UNIVERSITÀ
DI SIENA
1240

UNIVERSITY OF SIENA

Department of Biotechnology, Chemistry and Pharmacy

PHD SCHOOL IN BIOCHEMISTRY AND MOLECULAR BIOLOGY BiBiM 2.0

(Cycle XXXIII)

Coordinator of PhD school: Prof. Lorenza Trabalzini

SNAI1 target genes in myoblasts

S.S.D. BIO/11

Tutors:

Prof. Maurizio Orlandini

Prof. Federico Galvagni

PhD Candidate:

Ines Elia

Academic year: 2021

Digitally signed by ELIA INES
C=IT

SUMMARY

1. ABSTRACT

SNAI proteins are zinc finger transcription factors that act as transcriptional repressors through a conserved domain (SNAG domain) located in the N-terminus of the protein. These factors bind to a palindromic sequence of the E-box group (CANNTG) in the regulatory regions of their target genes. The role of SNAI11 and SNAI2 is well known in the epithelial mesenchymal transition, where they act as regulators increasing the capacity of tumor cells to metastasize. Less is known about their role as mediators in tissue homeostasis and differentiation. Recent studies have showed SNAI1 and SNAI2 as repressors of muscle differentiation, with the function of maintaining myoblasts in an undifferentiated state during the proliferative phase.

In this study, we explored the function of SNAI1 and SNAI2 in myogenesis both *in vitro* and *in vivo*. *In vitro*, we analyzed the expression of SNAI1 and SNAI2 in proliferating murine myoblasts, at various time points after inducing their differentiation. To evaluate their expression during myogenesis *in vivo*, we induced skeletal muscle regeneration by injecting the myotoxic agent Bupivacaine in the tibialis anterior muscles of wild-type and transgenic mice. We demonstrated that SNAI1 and SNAI2 are upregulated in proliferating myoblasts both *in vitro* and *in vivo.*

Through the analysis of the transcriptome in C2C12 myoblasts silenced for the expression of SNAI1, we have identified several target genes, among which *Fgf21* and *Atf3*. FGF21 is a growth factor involved in muscle differentiation as well as in glucose and lipid metabolism. In muscle differentiation, FGF21 expression is increased during myogenic differentiation and its knockdown impairs myogenic differentiation in C2C12 cells. ATF3 is a transcription factor that induces endoplasmic reticulum stress (ER-stress), phenomenon behind numerous physiological processes, including muscle differentiation and metabolism regulation. Recent studies have showed that ATF3 is able to regulate chemokine mRNA expression in C2C12 myotubes and it attenuates inflammation of skeletal muscle upon muscle-damaging eccentric exercise.

Herein, we analyzed the direct involvement of SNAI1 in the regulation of *Fgf21* and *Atf3*. For this purpose, several *Fgf21* and *Atf3* promoter deletion mutants, cloned in front of the reporter gene for luciferase, were generated in order to progressively exclude the possible binding sites for SNAI1. We used the Dual-Luciferase Reporter Assay System and ChIP-qPCR analysis to demonstrate that SNAI1 directly binds to the promoter region of *Fgf21* and *Atf3*, leading to the activation of *Fgf21* and *Atf3* expression in mouse C2C12 myoblasts.

Finally, we generated a SNAI1 knockout C2C12 cell line, using the CRISPR-Cas9 genome editing technique and we confirmed that SNAI1 acts as repressor of *Fgf21* and *Atf3* in proliferating myoblasts.

2. INTRODUCTION

2.1 *Snai* superfamily

The first member of the *Snai* superfamily, *Snai1*, has been initially described in *Drosophila melanogaster* (Grau *et al.*, 1984; Nüsslein-Volhard *et al.*, 1984), where it drives the development of the mesoderm (Leptin *et al.*, 1991). Later on, *Snai1* homologues have been found in many species within the Animalia kingdom. More than 50 Snai family members have been described, three of which in mammals: *Snai1* (also called *Snail*), *Snai2* (*Slug*) and *Snai3* (*Smuc*). They constitute a superfamily that groups two independent families, *Snail* and *Scratch*, originated by the duplication of an ancestral gene and by independent duplication events, that led to a different number of family members in each group (Manzanares *et al.*, 2001; Nieto *et al.*, 2002) (Figure 1).

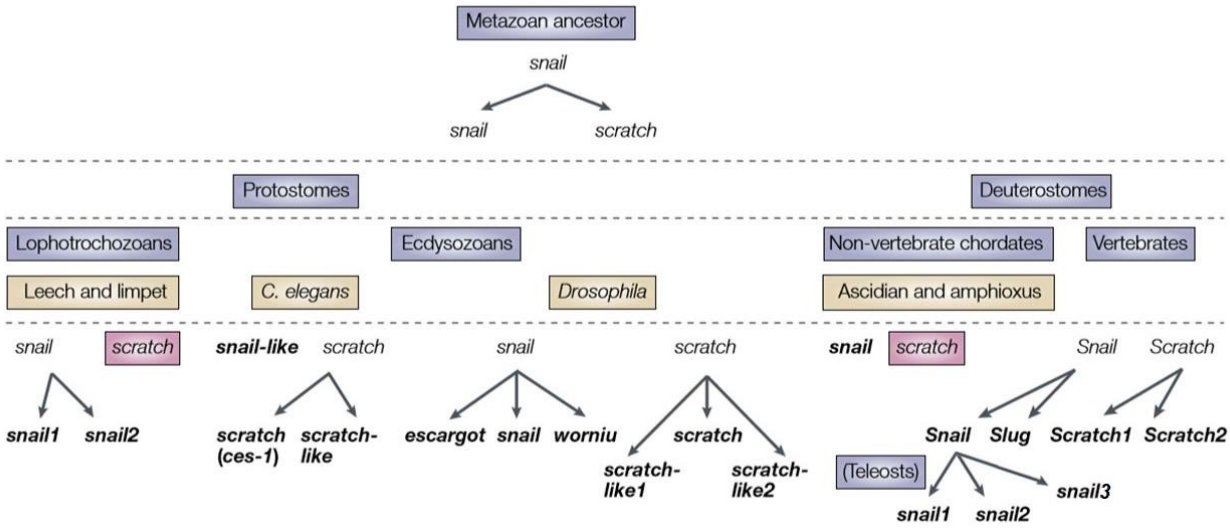

Figure 1. Proposed evolutionary history of the *Snai* superfamily. The duplication of a unique *Snail* gene in the metazoic ancestor gave rise to two genes: *Snail* and *Scratch*. Independent duplication events in *Protostomes* and *Deuterostomes* gave rise to a different number of family members in each group (Nieto *et al.*, 2002).

Snai family members encode zinc-finger transcription factors with have a conserved structure composed of a highly preserved C-terminal region, containing four-six zinc fingers and a divergent N-terminal region. These C_2H_2-type zinc fingers are sequence-specific DNA-binding motifs, structurally composed of 2 β-strands followed by an α-helix, the amino-terminal part which binds to the major groove of the DNA (Buorlay *et al.*, 1987; Nieto *et al.*, 2002). Through these domains, SNAI factors recognize and bind to an E-box, 5'CANNTG-3', a consensus sequence containing a core of six bases. This consensus motif is identical to the core binding site of basic helix-loop-helix (bHLH) transcription factors, such as MRFs (myogenic regulatory factors), which indicates that

SNAI proteins might compete with bHLH for the same binding sequences (Kataoka *et al.*, 2000; Braun *et al.*, 1991; Mauhin *et al.*, 1993).

Recently, Soleimani *et al.* have demonstrated that SNAIl-HDAC1/2 repressive complex binds and excludes MyoD from its targets. Notably, SNAIl binds E-box motifs that are G/C rich in their central dinucleotides and such sites are almost exclusively associated with genes expressed during differentiation. In ChIP-seq experiments, SNAI1/HDAC1/2 complex preferentially binds to G/C-rich E-boxes in myoblasts. Importantly, these sites are not enriched for MyoD in myoblasts (Figure 2). However, during differentiation, removal of SNAI1 and SNAI2 by miR-30a and miR-206 respectively results in MyoD occupancy on G/C-rich differentiation-specific E-boxes (Soleimani *et al.,* 2012).

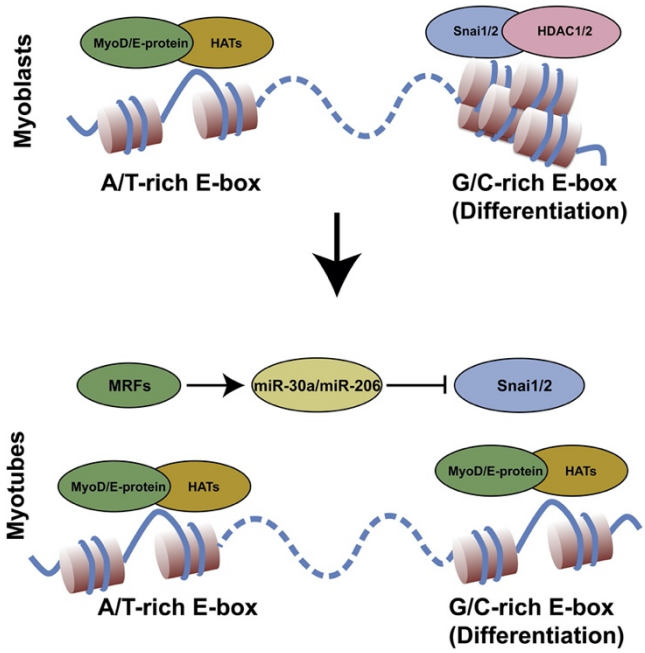

Figure 2. SNAIl/HDAC1/2 complex preferentially binds to G/C-rich E-boxes in myoblasts and excludes MyoD from its targets. During myoblasts differentiation, removal of SNAI1 and SNAI2 by miR-30a and miR-206, respectively, results in MyoD occupancy on G/C-rich differentiation-specific E-boxes (Soleimani *et al.,* 2012).

SNAI family members act as transcriptional repressors (Kataoka *et al.*, 2000; Batlle *et al.*, 2000; Bolos *et al.*, 2003). Their repressor capacity is dependent on both the zinc finger DNA-binding domain and the SNAG domain (Snai1/Gfi), a conserved short sequence (7-9 amino acids) localized in the N-terminal region of the protein (Nakayama *et al.*, 1998; Batlle *et al.*, 2000). The N-terminal regulatory domain is necessary for transcriptional repression and it mediates the repression by recruitment of chromatin-modifying enzymes (Peinado *et al.*, 2004). The serine-proline-rich domain in the central region of SNAI proteins is highly divergent between SNAI members. SNAI2 protein

contains the so-called SLUG domain in this region and its function is elusive. By contrast, SNAI1 protein has two functional domains in the central region: a regulatory domain containing a Nuclear Export Signal (NES) and a destruction box domain characterized by the DSGXXS amino acid sequence, which is recognized by the β-Trcp factor (Peinado *et al.*, 2007) (Figure 3). The phosphorylation on serine residues in both regions is involved in subcellular location of SNAI, protein stability and repressor activity. Thus, a mechanism based on phosphorylation can control the activity of these factors (Dominguez *et al.*, 2003; Zhou *et al.*, 2004).

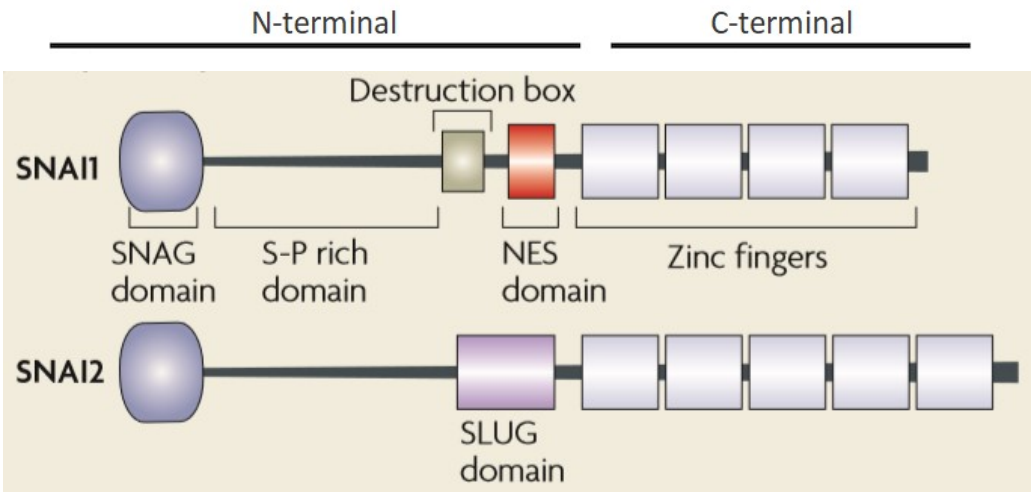

Figure 3. Main structural domains found in mammalian SNAI1 and SNAI2. SNAI factors are transcriptional repressor, characterized by the presence of a conserved domain (SNAG), a Serine/Proline rich domain and a C-terminal region containing 4-6 zinc fingers. In the central region of SNAI1 are present two different functional domain: destruction box (DB) and nuclear export signal (NES); by contrast, in SNAI2 is present the SLUG domain (Peinado *et al.*, 2007).

If studies on SNAI1 and SNAI2 family members are abundant, not so much is known yet about SNAI3. The SNAI3 protein contains five DNA-binding zinc finger domains in its C-terminal region, which bind the same E-box sequence recognized by the SNAI1 and SNAI2 proteins, acting as a transcriptional repressor (Kataoka *et al.*, 2000).

2.2 *Snai* functions

The functions of the *Snai* family as mesodermal determinants are essential during embryonic development; in fact, the expression of *Snai1* gene is important in the formation and morphogenesis of mesoderm (Barrallo-Gimeno *et al.*, 2005; Leptin *et al.*, 1991). SNAI members induce the conversion of epithelial cells into migratory mesenchymal cells (epithelial–mesenchymal transitions,

EMTs). They upregulate the mesenchymal markers, such as metalloprotease, fibronectin and vitronectin, and they downregulate the epithelial markers, such as E-cadherin, occludins and cytokeratins (Barrallo-Gimeno *et al.*, 2005; Cano *et al.*, 2000). EMT process is crucial for the formation of many different tissues and organs during embryogenesis, such as the mesoderm in amniotes, the neural crest in all vertebrates, as well as the heart cushions and the palate (Nieto *et al.*, 2002). Although *Snai* is required in all processes of EMT that have been studied, this does not necessarily mean that the induction of EMT is the prevalent role of *Snai* genes. One EMT-independent role of all *Snai* superfamily members is the protection of cells from death, acting as potent survival factors. SNAI-expressing cells survive to the loss of survival factors or to direct apoptosis and are resistant to DNA damage (Barrallo-Gimeno *et al.*, 2005; Kajita *et al.*, 2004; Martinez-Alvarez *et al.*, 2004; Vega *et al.*, 2004).

EMT is also well known to play an essential role in pathological processes, such as tumor progression, that occur concomitantly with the cellular acquisition of migratory and invasive properties following the downregulation of the E-cadherin, a cell-to-cell adhesion protein encoded by the CDH1 gene. E-cadherin is currently thought to be a suppressor of invasion during carcinoma progression, in fact the functional loss of this protein is one of the hallmarks of EMTs (Peinado *et al.*, 2004; Nieto *et al.*, 2002; Cano *et al.*, 2000). SNAI1 is a strong repressor of transcription of the *E-cadherin* gene, directly binding its promoter (Herranz *et al*., 2008; Peinado *et al*., 2007; Thiery *et al*., 2006). Deregulation of SNAI1 has been observed in a variety of tumors including breast cancer (Phillips *et al.*, 2014), gastric carcinoma (Yang *et al.*, 2016), colorectal cancer (Jägle *et al.*, 2017) and prostate cancer (Osorio *et al.*, 2016). Furthermore, SNAI1 directly suppresses the gene expression of proteins representing other adhesive complexes, such as claudins and occludins, integral membrane proteins localized at tight junctions (Ikenouchi *et al.*, 2003). SNAI1 factor represses also other epithelial markers, such as MUC1 and cytokeratin 18 (Guaita *et al.*, 2002). In addition, SNAI1 is involved in the decrease of proliferation. It impairs the transition from early to late G1 by maintaining low levels of Cyclins D and can block the G1/S transition by maintaining high levels of p21 (Vega *et al.*, 2004). SNAI1 is also involved in the resistance to apoptosis, reducing the levels of p53 (Kajita *et al*, 2004) (Figure 4). Other SNAI1 targets are vitamin D_3 receptor (Palmer *et al*, 2004) and the β-subunit of the Na^+/K^+ ATPase (Espineda *et al.*, 2004).

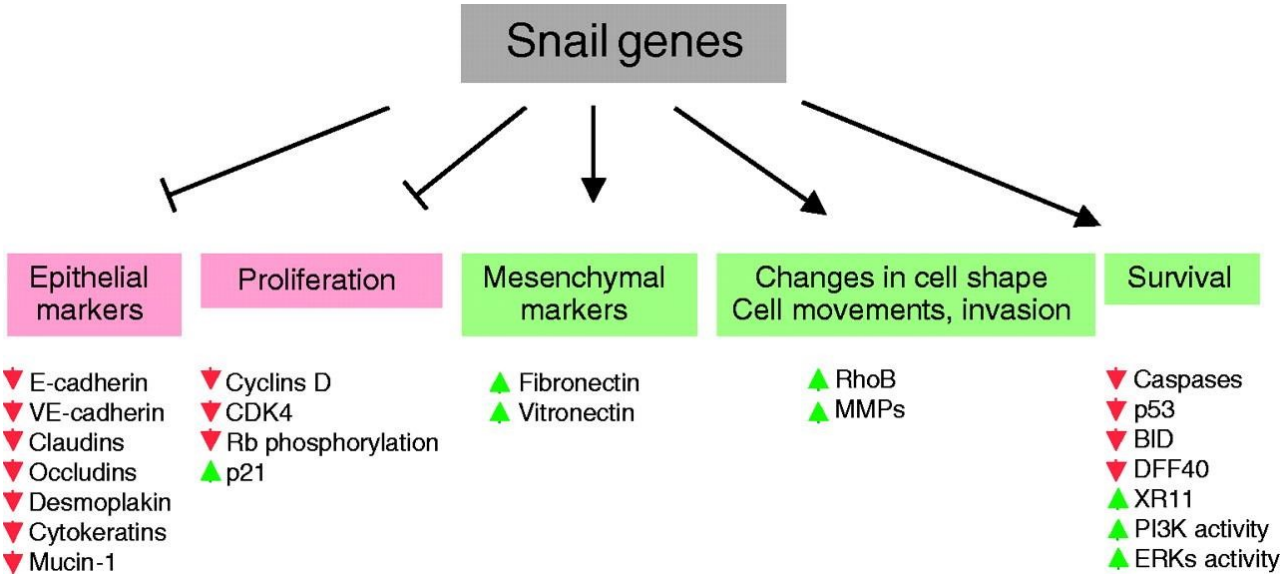

Figure 4. Downstream targets of *Snai1*. *Snai1* gene expression induces the loss of epithelial markers and the gain of mesenchymal markers, as well as inducing changes in cell shape and changes related to morphology and to the acquisition of motility and invasive properties. The *Snai1* genes also regulate cell proliferation and cell death. The molecules and processes shown in red are downregulated or impaired by *Snai1*, and those in green are upregulated or promoted by *Snai1* (upregulation might be due to the *Snai1* mediated repression of a repressor. However, their role as activators cannot be excluded) (Barrallo-Gimeno *et al.*, 2005).

Furthermore, SNAI1 and SNAI2 are expressed in myoblasts, since they are widely expressed in mesodermal cells. They are expressed in proliferating myoblasts and rapidly turned off as muscle differentiation proceeds. A molecular switch involving various actors, including MRFs and SNAI1/2, regulates transition from proliferating myoblasts to terminally differentiated myotubes (Soleimani *et al.*, 2012).

MRFs, such as myogenic differentiation antigen (MyoD), myogenic factor 5 (Myf5), myogenin (MyoG) and myogenic regulatory factor 4 (MRF4), are basic helix-loop-helix (bHLH) transcription factors that regulate myogenesis (Singh *et al.*, 2013). Myf5 and MyoD are required in myoblasts to establish their myogenic identity and act upstream of MyoG and MRF4, which instead drive myogenic differentiation (Jiménez-Amilburu *et al.*, 2013). SNAI1-HDAC1/2 repressive complex binds to multiple differentiation-specific genes under growth condition, allowing the exclusion of MyoD from these sites, therefore the block of differentiation. At the onset of differentiation, SNAI1/2 must be removed to allow the access of MyoD to differentiation genes sequences. Thus, a dynamic switch from a repressive to an activating complex on muscle-specific genes during differentiation (Soleimani *et al.*, 2012). In addition, SNAI1/2 are targets of microRNAs, such as miR-30a and miR206, which are MRFs targets (Sweetman *et al.*, 2008), when cells receive a differentiation signal

from a molecular cascade initiated by growth factors, MRFs activate the miRNAs that prevent *Snai* mRNA translation. As SNAI proteins turn over, MyoD gains access to differentiation-specific E-boxes (Soleimani *et al.*, 2012).

SNAI1 and SNAI2 functions have been studied extensively during vertebrate embryogenesis and tumor progression, while the role of SNAI3 still needs to be studied (Bradley *et al.*, 2013). SNAI3, also known as SMUC (Snail-related transcription factor of muscle cells), is highly expressed in the developing embryos and in the adult skeletal muscle and thymus. It is expressed in terminal T-cell and myeloid lineages, where it has been largely studied. It has been shown that this transcriptional repressor competes with MyoD for binding on a muscle-specific gene (Kataoka *et al.*, 2000), this means that it probably works as a regulator of muscle differentiation processes with mechanisms similar to the other *Snai* family members. However, still a lot needs to be studied about SNAI3 and its function during myogenesis needs to be clarified.

2.3 *Snai* regulation

The modification of chromatin structure has emerged as an essential regulatory event promoted by SNAI proteins during EMT. The N-terminal regulatory domain of these factors is necessary for both transcriptional repression and repression by recruitment of chromatin-modifying enzymes (Peinado *et al*., 2004). SNAI can recruit numerous chromatin enzymes, including members of the histone-deacetylase family (HDACs) and of the lysine-specific histone demethylase (LSDs) to the *E-cadherin* promoter. These enzymes are essential to generate heterochromatin and promote DNA methyltransferase (DNMT)-mediated DNA methylation at the promoter region (Lin *et al.*, 2014). SNAI factors repression of CDH1 involves the direct recruitment of a repressor complex formed by co-repressors and HDACs (Peinado *et al*., 2007) (Figure 5).

Snai activity is regulated both transcriptionally and post-transcriptionally. *Snai* genes are expressed in all EMT processes studied (Nieto *et al.*, 2002). EMT can be triggered by different signaling molecules, such as by fibroblast growth factor (FGF), bone morphogenetic proteins (BMPs), epidermal growth factor (EGF), hepatocyte growth factor (HGF), transforming growth factor β (TGFβ), WNTs and Notch. These signaling molecules have been shown to induce *Snai* genes in different cellular contexts (Barrallo-Gimeno *et al.*, 2005; De Craene *et al.*, 2005) (Figure 6).

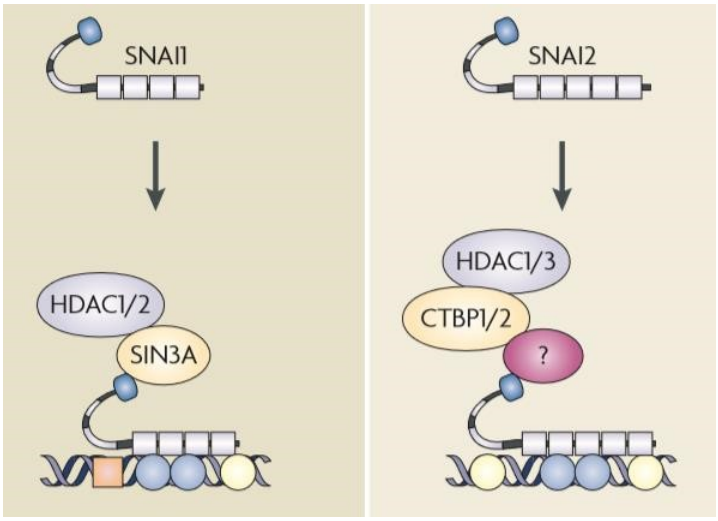

Figure 5. Schematic view of the main repression mechanism of SNAI factors, representing the main corepressor complexes or proposed interactions in the repressor mechanism of each transcription factor (Peinado *et al*., 2007).

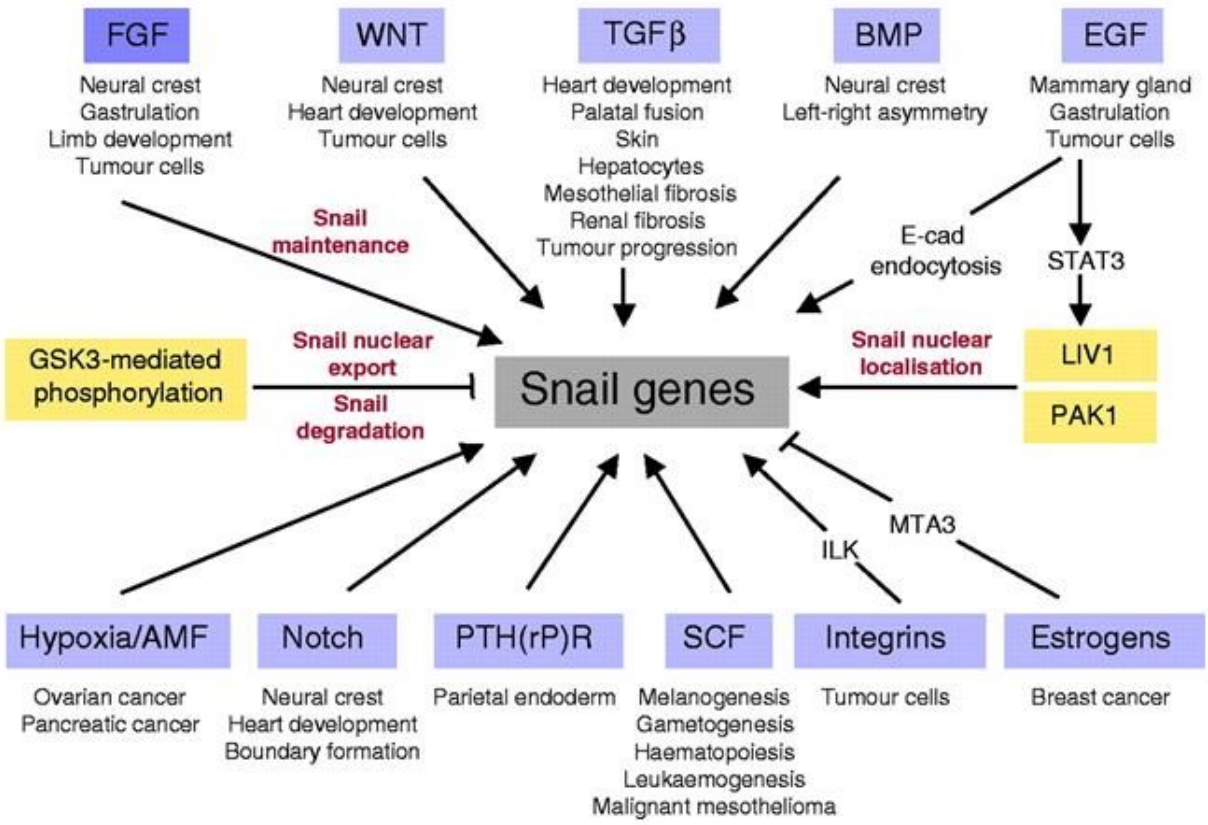

Figure 6. Transcriptionally and post-transcriptionally regulation of *Snail* genes. Numerous signaling pathways induce the epithelial to mesenchymal transition (EMT), and all have been shown to activate the expression of *Snail* genes (Barrallo-Gimeno *et al.*, 2005).

Snai promoter presents a functional 5′-CACCTG-3′ E-box that acts as a regulative negative element; in fact, SNAI factors bind to this element creating a negative loop that controls its own expression (Peirò *et al.*, 2006).

SNAI contains a serine-proline rich domain, and the phosphorylation of which is involved in the regulation of SNAI, in particular in the protein degradation and subcellular localization (Dominguez *et al.*, 2003; Zhou *et al.*, 2004). SNAI is regulated by glycogen synthase kinase 3 beta (GSK-3β). GSK-3β-mediated phosphorylation of SNAI factors controls their turnover and sub-cellular localization during EMT (Kim *et al.*, 2012). SNAI factors contain two GSK-3β phosphorylation motifs, separated by two proline residues. The phosphorylation of the second motif regulates their subcellular localization by induction of a conformational change that makes the NES domain more accessible to the transport proteins¸ allowing the nuclear export of these factors. Thus, the exportins, such as CRM1, which control the translocation of protein from the nucleus to the cytoplasm, are involved in exporting phosphorylated SNAI and in its inactivation as a transcription factor (Zhou *et al.*, 2004; De Craene *et al.*, 2005; Dominguez *et al.*, 2003).

The first GSK-3β phosphorylation motif overlapped with the destruction box, DSGXXS, recognized by the β-Trcp factor, determines the degradation of SNAI. The phosphorylation of these two motifs by GSK-3β is required for the binding of β-Trcp in the ubiquitination of SNAI and the protein degradation in the proteasome. (Zhou *et al.*, 2004).

Many upstream signaling pathways regulate the function of SNAI modulating the activity of GSK-3β. Oncogenic signals, such as PI(3)K/Akt, MAPK and Wnt, cause the inhibition of GSK-3β, the resulting increase of nuclear SNAI level and the initiation of EMT programs (Wu *et al.*, 2012; Yook *et al.*, 2005; Zhou *et al.*, 2004) (Figure 7).

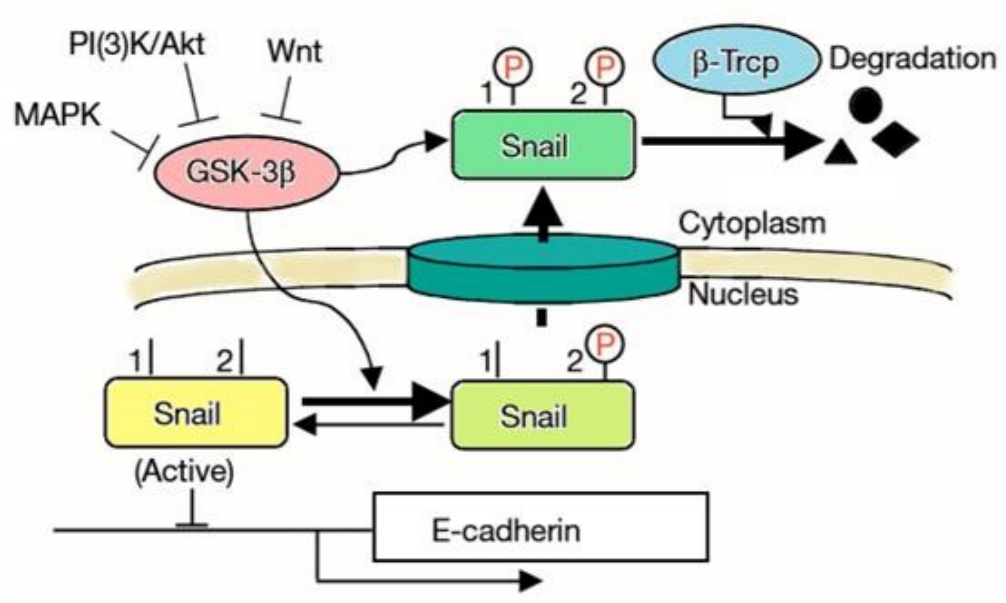

Figure 7. A model proposed to illustrate the inhibition of SNAI1 by GSK-3β. GSK-3β is a multi-tasking kinase involved in the Akt, Wnt and Hedgehog pathways, it is present in the nucleus and in the cytoplasm. It can phosphorylate several nuclear transcription factors, such as c-Myc and p53. GSK-3β binds and phosphorylates SNAI1 (at level of the motif 2) and thereby induces its nuclear export. Subsequent phosphorylation by GSK-3β (at level of the motif 1) results in the association of SNAI1 with β-Trcp and thus leads to the degradation of SNAI1 (Zhou *et al.*, 2004).

The p21-activated kinase (PAK1) is also able to phosphorylate SNAI. PAK1-induced phosphorylation determines the nuclear localization of SNAI, thus, its activity as a transcription factor (Yang *et al.*, 2005).

Furthermore, the small C-terminal domain phosphatase (SCP) is a specific phosphatase for SNAI. SCP interacts and colocalizes with SNAI in the nucleus, inducing SNAI dephosphorylation and stabilization, with a resulting increase of SNAI activity (Wu *et al.*, 2009).

2.4 FGF21

Fibroblast Growth Factor 21 (FGF21) is an endocrine hormone expressed in numerous tissues including liver, brown adipose tissue, white adipose tissue and pancreas (Markan *et al.*, 2014). Although the liver is generally considered the main site of FGF21 production, FGF21 could be considered a myokine since many studies indicate that the skeletal muscle may be a relevant source of FGF21 production, especially in response to insulin stimulation. In the skeletal muscle, expression and release of FGF21 are essential because they are related to myogenic differentiation, in both rodent and human cell models of myogenesis (Izumiya *et al.*, 2008; Ribas *et al.*, 2014). Recent studies have demonstrated that MyoD binds directly to the promoter region of *Fgf21,* leading to the activation of *Fgf21* expression in mouse C2C12 myoblasts. In this cellular context, FGF21 activates expression of the early myogenic genes, promotes cell cycle exit and enhances myogenic differentiation of C2C12 cells. Even if the mechanism involved in these processes is not so clear, it is known that FGF21 not only regulates myogenesis, but also myofiber type transformation, promoting aerobic myofiber formation (Liu *et al.*, 2016).

FGF21 is also a pivotal modulator involved in the regulation of several physiological processes, such as glucose and lipid metabolism, sensitivity to insulin and cardioprotection (Liu *et al.*, 2016). As a member of the FGF family, FGF21 was initially identified as critical regulator of lipid metabolism and energy homeostasis. It stimulates glucose uptake and fatty acid oxidation (Guridi *et al.*, 2015) and suppresses the accumulation of lipids in muscles (Wang *et al.*, 2016). Several studies have reported that FGF21 is involved in the improvement of insulin sensitivity: long acting of this growth

factor improves liver metabolism and insulin signaling without side effects (Camporez *et al.*, 2015). Moreover, it has been shown that in the cardiovascular system FGF21 released by cardiomyocytes could protect cardiac cells from hypertrophic injury (Planavila *et al.*, 2013). Other studies show that FGF21 regulates the expression of genes involved in antioxidant pathways in heart tissue, preventing the induction of pro-oxidative pathways, and protects against cardiac apoptosis (Planavila *et al.*, 2015; Zhang *et al.*, 2015).

FGF21 expression is not only correlated with physiological processes, but also with metabolic disease and it is strongly induced in animal and human subjects with metabolic diseases, but little is known about the molecular mechanism of this induction (Wan *et al.*, 2014; Itoh *et al.*, 2014).

2.5 ER stress and ATF3

The development of skeletal muscles is an elaborated process that involves myoblasts proliferation and myofibers differentiation, which are mainly controlled by MyoD-Myf5 and MyoG-MRF4 transcription factors, respectively (Singh *et al.*, 2013; Jiménez-Amilburu *et al.*, 2013). In addition, numerous studies have shown that endoplasmic reticulum (ER) stress plays an essential part in the regulation of the skeletal muscle development (Chen *et al.*, 2006; Nakanishi *et al.*, 2015; Wei *et al.*, 2016); in particular, ER stress occurs transiently during differentiation and myofiber formation, although its cause remains unknown (Nakanishi *et al.*, 2015). ER stress plays a critical role both in physiological processes, such as in metabolic homeostasis and myogenesis, and in pathological processes, such as in the contribution of triggering insulin resistance, obesity, and type 2 diabetes (Wan *et al.*, 2014; Cao *et al.*, 2013).

ER is a specialized organelle required for its crucial role in the synthesis, assembly, folding, routing and degradation of a large numbers of proteins and in Ca^{2+} storage. ER stress is a compensatory process that aims to restore ER homeostasis in order to preserve cellular functions and survival (Kaufman *et al.,* 1999). A variety of agents causes ER stress, *e.g.,* ER redox imbalance or disruption of ER Ca^{2+} homeostasis, resulting in accumulation of misfolded or unfolded proteins in the ER lumen (Malhotra *et al.*, 2007; Wang *et al.*, 2016). This triggers an adaptive response called unfolded protein response (UPR). The UPR is mediated by three ER transmembrane sensors: protein kinase R (PKR)-like endoplasmic reticulum kinase (PERK), inositol-requiring protein 1α (IRE1α) and activating transcription factor 6 (ATF6) (Edagawa *et al*., 2014). Initially, the activation of these stress sensors results in a transient repression of protein synthesis, followed by a transcriptional modification that promotes the correct protein folding and the degradation of misfolded proteins and enhances ER folding capacity, thereafter the inhibition of protein synthesis is relieved. In case of prolonged or

strong ER stress, apoptotic pathways are activated (Schaap *et al.*, 2013). Evidence suggests that ER stress induced UPR pathways may regulate various aspects of myogenesis. Specifically, levels of ER stress-related proteins, such as ATF6, CHOP and GRP74, and the activity of caspase-12 are increased in myoblasts undergoing apoptosis during myogenic differentiation (Afroze *et al*., 2019; Nakanishi *et al*., 2005). Heightened ER stress seems to be essential for proper progression of myogenesis because the inhibition of ATF6 or caspase-12 reduces the formation of multinucleated myotubes. An increase in caspase-12 activity is also observed during embryonic development of skeletal muscle, suggesting that the ATF6 arm of the UPR is required for the removal of a subpopulation of myoblasts that may not be able to sustain cellular stress (Afroze *et al*., 2019; Nakanishi *et al*., 2005; Nakanishi *et al*., 2007). ER stressors, such as tunicamycin and thapsigargin, increase cell death in C2C12 myoblast cultures after induction of differentiation. However, the surviving myoblasts more efficiently differentiate into functional myotubes, further suggesting that ER stress is a mechanism to remove differentiation-incompetent myoblasts during myogenesis (Nakanishi *et al*., 2007).

It has been reported that the phosphorylation of PERK and eIF2α and levels of CHOP are transiently increased in a subset of myoblasts, after incubation in differentiation medium. CHOP inhibits myogenic differentiation repressing the expression of transcription factor MyoD, which could be a mechanism to prevent premature differentiation of myoblasts (Alter *et al*., 2011). IRE1α has an endonuclease activity that mediates the unconventional splicing of XBP1 mRNA. Spliced XBP1 (sXBP1) is a powerful transcription factor that induces UPR target genes. In myogenic cells, the expression of *Xbp1* is regulated by MyoD and myogenin. *Xbp1* is able to inhibit myotube formation through upregulation of Mist1 (Blais *et al.,* 2005; Acosta-Alvear *et al.,* 2007). Furthermore, Afroze *et al*. found that PERK is required for the survival of satellite cells and the regeneration of myofibers upon injury. Altogether, these studies suggest that the UPR plays an important role in satellite cells homeostasis and myogenesis both *in vitro* and *in vivo* (Afroze *et al*., 2019).

Several signals that cause the UPR pathway induce also the activating transcription factor 3, ATF3 (Edagawa *et al.*, 2014; Xu *et al.*, 2012; Gjymishka *et al.*, 2009). ATF3 is a member of the ATF/cyclic adenosine mono-phosphate response element binding (CREB) family of basic-region leucine zipper (bZIP) proteins (Hai *et al.*, 1989); it is considered to be a regulatory factor of gene transcription. The *ATF3* gene consists of four exons that encode a 181-amino acid protein with a molecular weight of 22 kDa (Hai *et al.,* 1989). ATF3 has been demonstrated to be a transcriptional repressor by forming a homodimer. In addition, the transcription factor cooperates with other ATF/CERB family proteins or CCAAT/enhancer-binding protein (C/EBP) family proteins to form heterodimers producing inhibitory or stimulatory effects in a cell- and promoter-dependent context (Chen *et al.*, 1994; Hai *et al.,* 1991). ATF3 is induced in response to ER stress by a mechanism requiring PERK pathway.

Transcriptional regulator ATF4 is necessary to allow an increased expression of ATF3 protein in early response to stress (Schmitz *et al.*, 2018; Jiang *et al.*, 2004). In fact, ATF3 levels are dramatically induced in many different tissues in response to a variety of cellular stressors; thus, while ATF3 expression is maintained at low levels in normal quiescent cells, it is induced by several stress conditions (Yang *et al.*, 2016). A strong body of evidence shows that *ATF3* is an adaptive-response gene and that its expression is increased by numerous signals, including those triggered by genotoxic agents, cytokines, cell death-inducing agents and physiological stress. Indeed, overwhelming evidence indicates that ATF3 plays an important role in metabolic regulation, immune response and oncogenesis (Hui-Chen *et al.,* 2020; Lu *et al.*, 2006; Hashimoto *et al.,* 2002; Hai *et al.,* 1999). Recent studies showed that ATF3 is a negative regulator of some inflammatory genes in skeletal muscle. ATF3 is able to regulate chemokine mRNA expression in C2C12 myotubes and to attenuate inflammation of skeletal muscle upon muscle-damaging eccentric exercise (Fernández-Verdejo *et al.,* 2017).

2.6 Skeletal muscle regeneration

Skeletal muscle is an excitable, contractile tissue responsible for maintaining posture and moving the orbits, together with the appendicular and axial skeletons. It attaches to bones and the orbits through tendons. Excitable tissue responds to stimuli through electrical signals. Contractile tissue is able to generate tension of force. Skeletal muscle tissue is also extensible and elastic. Extensible tissue can be stretched, and elastic tissue is able to return to its original shape following distortion. Skeletal muscle is a type of striated muscle tissue, accounting for ~40% of adult human body weight. Skeletal muscles consist of myofibers, neurons, vasculature networks and connective tissues, of which the structural and functional element of skeletal muscle is the myofiber. During development, myofibers are formed by fusion of mesoderm progenitors called myoblasts. In neonatal/juvenile stages, the number of myofibers remains constant, but each myofiber grows in size by fusion of satellite cells, a population of postnatal muscle stem cells. Each myofiber is surrounded by the endomysium. Bundles of myofibers are surrounded by the perimysium, while the entire muscle is contained within the epimysium. Each myofiber is anchored at its extremities to tendons or tendon-like fascia at the myotendinous junctions (MTJs) (Yin *et al., 2013;* Tidball *et al.,* 1986). Myofibers are composed of actin and myosin myofibrils repeated as a sarcomere, which is the basic functional unit of skeletal muscle. Responding to the signals from motor neurons, myofibers depolarize and release calcium from the sarcoplasmic reticulum (SR). This drives the movement of actin and myosin filaments relative to one another and leads to sarcomere shortening and muscle contraction (Decary *et al.*, 1997; Schmalbruch *et al*., 1991) (Figure 8).

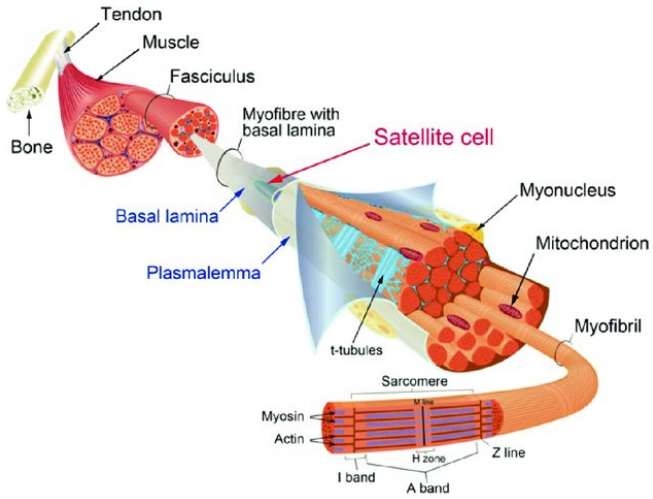

Figure 8. Skeletal muscle structure and satellite cells niche. Individual muscle cell fibers are surrounded by delicate connective tissue called endomysium. Skeletal muscle fibers are aligned in bundles called fascicles and these fascicles are surrounded by a stronger sheath of connective tissue called the perimysium. The fascicles are finally packaged in a stronger connective tissue encasement called the epimysium. Satellite cells are small mononuclear cells located between the plasmalemma of the myofibers and the basal membrane (Meiliana *et al.* 2015, adapted from The Company of Biologist, Ltd).

Skeletal muscle is a tissue that is able to regenerate after injury. Responding to injury, skeletal muscle undergoes a highly orchestrated degeneration and regenerative process that takes place at the tissue, cellular and molecular levels (Yin *et al.,* 2013; Seale *et al*., 2000). The initial event of muscle degeneration is necrosis of the muscle fibers. This event is generally triggered by disruption of the myofiber sarcolemma resulting in increased myofiber permeability. The disruption of myofiber integrity is proved by increased serum levels of muscle proteins, such as MCK (Muscle Creatine Kinase, usually restricted to the myofiber cytosol). It has been hypothesized that increased Ca^{2+} influx after sarcolemma or sarcoplasmic reticulum damage results in a loss of Ca^{2+} homeostasis and increased $Ca2^{+}$ dependent proteolysis that drives tissue degeneration resulting in focal or total autolysis depending on the extent of the injury. The early phase of muscle injury is usually accompanied by the activation of mononucleated cells, mainly inflammatory cells and myogenic cells (Chargè *et al., 2004;* Rappolee *et al*, 1992). Neutrophils are the first immune cells to invade the injured muscle, with a significant increase in their number being observed as early as 1–6 h after myotoxin or exercise-induced muscle damage. After neutrophil infiltration and 48 h post injury, macrophages become the predominant inflammatory cell type within the site of injury (Tidball *et al.,* 2017; Seale *et al*., 2000). Macrophages infiltrate the injured site, through phagocytosis remove cellular debris and may affect other aspects of muscle regeneration by activating myogenic cells. Following proliferation, myogenic cells differentiate and fuse to existing damaged fibers or fuse with one another to form myofibers *de novo*. Newly formed myofibers have small caliber and centrally located myonuclei. At the end of muscle regeneration, newly formed myofibers increase in size, and myonuclei move to the periphery of the muscle fiber (Yin *et al.,* 2013; Chargè *et al.,* 2004).

This process, in many but not all aspects, recapitulates embryonic myogenesis. Skeletal myogenesis begins in the somites where multipotent mesodermal cells commit to the myogenic lineage. These mononucleated myoblasts then fuse and form multinucleated cells (myotubes) that, ultimately, develop into mature myofibers. During the course of muscle development, some myoblasts fail to differentiate and remains associated with the surface of the developing myofiber as quiescent muscle satellite cells in fully developed mature skeletal tissue (Yin *et al.,* 2013; Chargè *et al.,* 2004).

Satellite cells activation may result from the ligation of the integrin molecule VL4 (4integrin $\alpha 4\beta 1$) on PMNL (infiltrating polymorphonuclear leukocytes) and VCAM1 (vascular cell adhesion molecule-1) on resident satellite cells. HGF (Hepatocyte growth factor) is also postulated to activate satellite cells through its receptor c-Met, expressed in quiescent satellite cells. HGF may be produced by undamaged myofibers in response to physiological stimuli or to the damage to the basal lamina or extracellular matrix. Several growth factors have been implicated in the proliferation of satellite cells,

including PDGF (platelet derived growth factor), LIF (leukemia inhibitory factor), IL-6 (interleukin-6), FGF (fibroblast growth factor), IGF-1 (insulin-like growth factor-1) (Seale *et al*., 2000).

2.7 Transcriptional regulation of skeletal muscle regeneration

Discovery of the myogenic regulatory factor family of transcription factors MYF5, MYOD, Myogenin and MRF4 was a seminal step in understanding specification of the skeletal muscle lineage and control of myogenic differentiation during development. These factors are also involved in specification of the muscle satellite cell lineage, which becomes the resident stem cell compartment in adult skeletal muscle. While MYF5, MYOD, Myogenin and MRF4 have minor roles in mature muscle, they play a crucial role in directing satellite cells function to regenerate skeletal muscle, linking the genetic control of developmental and regenerative myogenesis. MRFs present highly related proteins structure. These class II basic helix-loop-helix (bHLH) transcription factors contain three conserved domains: the amino terminal transactivation domain with a histidine/cysteine-rich zone, the central region with the bHLH motif including the α-helical basic domain and Helix I and II and another transactivation domain in the carboxyl terminal containing Helix III . The basic domain directs DNA binding to the E-box consensus sequence CANNTG, but only specific 'private' sequences are associated with activating transcription (e.g. CAGGTG for MYOD), and E-box accessibility is epigenetically controlled (Zammit *et al.,* 2017).

In intact muscle, satellite cells are sublaminar and mitotically quiescent (G_0phase). Quiescent satellite cells are characterized by the expression of Pax7 but not MyoD or Myogenin. Upon exposure to signals from a damaged environment, satellite cells exit their quiescent state and start to proliferate (satellite cells activation). Proliferating satellite cells and their progeny are often referred as myogenic precursor cells (MPC) or adult myoblasts. Unlike quiescent satellite cells, myogenic precursor cells are characterized by the rapid expression of myogenic transcription factors MyoD and Myf5. Of note, the presence of MyoD, Desmin, and Myogenin in satellite cells was observed as early as 12 h after injury, which is before any noticeable sign of satellite cells proliferation. This early expression of MyoD is proposed to be related to a subpopulation of committed satellite cells, which are poised to differentiate without proliferation. In contrast, the majority of satellite cells express either MyoD or Myf5 by 24 h following injury and subsequently express both factors by 48 h (Yin *et al.,* 2013). The ability of satellite cells to upregulate either MyoD or Myf5 suggests these two transcription factors may have different functions in adult myogenesis. *MyoD*$^{-/-}$ mutant mice display markedly reduced muscle mass. This atrophy phenotype is reportedly due to delayed myogenic differentiation. Similarly, muscle regeneration is also impaired in *MyoD*$^{-/-}$ mice, resulting in an increased number of myoblasts within the damaged area. These *MyoD*$^{-/-}$ myoblasts persist for prolonged periods of time,

fail to differentiate and do not fuse into myotubes. Expression of MyoD is an important determinant of myogenic differentiation, and in the absence of MyoD, activated myoblasts have a propensity for proliferation and self-renewal (Yin *et al.,* 2013; Chargè *et al.,* 2004).

Compared to the *MyoD*$^{-/-}$ mice, *Myf5*$^{-/-}$ mutant mice show a myofiber hypertrophy phenotype, and the proliferation of *Myf5*$^{-/-}$ myoblasts is compromised. Together, these results implicate a distinct role for Myf5 in adult myoblasts proliferation, while MyoD is essential for differentiation. Together, the aforementioned observations suggest the hypothesis that satellite cells enter different myogenic programs depending on whether Myf5 or MyoD expression predominates. Predominance of MyoD expression would drive the program toward early differentiation, as exemplified by the behavior of *Myf5*$^{-/-}$ myoblasts. In contrast, predominance of Myf5 expression would direct the program into enhanced proliferation and delayed differentiation, as shown by the behavior of *MyoD*$^{-/-}$ myoblasts. MyoD expression peaks in mid G_1, whereas Myf5 expression is maximal at the G_0 and G_2 phases of the cell cycle (Ustanina *et al.,* 2009; Yin *et al.,* 2013; Chargè *et al.,* 2004). After limited rounds of proliferation, the majority of satellite cells enters the myogenic differentiation program and it begins to fuse to damaged myofibers or fuse to each other forming new myofibers. The initiation of terminal differentiation starts with the expression of Myogenin and Myf6 (also called Mrf4). In this hypothesis, myogenic differentiation is an irreversible procedure and is driven by the sequential expression of key transcription factors (master regulators), which are destined to transduce gene expression signals to their target genes. The expression of these genes is essential for the proper formation, morphology, and function of skeletal muscle; thus they are regulated by multiple mechanisms. MyoD also induces the expression of p21 and subsequent permanent cell cycle arrest. The terminal differentiation ends with the expression of specific muscle proteins such as the Muscle Creatine Kinase (MCK) and the Myosin Heavy Chain (MHC) (Yablonka-Reuveni *et al.,* 2011; Chang *et al.,* 2014) (Figure 9).

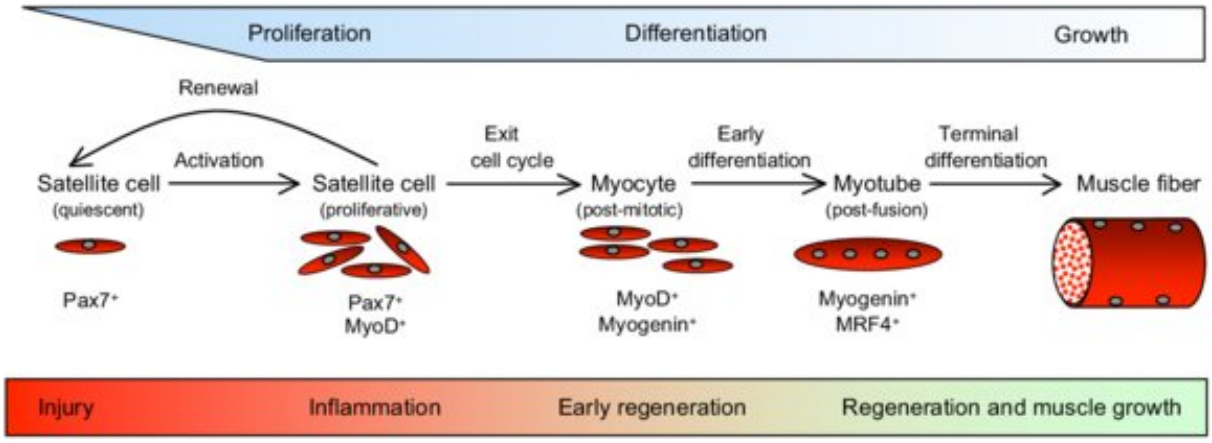

Figure 9. Transcription regulation of skeletal muscle regeneration. During the initial stages of injury, $Pax7^+$ satellite cells are activated, proliferate and begin to express MyoD, initiating transcription of muscle-specific genes necessary for early differentiation. As myogenesis proceeds, some activated satellite cells return to quiescence and renew the satellite cell reserve population, while others exit the cell cycle to undergo further differentiation. Those post-mitotic myocytes display a shift in gene expression that enables their fusion to form multinucleated myotubes that are able to undergo terminal differentiation (Tidball *et al.*, 2014).

2.8 Animal models of muscle injury

Although the degenerative and regenerative phases of the muscle regeneration process are similar among several muscle types and after different causes of injuries, the kinetics and amplitude of each phase may be dependent on the extent of the injury, the muscle injured, or the animal model. To study the process of muscle regeneration in a controlled and reproducible way, it has therefore been necessary to develop animal models of muscle injury. The use of myotoxins, such as Bupivacaine (Marcaine), cardiotoxin (CTX), and notexin (NTX) is perhaps the easiest and most reproducible way to induce muscle regeneration (Chargé *et al*., 2004). These toxins have a wide range of biological activities that are not entirely understood. For example, NTX is a phospholipase A_2 neurotoxin peptide extracted from snake venoms that blocks neuromuscular transmission by inhibition of acetylcholine release; CTX, also a peptide isolated from snake venoms, is a protein kinase C-specific inhibitor that induces the depolarization and contraction of muscular cells, leading to the disruption of membrane organization and the lysis of various cell types. Bupivacaine is a local anesthetic drug that induces Ca^{2+} release from the Sarcoplasmic Reticulum (SR) and simultaneously inhibits Ca^{2+} reuptake into the SR, resulting in persistently elevated intracellular Ca^{2+} concentrations. It also has a Ca^{2+} sensitizing effect on the contractile proteins. These mechanisms result in increased intracellular Ca^{2+} concentrations and contribute to pronounced skeletal muscle toxicity. Muscle fiber necrosis is extremely rapid after Bupivacaine induced injury. Injection of the drug into small skeletal muscles of

rat or mouse leads to immediate and massive myonecrosis followed by phagocytosis of necrotic debris and a rapid, complete regeneration of muscle fibers 3-4 weeks after injection (Zink *et al*., 2002). In our laboratory, 25 µl of Bupivacaine injected in adult mouse tibialis anterior muscle induced muscle degeneration leading to a wound coagulum with mononuclear cell infiltration within 1 day of injection. Inflammatory response and mononuclear cell proliferation were active the most within 1–4 days of injection. Myogenic cell differentiation and new myotube formation were observed ~5–6 days post injection. By 10 days post injection, the overall architecture of the muscle was restored, although most regenerated myofibers were smaller and displayed central myonuclei. The return to a morphologically and histochemical normal mature muscle was seen at ~3–4 weeks post injection (Figure 10).

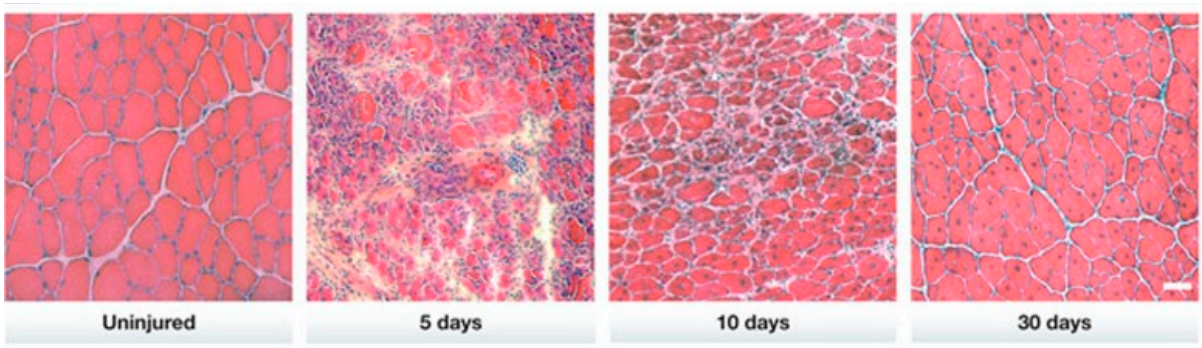

Figure 10. Overview of tissue histology during mouse skeletal muscle regeneration. A time course of histological changes in regenerating skeletal muscle. H&E staining of uninjured TA muscles and regenerating TA muscles at 5, 10 and 30 days after injury. Regenerating muscles are reduced to mostly mononuclear cells at day 5 but are able to re-establish multinucleated myofibers by day 10. Notably, the nuclei of uninjured myofibers are located at the periphery, whereas those of regenerating muscle fibers are centrally located. Scale bar, 50 µm, (Rudnicki *et al.,* 2013).

3. MATERIALS AND METHODS

3.1 Animals

In vivo experiments on wild-type mice, were performed in collaboration with Prof. Libero Vitiello from the University of Padua. *In vivo* experiments on transgenic mice, were performed in collaboration with the Medical Doctor Stephen J. Weiss from the University of Michigan. *Snai1*$^{flox/flox}$ mice have been generated in Stephen J. Weiss laboratory as described in Rowe *et al*., 2009. The S*nai1*$^{+/LacZ}$ embryonic stem cells (ESCs) were generated by the International Knockout Mouse Consortium (EUCOMM/KOMP) with the details described at the Consortium website. *Snai*1$^{+/LacZ}$ mice were bred and maintained on a C57/B6 background. Mice carrying *Snai*1 $^{fl/fl}$ alleles were bred with Tamoxifen-inducible CAG-Cre/Esr1* mice (Jackson Laboratory: 004453) to generate *Snai*1$^{fl/fl}$; *CAG-Cre* + conditional knockout mice (Yongshun *et al.,* 2014).
*Snai*2$^{+/LacZ}$ mice were obtained from T. Gridley (Jiang *et al, 1998;* Grande *et al*., 2015). *Snai*1$^{+/YFP}$ mice were obtained from Robert Weinberg's lab (Ye *et al*., 2015).
*Snai*1$^{flox/flox}$, *Snai*1$^{+/LacZ}$, *Snai*2$^{+/LacZ}$ and *Snai*1$^{+/YFP}$ mice were bred and maintained on a C57BL/6 genetic background. All mouse work was performed with IACUC approval and in accordance with a protocol approved by University of Michigan Institutional Animal Care & Use Committee.

3.2 Genotyping

Transgenic mice tails were cut (~2 mm) and digested at 95 °C for 30 min in 50 µl of buffer 1 (10 N NaOH and 0.5 M EDTA, pH 12.0). An equal amount of buffer 2 (40 mM Tris-HCl, pH 5.0) was added to neutralize buffer 1. The mixtures were immediately vortexed and centrifuged at 12.000 x*g* for 5 min. The supernatants containing the tail genomic DNA were collected and stored at −20 °C for further use. For genotyping, 1 µl of extracted genomic DNA was used as a template in 20 µl of PCR reaction mixture containing 10 µl 2× GoTaq GreenMaster Mix (Promega), 2.5 µl forward/reverse primers 10 µM and 8.5 µl H_2O. PCR primers for amplifying the indicated mice transgenes are listed in the Table 1.

Table 1. List of oligonucleotides used for the genotyping.

Primers	Description	5'>3' sequence
Snai1-flox	Forward Reverse	CTGCCAGGT GGGAAGGACT CAAGGACATGCGGGAGAAGGT
Snai1-LacZ	Forward Reverse	GCAGCCTCTGTTCCACATACACTTCA GTCTGTTGTACCTCAAAGAAGGTGGC
Snai2-LacZ	Forward Reverse	TCGCCTTCTATCGCCTTCTTG CTATTTGGTTGGTAAGCACATGAG
Snai1-YFP	Forward Reverse	AACCTTCTCCAGAATGTCGCTTCTG TGCAGGTGTATCTTATACACGTGGC

3.3 *In vivo* assay

For the *in vivo* analysis, three-months mice received a pre-emptive dose of the analgesic Carprofen and then were anaesthetized with Isoflurane. Skin adjacent to the tibial anterior muscle was shaved, wiped clear of debris with sterile water, and sterilized with alternating scrubs of Iodine/Betadine and alcohol three times. 25 µl of Bupivacaine 0.5% were injected into the tibialis anterior muscles to induce acute skeletal muscle regeneration through a single intramuscular injection. Following Bupivacaine injection, mice were sacrificed at different time points and the tibialis anterior muscles were dissected, frozen and processed for further analysis.

3.4 *X-Gal* Staining

To detect βGal/LacZ activity, the dissected tibial anterior muscles were fixed in fixative solution (4% formaldehyde, 0.5% glutaraldehyde, 1.25 mM EGTA, 2 mM $MgCl_2$, 0.1M sodium phosphate, pH 7.4), washed in rinse buffer (2 mM $MgCl_2$, 0.2% deoxycholate, 0.2% NP-40. 0.1 M sodium phosphate, pH 7.4) and incubated overnight in X-gal staining buffer (2 mM $MgCl_2$, 0.2% deoxycholate, 0.2% NP-40, 1 mg ml^{-1} X-gal, 5 mM potassium ferrocyanide, 0.1 M sodium phosphate, pH 7.4). After being stained, whole-mount tissues were washed with phosphate buffered saline (PBS), transferred to 70% alcohol and then visualized under a Leica dissecting microscope.

3.5 Muscle embedding and cryosectioning

After dissection, skeletal tibialis anterior muscles were embedded with minimum amount of Tissue-Tek O.C.T (Sakura Finetek USA). The embedded muscles were frozen by placing them into the cooled 2-methylbutane for 5 min and then the muscle samples were transferred to a −80 °C freezer

for storage. Before cryosectioning, the cryostat with the blade was pre-cooled to −22 ± 2 °C. Samples were placed in cryostat for at least 20 min for thermal equilibration, attached on the round metallic holders of the cryostat with Tissue-Tek O.C.T. 10 µm-thick sections were made and collected on room temperature positive charged microscope slides and then stored at −80 °C. These slides were further processed for Hematoxylin and Eosin staining or immunostaining.

3.6 Hematoxylin and Eosin staining

The slides were brought from the −80 °C freezer to room temperature and incubated with hematoxylin solution in a staining jar for 10 min to stain the nuclei. Slides were transferred to a staining jar with running water and then to a staining jar with Eosin solution for 3 min. Successively, the slides were transferred into staining jars with 70% ethanol for 20 sec, 90% ethanol for 20 sec, 100% ethanol for 1 min and xylene for 3 min. Finally, the slides were mounted with xylene-based mounting media and covered with cover slides. Clips were used to press the slides to squeeze bubbles. Hematoxylin and Eosin-stained images were captured with Leica DMI 6000B microscope.

3.7 Tissue Immunostaining

Sections were blocked with 0.5% normal goat serum (Jackson ImmunoResearch Laboratories) in PBST (PBS+0.3% Triton-X100) for one hour at room temperature. Sections were incubated with the anti-GFP primary antibody (Rockland) at 4 °C overnight. After three washes with PBS, sections were incubated with secondary antibody (Biotium) and DAPI for two hours at room temperature, washed three times with PBS and mounted in Prolong gold Antifade reagent (Invitrogen). Immunostained samples were imaged using Zeiss LSM700 confocal microscope.

3.8 Cell culture, differentiation and treatment

The C2C12 myoblasts, an immortalized mouse myoblast cell line established by Yaffe and Saxel (Yaffe *et al.,* 1977) (www.atcc.org), were used as in vitro model for mammalian muscle differentiation. The cells were cultured in Dulbecco's modified Eagle's medium (DMEM) High Glucose medium (EuroClone), supplemented with 2 mM L-Glutamine, 100 µg/ml streptomycin, 100 U/ml penicillin and 20% (v/v) fetal bovine serum (FBS), at 37°C in humidified atmosphere

containing 5% (v/v) CO_2. To induce myotube differentiation, the C2C12 were cultured in DMEM High Glucose, supplemented with 2 mM L-Glutamine, 100 µg/ml streptomycin, 100 U/ml penicillin and 2% (v/v) horse serum (HS).

The primary mouse satellite cells were cultured in DMEM High Glucose supplemented with 2 mM L-Glutamine, 100 µg/ml streptomycin, 100 U/ml penicillin 20% (v/v) fetal bovine serum, 10% (v/v) horse serum and 1% chicken embryo extract (CEE) at 37°C in humidified atmosphere containing 5% (v/v) CO_2.

To induce ER stress, we used Thapsigargin 0.2 µM diluted in dimethyl sulfoxide (DMSO). The control cells were treated only with DMSO.

Lenti-X 293T cell line, a subclone of the transformed human embryonic kidney cell line HEK 293, was used to produce lentivirus particles, since they are highly transfectable and able to support high levels of viral protein expression. Lenti-X 293T cells were grown in the DMEM High Glucose supplemented with 2 mM L-Glutamine, 100 µg/ml streptomycin, 100 U/ml penicillin and 10% (v/v) fetal bovine serum (FBS), at 37°C in humidified atmosphere containing 5% (v/v) CO_2.

3.9 *Fgf21* plasmid construction

Based on the mouse *Fgf21* promoter sequence, specific primers were designed (Table 2) to amplify a full-length promoter, spanning from -1775 bp respect to the transcription start site to +166 bp, and progressively shorter promoter fragments excluding the putative binding sites for SNAI1, previously identified by bioinformatic analysis. In total, four promoter fragments were amplified by PCR from *Mus musculus* genome using the Q5® High-Fidelity DNA Polymerase (BioLabs), cloned into the pGL3-Basic vector (Promega) (Figure 11) and named as follows: -1775, -1681, -1091 and -926.

Table 2. List of oligonucleotides used for the amplification of the *Fgf21* promoter region.

***Fgf21* promoter fragments**	**Primers for amplification**	**5'>3' sequence**
-1775	Forward A160 Reverse A164	GGGGTACCATGCTCTGGGAGTAGCCACG GCTCTAGACAGGGCTGCGCTCCGTTCGG
-1681	Forward A161 Reverse A164	GGGGTACCGGAGGATGGAGAACCTGTTT GCTCTAGACAGGGCTGCGCTCCGTTCGG
-1091	Forward A162 Reverse A164	GGGGTACCACCCCCCAAAGCATCTGGAG GCTCTAGACAGGGCTGCGCTCCGTTCGG
-926	Forward A202 Reverse A164	GGGGTACCGGGCTGAGGACTCCTCTTACAC GCTCTAGACAGGGCTGCGCTCCGTTCGG

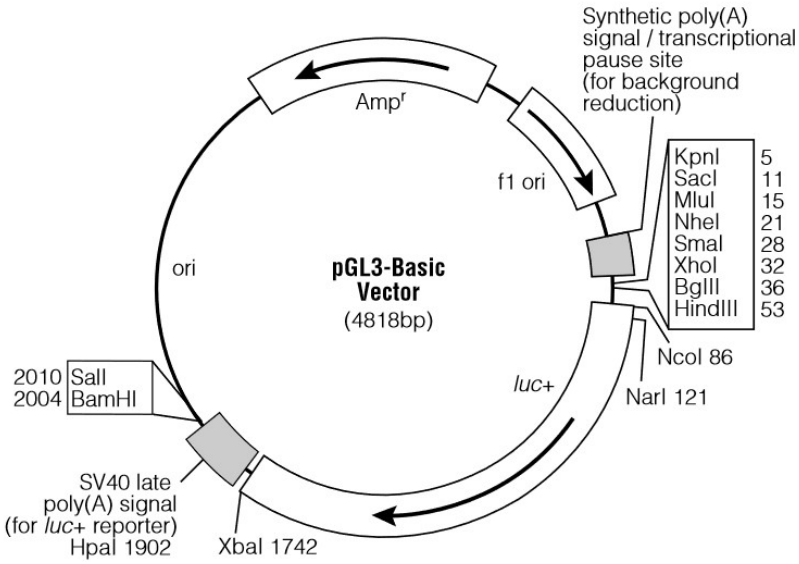

Figure 11. pGL3-Basic vector circle map. Graphic representation of the pGL3-Basic vector used for cloning. Additional description: luc+ (cDNA encoding the modified firefly luciferase); Amp^r (gene conferring ampicillin resistance in *E. coli*); f1 ori (origin of replication derived from filamentous phage); ori (origin of replication in *E. coli)*.

The four promoter fragments and the pGL3-Basic vector were digested with KpnI-HF/XbaI and KpnI-HF/NheI-HF restriction enzymes (NEB), respectively and then ligated by using the T4 DNA ligase (NEB). The ligation reaction was precipitated by adding 0.1 volumes of Sodium Acetate (3M, pH 5.2) and 2.5 volumes of 95% (v/v) ethanol. The DNA was resuspended in 5 µl of deionized sterile water and transformed into DH5α E. *coli* stain.

3.10 Site directed mutagenesis

The point-mutations on the -926 *Fgf21* promoter E-boxes were introduced by using the *QuickChange XL Site-Directed Mutagenesis* kit (Agilent), according to manufacturer's instructions. The primers used for PCR amplification are listed in Table 3.

Table 3. List of oligonucleotides used for the mutagenesis of the -926 *Fgf21* promoter region.

***Fgf21* promoter point-mutants**	**Primers fo amplification**	**5'>3' sequence**
-926 m1	Forward A210 Reverse A211	GAACACAATTCCAGCAAGCTTGGCTCCTCAGCC GGCTGAGCAGCCAAGCTTGCTGGAATTGTCTTC
-926 m2	Forward A218 Reverse A219	GACAGCCTTAGTGTCTTCTAGACTGGGGATTCAACACAGG CCTGTGTTGAATCCCCAGTCTAGAAGACACTAAGGCTGTC
-926 m3	Forward A208 Reverse A209	TCAGGAGTGGGGAGGATCCGTGGGCGGGCCTGT ACAGGCCCGCCCACGGATCCTCCCCACTCCTGA

The primers were designed in order to obtain point-mutations of the E-boxes 1, 2, and 3, surrounding the TSS (see Figure 25), in the construct carrying the -926 *Fgf21* promoter. To easily identify mutated clones, E-boxes were mutated by inserting the restriction sites for the enzymes HindIII (A210-A211), XbaI (A218-A219) or BamHI (A208-A209). After PCR amplification, the *Dpn*I endonuclease was used to digest the methylated parental DNA template allowing the selection of the mutation-containing PCR-synthesized plasmids. The nicked vector DNA containing the desired mutations was then transformed into XL10-Gold Ultracompetent Cells.

3.11 *Atf3* plasmid construction

The full length of *Atf3* promoter (-1943) and a deletion fragment excluding putative binding sites for SNAI1 (-1235) were generated by PCR amplification of *Mus musculus* genome. Considering the difficulty in cloning *Atf3* promoter directly into the pGL3-Basic vector, the -1943 and -1235 fragments were cloned using the pCR®-Blunt II-TOPO® system (Invitrogen), within which successively was cloned the fragment Luc+-SV40 late poly(A) signal, derived from the pGL3-Basic vector.

Table 4. List of oligonucleotides used for the amplification of the *Atf3* promoter region.

***Atf3* promoter fragments**	**Primers for amplification**	**5'>3' sequence**
-1943	Forward A173 Reverse A175	GGGGTACCATTTATTCCAGGGCAGCCTG GCTCTAGATTAGCCGATTGGCTCCACTG
-1235	Forward A174 Reverse A175	GGGGTACCGCAGTCTGTGCACGTGTAAC GCTCTAGATTAGCCGATTGGCTCCACTG

After the amplification, the PCR products were cloned into pCR®-Blunt II-TOPO® (Figure 12), using the Zero Blunt® TOPO® PCR Cloning kit (Invitrogen). The plasmid constructs were digested with NotI-HF restriction enzyme (NEB), purified by means of QIAquick PCR purification kit (QIAGEN), and blunt ends were generated by means of Large (Klenow) Fragment (NEB).

At the same time, the fragment Luc+-SV40 late poly(A) signal was obtained by digesting the pGL3Basic vector with XhoI and BamHI (NEB) restriction enzymes, separated by agarose gel electrophoresis and extracted from the 1% agarose gel by means of QIAquick gel extraction kit (QIAGEN). Successively, blunt ends were obtained as above. Then, the fragment Luc+-SV40 late poly(A) signal was inserted into the pCR®-Blunt II-TOPO® promoter constructs by ligase reaction with T4 DNA ligase (NEB). Subsequently, DNA was precipitated as described above and used to transform the DH5α *E. coli* strain.

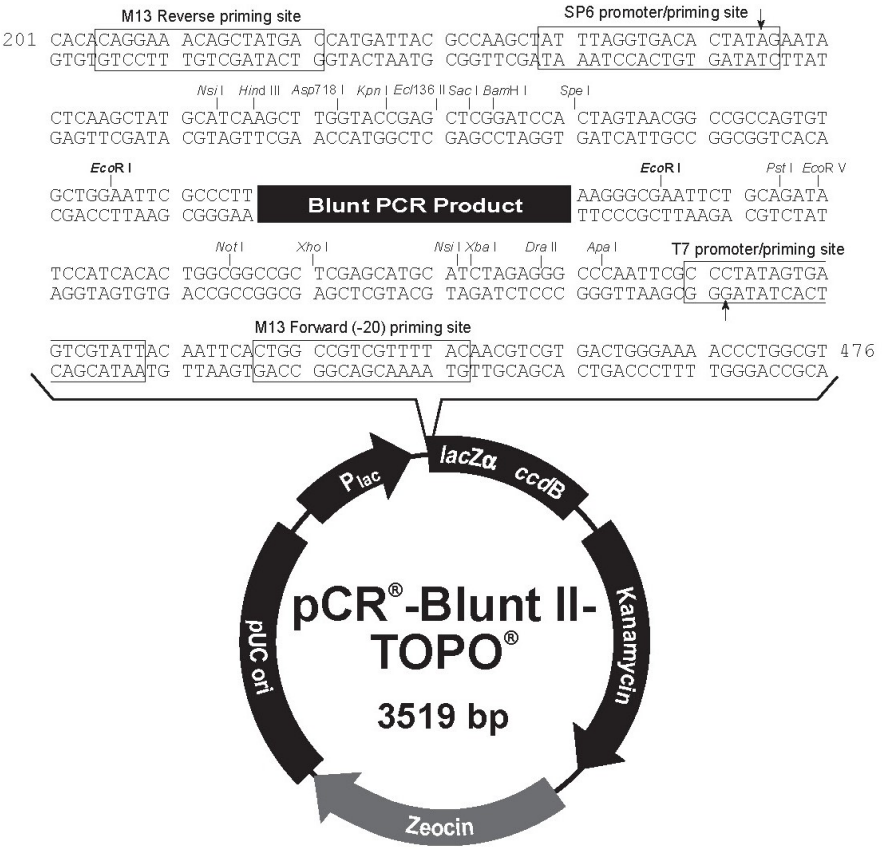

Figure 12. pCR-Blunt II-TOPO vector. Graphic representation of the pCR-Blunt II-TOPO vector, where *Atf3* promoter has been cloned adding the fragment Luc+-SV40 late poly(A) signal, derived from pGL3-Basic vector.

3.12 Expression vectors

The pCMV6 expression vectors for murine ATF3 and SNAI1 (OriGene) were used in experiments of co-transfection and pCMV6-Entry vector was used as control (Figure 13).

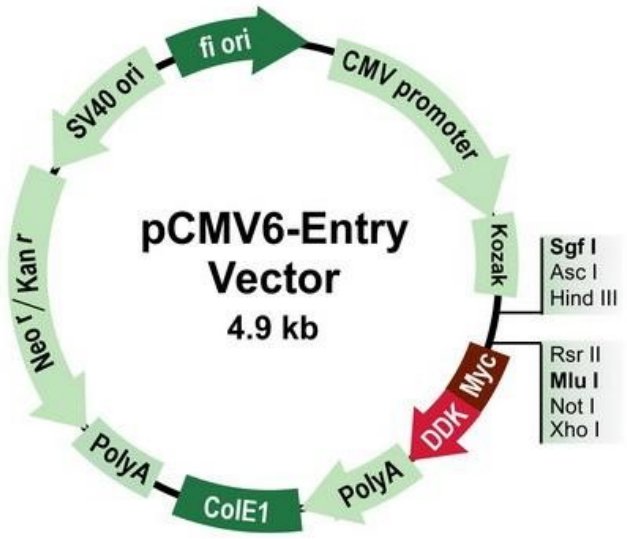

Figure 13. pCMV6-Entry vector. A mammalian vector with C-terminal Myc- DDK Tag, containing cDNA clones. In this vector, a TrueORF sequence is fused with a MYC/DDK tag at its carboxy terminus. The antibiotic selection marker for *E. coli* is kanamycin (25µg/ml), and neomycin (G418) for mammalian cells. The small dual tags facilitate the detection and purification of the ORF product with anti-Myc or anti-DDK antibody.

3.13 Bioinformatic analysis

The GC content of the *Atf3* promoter sequence was assessed with the GC Content Calculator (https://www.biologicscorp.com/tools/GCContent/). GC content is usually calculated as a percentage value and sometimes called G+C ratio or GC-ratio. GC-content percentage is calculated as Count (G + C) / Count (A + T + G + C) * 100% in a defined window of nucleotides.

3.14 Plasmid DNA preparation

For the mini preparation of plasmid DNA, the NucleoSpin® Plasmid (Macherey-Nagel) kit was used according to manufacturer's instructions. The protocol provides essentially three steps: cell lysis, plasmid DNA binding to a silica resin and washing step following by the plasmid DNA elution. For a greater plasmid production, the midi preparation of plasmid DNA was used the NucleoSpin® Xtra plasmid purification kit (Macherey-Nagel), according to manufacturer's instructions.

3.15 Transfection

C2C12 cells were transfected using Attractene Transfection Reagent (Qiagen), a non-liposomal lipid that ensures highly efficient DNA transfection of all adherent eukaryotic cells.
C2C12 cells were seeded at a density of $9x10^4$ cells/well in 6-well culture plate and grown 24 hours. Before proceeding with transfection, the media was replaced with fresh media and 0.8 µg of luciferase reporter vector, 0.4 µg of the pCMV6 expression vectors (for SNAI1, ATF3 or empty vector), 0.025 µg of *Renilla* luciferase control vector (pNL1.1 TK[*Nluc*/TK]; Promega) and 4.5 µl of Attractene were added into 100 µl of DMEM and incubated for 15 minutes at room temperature. The transfection complexes were added to the cells, that were incubated with the transfection complexes under their normal growth condition. After 24 hours, the growth medium was removed from the cultured cells and replaced with 2 ml of differentiation medium when necessary. The day after, the cells were assayed for the expression of the transfected gene.

3.16 Dual-luciferase reporter assay

Following transfection, the cells were harvested in Passive Lysis Buffer (Promega) and the luciferase activity of the samples was measured by the Nano Dual-luciferase report™ assay system (Promega), following the manufacturer's instructions. Luciferase activity was normalized to the *Renilla* luciferase internal control.

3.17 C2C12 transfection by electroporation

C2C12 transfection by electroporation was used to overexpress SNAI1 in order to analyze *Fgf21* and *Atf3* expression and to perform ChIP assay. C2C12 cells were trypsinized and 2.0 x 10^6 cells/point were centrifuged three times for 5 minutes, at 190 xg with DMEM/F12 supplemented with 2.5% (v/v) FBS and 0.25% (w/v) bovine serum albumin (BSA). Then, the cells were resuspended in 200 μl of the same DMEM/F12 used for washing, and 10 μg of DNA (pcMV6-entry vector or pcMV6- SNAI1) were added. Each mix was put into an electroporation cuvette (Gene Pulser electroporation cuvette, Gap Width 0.2 cm, Bio-Rad). Electroporation was performed using the following parameters: 290 V, 1.000 µF, 200 Ω. After the electroporation, the cuvette content was resuspended with pre-warmed complete C2C12 medium and plated in six-wells dishes. 24 hours later the medium was changed, and after other 24 or 48 hours the cells were harvested for the analyses.

3.18 ChIP-qPCR

For the ChIP-qPCR analysis, we used the CUT&RUN Assay Kit (Cell Signaling**)** following the manufacturer instructions. Cleavage Under Target & Release Using Nuclease (CUT&RUN) is a new technology that can be used for chromatin profiling.

Briefly, to isolate the protein-DNA complex of interest, C2C12 cells transfected with pCMV6 or pCMV6-SNAI1 were first trypsinized, centrifuged and the pellet was resuspended in wash buffer containing spermidine and protease inhibitor cocktail. The input samples were collected at this time while the other cells were bound to Concanavalin A-coated magnetic beads. Cell membranes were permeabilized with digitonin to facilitate the entry of the primary antibody (FLAG M2, Sigma Aldrich) into the nuclei. At this point, the primary antibody could bind the transfected FLAG-tagged SNAI1. The pAG-MNase enzyme, a fusion of Protein A and Protein G to Micrococcal Nuclease, was then added to the reaction mixture, where it bound the primary antibody heavy chain, targeting the enzyme to the chromatin region of interest. The pAG-MNase was activated with the addition of Ca^{2+} in order to initiate DNA digestion around the target protein on the chromatin. The digestion products were about 200 bp in size. This allowed the cleaved chromatin complex to diffuse away from the genomic chromatin, out of the nuclei, into the sample supernatant (Figure 14). Then the digestion was stopped with the Stop Buffer containing digitonin, RNAse A and Spike-in DNA. The Sample Normalization Spike-In DNA is fragmented genomic DNA from the yeast *S. cerevisiae* that facilitate normalization between samples and between experiments during qPCR analysis.

At the end, input and enriched chromatin samples were collected with the phenol/chloroform extraction followed by ethanol precipitation. The purified, enriched DNA was quantified by qPCR with QuantiTec SYBR Green PCR Master Mix (Qiagen), following the manufacturer instructions, and results were analyzed using the Percent Input Method (Haring *et al.,* 2007). qPCR amplification reaction of Spike-In DNA was performed for sample normalization and were analyzed using the Percent Input Method (Haring *et al.,* 2007). Signals obtained from each immunoprecipitation were expressed as a percent of the total input chromatin.

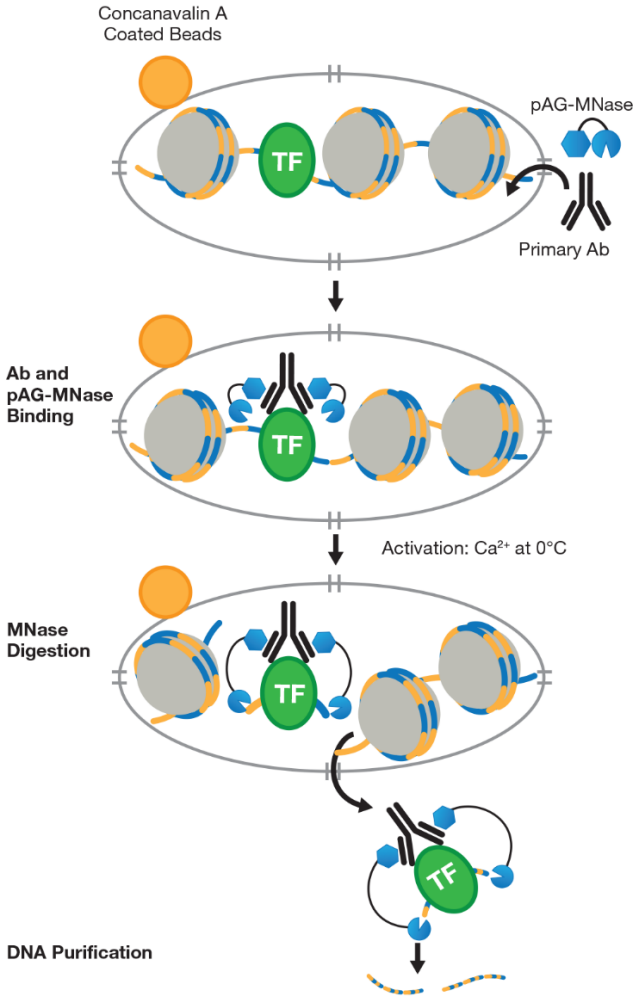

Figure 14. Schematic representation of the CUT&RUN technology. CUT&RUN works by using the DNA cutting activity of a Protein A fused micrococcal nuclease (MNase) to specifically isolate DNA that is bound by a protein of interest. First, nuclei from tissue or cell culture are isolated using Concavalin A-coated magnetic beads. Nuclei are then incubated with a primary antibody against the protein of interest. The Protein A fused MNase is then added and Protein A binds Immunoglobulin G (IgG) thus targeting MNase to antibody bound proteins. Once MNase has been localized to target sites, the nuclease is briefly activated to digest the DNA around the target protein. This targeted digestion is controlled by the addition of calcium, which MNase requires for its nuclease activity and is chelated from the reaction up until this point. After MNase digestion, fragments are released from nuclei by a short incubation at 37 °C. These short DNA fragments can then be purified for subsequent analysis.

Table 5. List of oligonucleotides used for the *Fgf21* ChIP.

***Fgf21* ChIP sites**	**Primers for amplification**	**5'>3' sequence**
E-Box Cluster A	Forward A186 Reverse A187	AGATGCTCTGGGAGTAGCCA CGGGGTACGAAGAAGAAGCA
E-Box Cluster B	Forward A190 Reverse A191	GGACGCTGTCTGGTGAAAGA CCTCACCAACCCCTGCTTAG
E-Box Cluster C	Forward A194 Reverse A195	GCTGGGGATTCAACACAGGA AGGGATGGGTCAGGTTCAGA
Exon 2 CTRL	Forward A198 Reverse A199	AGGTTCCTGCCAAGTGTGTC TCCTGTGTTGAATCCCCAGC

Table 6. List of oligonucleotides used for the *Atf3* ChIP.

***Atf3* ChIP sites**	**Primers for amplification**	**5'>3' sequence**
-1873	Forward A325 Reverse A326	AAAAGATGGGGCAGGTAGGAG GGCACAACCCCGAAGAAAG
-1257	Forward A321 Reverse A322	CTTTACACCTCAGCGTCCTG GACTGCGGCCCAGGAAT
-607	Forward A332 Reverse A333	TACGTTAACCCACAGCTGCTA CTCCGATGAATCCACACCGT
Exon 1 CTRL	Forward A329 Reverse A330	CATCCATCACTTCTTGTCCCG GCCTCTACGCGGACTTAGG

3.19 RNA extraction and RT-qPCR

Total RNA was extracted from C2C12 cells by using RNeasy® Plus Mini Kit (Qiagen), according to manufacturer's instruction.

Total RNA was quantified through QIAxpert by measuring the UV/VIS absorption spectrum and used to evaluate the gene expression by means of RT-qPCR (Reverse Transcription quantitative Polymerase Chain Reaction). In our experiments, the kit Brilliant III Ultra-Fast SYBR Green RT-qPCR Master Mix (Agilent Technologies) was used. Primers for RT-qPCR are shown in Table 7.

Table 7. Primers used for the RT-qPCR analysis.

Name	Use	5'>3' sequence
O1029	RT-qPCR forward *Fgf21*	ACCAAGCATACCCCATCCCT
O1030	RT-qPCR reverse *Fgf21*	GCTTCAGTGTCTTGGTCGTCAT
O986	RT-qPCR forward *Atf3*	AGACAGAGTGCCTGCAGAAAGA
O987	RT-qPCR reverse *Atf3*	TCCGGTGTCCGTCCATTCTGA
N268	RT-qPCR forward *Snai1*	TTGGGCCAACTTCCCAAGCA
N270	RT-qPCR reverse *Snai1*	AGGAAGGCCTTTCCACAGGT
H237	RT-qPCR forward *Gapdh*	GGTCACCAGGGCTGCCATTG
H238	RT-qPCR reverse *Gapdh*	TTCCAGAGGGGCCATCCACAG
0611	RT-qPCR forward *MyoD*	CGGAGTGGCAGAAAGTTAAGACGA
0612	RT-qPCR reverse *MyoD*	AAAAGCGCAGGTCTGGTGAGT
0615	RT-qPCR forward *Pax7*	GTTTCCCATGGTTGTGTCTCCAAG
0617	RT-qPCR reverse *Pax7*	TTCTGAGCACTCGGCTAATCGAAC

3.20 Western blot analysis

The total protein extraction was performed as described below: once removed the medium, cells were washed twice with phosphate buffered saline (PBS) (pH 7.4) and lysed in RIPA buffer (50 mM Tris-HCl pH 7.2, 100 mM NaCl, 1% (v/v) Triton X100. 1% (w/v) deoxycholic acid, 0.1% (w/v) SDS, 50 mM NaF, 2 mM EDTA) freshly supplemented with anti-protease cocktail (Sigma Aldrich); then, by means of a scraper, cells were mechanically removed from the plate and collected in 1.5 ml centrifuge tube. The samples were sheared using Diagenode's Bioruptor 300 at HIGH setting, 5 cycles of 30 seconds and centrifuged at 16200 xg, for 5 minutes at 4°C. Finally, the supernatant was recovered and stored at -20°C. The protein concentration in each sample was measured by using Pierce™ BCA Protein Assay Kit (Thermo Fisher). After quantification, proteins were diluted in Sample Buffer (50 mM Tris-HCl pH 6.8, 2% (w/v) SDS, 1.5% (w/v) DTT, 10% (w/v) glycerol, 0.02% (w/v) bromophenol blue) and incubated at 95°C for 5 minutes to allow the complete protein denaturation. Cell lysates in sample buffer with equivalent concentration of total proteins were separated on SDS-polyacrylamide gel and transferred onto a Polyvinylidene fluoride (PVDF) membrane (GE Healthcare Life Science). Subsequently the membrane was blocked in a PBS solution containing 5% (w/v) non-fat dry milk and 0.1% (v/v) Tween-20, by gentle shaking for 1 hour at room temperature, and incubated overnight at 4°C with specific primary antibodies. The day after, the membranes were

washed 3 times (15 min) with PBS solution containing 0.1% (v/v) Tween-20 (PBS-T) and incubated for 1 hours at room temperature with the species-specific horseradish peroxidase-labelled secondary antibodies. Finally, the membranes were washed 4 times (15 min) with PBS-T. The membranes were reacted with chemiluminescent substrate (Luminata Crescendo Western HRP Substrate; Millipore) and blots were visualized by means of the instrument ImageQuantTM LAS 4000 (GE Healthcare). Primary and secondary antibodies, with respective working concentrations, were reported in Table 8.

Table 8. Primary and secondary antibodies used in the Western blot analysis.

Primary antibodies	Isotype	Concentration	Source
Anti-ATF3	Rabbit	1:1000	SCBT
Anti-Histone H3	Rabbit	1:1000	Abcam
Anti-Flag M2	Mouse	1:1000	Sigma
Anti-SNAI1	Rabbit	1:1000	Cell Signaling
Anti-MyoD1	Mouse	1:500	DAKO
Anti.Myogenin	Rabbit	1:1000	SCBT
Anti-P21	Rabbit	1:1000	BD-Pharmigen
Anti-Pax7	Rabbit	1:500	Abcam
Anti-SNAI2	Rabbit	1:1000	Cell Signaling
Anti-FGF21	Rabbit	1:1000	Abcam
Secondary antibodies	**Conjugated**	**Concentration**	**Source**
Anti-rabbit	HRP	1:5000	GE Healthcare Life Science
Anti-mouse	HRP	1:4000	GE Healthcare Life Science

3.21 SNAI1 CRISPR-Cas9 editing

In order to obtain SNAI1 editing in the C2C12 cell line, the plasmid LentiCRISPRv2 (pLCv2) (Addgene plasmid #52961) (Figure 15) was used. It contains two expression cassettes, hSpCas9 and the chimeric guide RNA. The vector was digested using the restriction enzyme BsmBI (NEB) and a pair of annealed synthetic oligonucleotides was cloned into the single guide RNA scaffold. The oligonucleotides were designed based on a target site sequence of 23 bp.

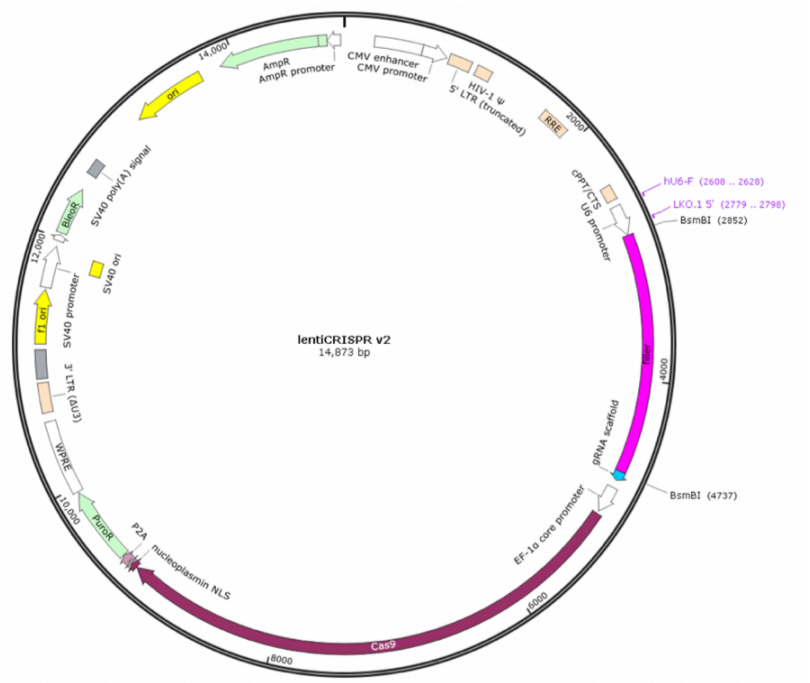

Figure 15. LentiCRISPR v2 plasmid. The 14873 bp long LentiCRISPRv2 (pLCv2) presents the restriction sites for BsmBI located at 2852 bp and 4737 bp, for the removal of the "filler" DNA sequences and its substitution with the target sequence of interest to generate the gRNA. The "filler" DNA sequences is located between the U6 promoter for the synthesis of the gRNA and the gRNA scaffold sequence necessary for Cas9 binding. This vector carries the Cas9 gene under the control of the EF- 1alpha core promoter, the ampicillin and puromycin resistance gene (Amp R and Puro R) and the sequences for lentiviral particle packaging (3' LTR and 5'LTR).

The online tool CHOPCHOP (https://chopchop.cbu.uib.no/) was used to design the sgRNAs (sgRNA-1, 2 and 3). The sequences of the oligonucleotide couples obtained by the software are listed below (in black is reported the target sequence, while in red the sequences of the BsmBI site with the two overhangs (5'-CACC-3' on the forward, 5'-AAAC-3' on the reverse strand) necessary to clone the double stranded oligonucleotides in the pLCv2 vector digested by BsmBI. Three couples of oligonucleotides have been tested as sgRNA and are listed in the Table 9.

Table 9. List of oligonucleotides used for the CRISPR-Cas9 sgRNA.

sgRNA	Description	5'>3' sequence
sgRNA-1	Forward Reverse	CACCGTTGAAGATCTTCCGCGACTGGGG AAACCCCCAGTCGCGGAAGATCTTCAAC
sgRNA-2	Forward Reverse	CAAACCCCTCCGCCCGAGGTCCTCAACCC ACCGGGTTGAGGACCTCGGGCGGAGGG
sgRNA-3	Forward Reverse	CACCGCGCTATAGTTGGGCTTCCGGCGG AAACCCGCCGGAAGCCCAACTATAGCGC

The oligonucleotide pairs (100 pmol of each oligonucleotide in 1X NEB buffer 2; 5 mM NaCl, 1 mM Tris-HCl, 1 mM MgCl2, 0.1 mM DTT, pH 7.9) were annealed in a thermocycler at 95° C for 5 min and then ramp down to 25 °C at 5°C/min. In order to ligate the annealed oligonucleotides in the digested vector, 200 ng of pLCv2 and 100 pg of annealed oligonucleotides were incubated overnight at 16 °C in 1x T4 DNA Ligase Reaction Buffer (50 mM Tris-HCl, pH 7.5; 10 mM MgCl2; 1 mM ATP; 10 mM DTT) with 1 µl of T4 DNA ligase enzyme (NEB). Finally, the ligation products were concentrated by standard ethanol precipitation and resuspended in 15 µl of sterile MilliQ water. To allow plasmid DNA amplification, the ligation products were transformed in competent *E. Coli* bacteria cells by electroporation using the following parameters: 2000 V, 25 µF, 200 Ω in Gene Pulser electroporation cuvette, gap width 0.1 cm, (Bio-Rad). After electroporation, the bacteria were incubated at 37 °C in rotation for 1 hour and then the solution from each tube was spread on a LB agar plate, containing 100 µg/ml ampicillin and incubated at 37°C overnight.
The day after, bacterial colonies were picked to check for the proper sgRNA insertion. Each single colony was inoculated into a 3ml LB medium culture containing 100 µg/ml ampicillin, at 37°C. The sequence of the plasmid was analyzed for the presence of sgRNA by sequencing service (Eurofins genomic).

3.22 Lentiviral particle production

For viral packaging pRSV-Rev, pMDLG/pRRE, and pMD2.VSVG plasmids were co-transfected with a lentiviral transfer plasmid. pMDLg/pRRE plasmid contains HIV-1 gag/pol genes, which provide structural proteins and reverse transcriptase. pRSV-Rev encodes Rev which binds to the RRE for efficient RNA export from the nucleus. pMD2.VSVG encodes the vesicular stomatitis virus glycoprotein (VSV-G) that replaces HIV-1 Env. VSV-G expands the tropism of the vectors and allows concentration via ultracentrifugation. All the genes encoding the accessory proteins, including Vif, Vpr, Vpu, and Nef are excluded in the packaging system. For the RNA interference-mediated

knockdown of SNAI1, we used the lentiviral transfer plasmid pLKO.1 from the TRC shRNA library (Open Biosystems) expressing specific shRNA for mouse SNAI1 (Table 10).

Table 10. List of shRNA used for the mouse SNAI1 knockdown.

shRNA	5'>3' sequence
shRNA-1	CCGGCCACTCGGATGTGAAGAGATACTCGAGTATCTCTTCACATCCGAGTG GTTTTTG
shRNA-2	CCGGGCAAATATTGTAACAAGGAGTCTCGAGACTCCTTGTTACAATATTTG CTTTTTG

For the SNAI1 CRISPR-Cas9 gene editing we used the lentiviral transfer plasmid pLCv2 with the sgRNA mentioned above.

To transfect Lenti-X 293T cell line, the TransIT-VirusGen Transfection kit (Mirus) was used according to manufacturer's instructions. For each transfection 1.5 μg of pMD2.VSVG, 2.4 μg of pMDLG/pRRE and 1.2 μg of pRSV-Rev were mixed and added to 5.1 μg of lentiviral transfer plasmid DNA. The mix (virus packaging-DNA) were transferred in a sterile tube containing 1 ml of Optimem (GIBCO), and 30 μl of Transit reagent were added and gently mixed. To allow the formation of transfection complexes, the mixture was incubated 20 minutes at room temperature, and subsequently added drop-by-drop on 80% confluent Lenti-X 293T cell line. An extra sample was transfected with GFP-expressing lentiviral transfer plasmid (pCCLsin.PPT.hPGK.GFPpre) to check the transfection and transduction efficiency by means of the fluorescence signal. At 24 and 48 h post-transfection, supernatants of Lenti-X 293T cells containing the lentiviral particles were transferred in a 50 ml centrifuge tube. The medium was filtered by using 0.45 μm filters, aliquoted and stored at -80°C.

3.23 C2C12 transduction

C2C12 cells were plated in 6-well plates at a concentration of $9.6x10^4$ cells per well. After 24 hours, the culture medium was replaced with 1 ml of complete C2C12 medium, 1 ml of Lenti-X 293T supernatant containing lentiviral particles and 2 μg of polybrene (Hexadimethrine bromide), per well. After 24 hours, medium was changed, and after other 48 hours, puromycin (2 μg/ml) selection was started for C2C12 cell carrying pLCv2-sgRNA 1, 2 or 3 or analyzed through western blot or transcriptome analysis for cells carrying the pLKO.1-shRNA 1 or 2. The drug was added at each medium change or cell passage. In such way, only cells that have integrated in the genome the

lentiviral genome of the pLCv2-sgRNA 1, 2 and 3, containing the puromycin resistance gene, survived and grew during and after the treatment. After 3 weeks of selection, western blot was performed to check the editing efficiency.

3.24 Immunofluorescence

Immunofluorescence was used to measure cell proliferation ability of SNAI1 knockout and control cells. C2C12 cells were fixed with 4% paraformaldehyde for 20 min at room temperature, permeabilized and incubated at 4°C with the primary mouse antibody anti-Ki-67, conjugated with Alexa Fluor® 647 (Santa Cruz Biotechnology). Total nuclei were detected by subsequent 4′,6-diamidino-2phenylindole (DAPI) staining. Images were captured with a Leica confocal microscope.

3.25 Statistical analysis

The data analysis was performed using Prism 6 statistical software (GraphPad Software Inc., San Diego, CA). Significance was estimated by one-way or two-way ANOVA. The significant differences were estimated using Tukey's multiple comparison test (*, $p < 0.05$; **, $p < 0.01$; ***, $p < 0.001$; ****, $p < 0.0001$). Student's t test was used to confirm significant differences between treatments. Two-tailed probabilities of less than 0.05 were considered significant.

4. AIM OF THE THESIS

SNAI1 and SNAI2 transcription factors are well known for their role as regulators of the epithelial-mesenchymal transition that increases the capacity of tumor cells to metastasize. However, much less is known about their role as mediators of differentiation and tissue homeostasis. Recent studies have shown SNAI1 and SNAI2 as repressors of muscle differentiation, with the function of maintaining myoblasts in an undifferentiated state, during the proliferative phase (Soleimani *et al*., 2012). The aim of this thesis was to identify new SNAI1 target genes and promoter binding sites in myoblasts to clarify their role in myogenesis.

5. RESULTS

5.1 SNAI1 and SNAI2 are upregulated during early stages of skeletal muscle regeneration

It has been recently reported that SNAI1 and SNAI2 are expressed in proliferating myoblasts *in vitro* (Soleimani *et al.,* 2012). To evaluate their expression during myogenesis *in vivo*, experiments were performed in collaboration with the Prof. Libero Vitiello. We injected the myotoxic agent Bupivacaine in mouse tibialis anterior muscles and analyzed their mRNA and protein levels at different muscle regeneration stages. Muscle regeneration after an acute Bupivacaine-induced degeneration is a useful *in vivo* experimental model for studying factors involved in muscle differentiation and muscle plastic adaptation to functional demand (Galvagni *et al.,* 2002). Regeneration requires the activation of undifferentiated satellite cells, which proliferate, differentiate into myoblasts expressing muscle-specific markers, fuse into myotubes, and finally mature into myofibers. After Bupivacaine injection in adult mouse tibialis anterior muscle, inflammatory response and mononuclear cell proliferation were most active within 1–4 days of injection (Zink *et al*., 2002). Myogenic cell differentiation and new myotube formation were observed ~5–6 days post injection. 10 days after the injection, the overall architecture of the muscle was restored, although most regenerated myofibers were smaller and displayed central myonuclei (Figure 16A). We therefore analyzed the expression of SNAI1 and SNAI2 at early time points after Bupivacaine treatment. Protein level of both SNAI transcription factors were induced early in regenerating muscle at 2-4 days after the injury, corresponding with the maximum activation of satellite cells, as defined by MyoD expression (Figure 16B). SNAI1 and SNAI2 expression rapidly decreased at day 6, at the beginning of myotubes differentiation program, as defined by the maker Myh3 (embryonic skeletal muscle myosin heavy chain), appearing concurrently with the decline of MyoD expression. *Snai1* and *Snai2* induction was also confirmed at mRNA level by RT-qPCR (Figure 16C). These results suggested a role of SNAI1 and SNAI2 during the early stages of muscle regeneration.

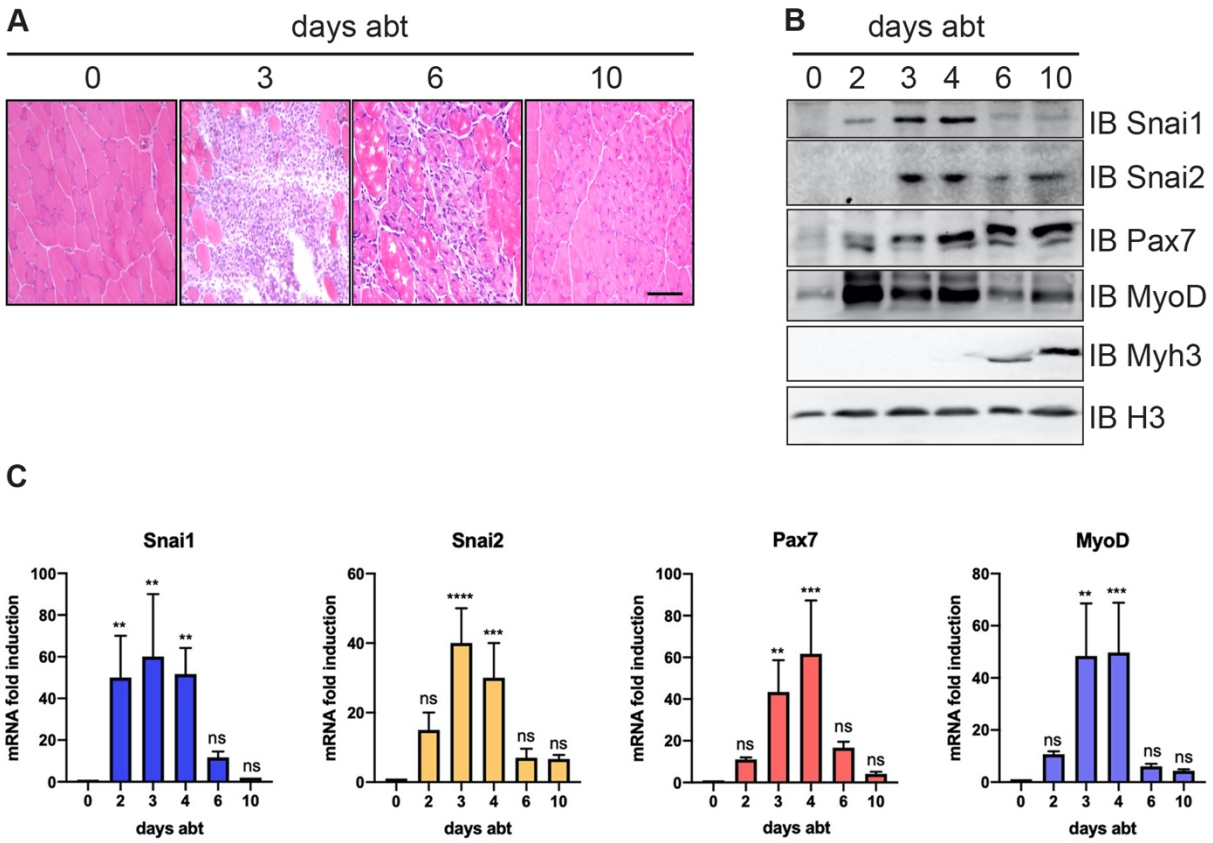

Figure 16. Expression of SNAI proteins and mRNA during muscle regeneration. A) Eosin-hematoxylin staining of cross-sections from tibialis anterior muscles at day 0 (untreated), 3, 6 and 10 after Bupivacaine treatment (abt). Bar, 50 µm. B) SNAI1 and SNAI2 protein expression was detected by Western blot analysis of whole extracts prepared from regenerating muscles at the indicate days abt. Histone H3 expression was used to confirm equal loading. Pax7, MyoD and Myh3 expression was detected as control of satellite cell-derived myoblasts proliferation and differentiation. C) Quantitative evaluation of *Snai1* and *Snai2* transcripts in regenerating muscle by reverse transcription quantitative PCR (RT-qPCR). *MyoD* and *Pax7* transcripts were measured as muscle regeneration control. The values normalized to the glyceraldehyde-3-phosphate dehydrogenase (*Gapdh*) mRNA levels are expressed as the mean ± SD of 3 independent experiments. Asterisks indicate significant differences (p-values) between expression in untreated muscle (0) and each time point after Bupivacaine treatment (abt). Data were evaluated using the one-way analysis of variance ANOVA: **** = P< 0.0001, *** = 0.0001<P< 0.001, ** = 0.001<P< 0.01, ns = not statistically significance.

5.2 *Snai1* and *Snai2* are expressed in myoblasts during muscle regeneration

Several factors act in concert to guide muscle repair, however the role of SNAI family members need to be clarified. While muscle regeneration occurs, satellite cells are activated, proliferate and differentiate to form multinucleate myofiber (Hang *et al*., 2013). To examine *in situ* the expression of *Snai1* and *Snai2* during muscle regeneration, experiments were performed in collaboration with the Medical Doctor Stephen J. Weiss. Muscle injury was induced by intramuscular injection of Bupivacaine into the tibialis anterior muscle of *Snai1*$^{+/LacZ}$ and *Snai2*$^{+/LacZ}$ knock-in mice. *Snai1*$^{+/LacZ}$ and *Snai2*$^{+/LacZ}$ is a system in which the *lacZ* reporter gene, with a nuclear localization signal, is under

the control of the *Snai*1 and *Snai*2 promoters allowing us to evaluate their expression through the measurement of the nuclear β-galactosidase activity. Using this system, β-galactosidase was observed in the tibialis anterior muscles 4 days after Bupivacaine injection, when activated satellite cell progeny undergoes to population expansion (Figure 17A).

Furthermore, using *Snai1*$^{+/LacZ}$ knock-in mice, *Snai1* was detected in the tibialis anterior muscles 3-4 days after Bupivacaine injection and its expression decreased at 6-10 days (figure 17B). We also observed the cytoplasmatic YFP expression at day 4 after the Bupivacaine injection in *Snai1*$^{+/YFP}$ knock-in transgenic mice but not in the untreated muscle (Figure 17C). Using *Snai2*$^{+/LacZ}$ knock-in mice, β- galactosidase activity was observed in the tibialis anterior muscles at 3-4-6 days and its activity decreased 10 days after the injury (Figure 17D). This confirms our previous data and suggests that *Snai1* and *Snai2* could play a role during muscle regeneration. It is necessary to confirm in which cell type *Sna1* and *Snai2* are expressed during muscle regeneration. Our data make us suppose that *Snai1* and *Snai2* are expressed in proliferative satellite cells (3-4 days after injury) and their expression decreases when myoblasts start to terminally differentiate. Moreover, *Snai2* is highly expressed at day 6, when its expression is not in the myofibers. This indicates that it could also have a role at the beginning of the satellite cells differentiation or in other cell types involved in muscle regeneration.

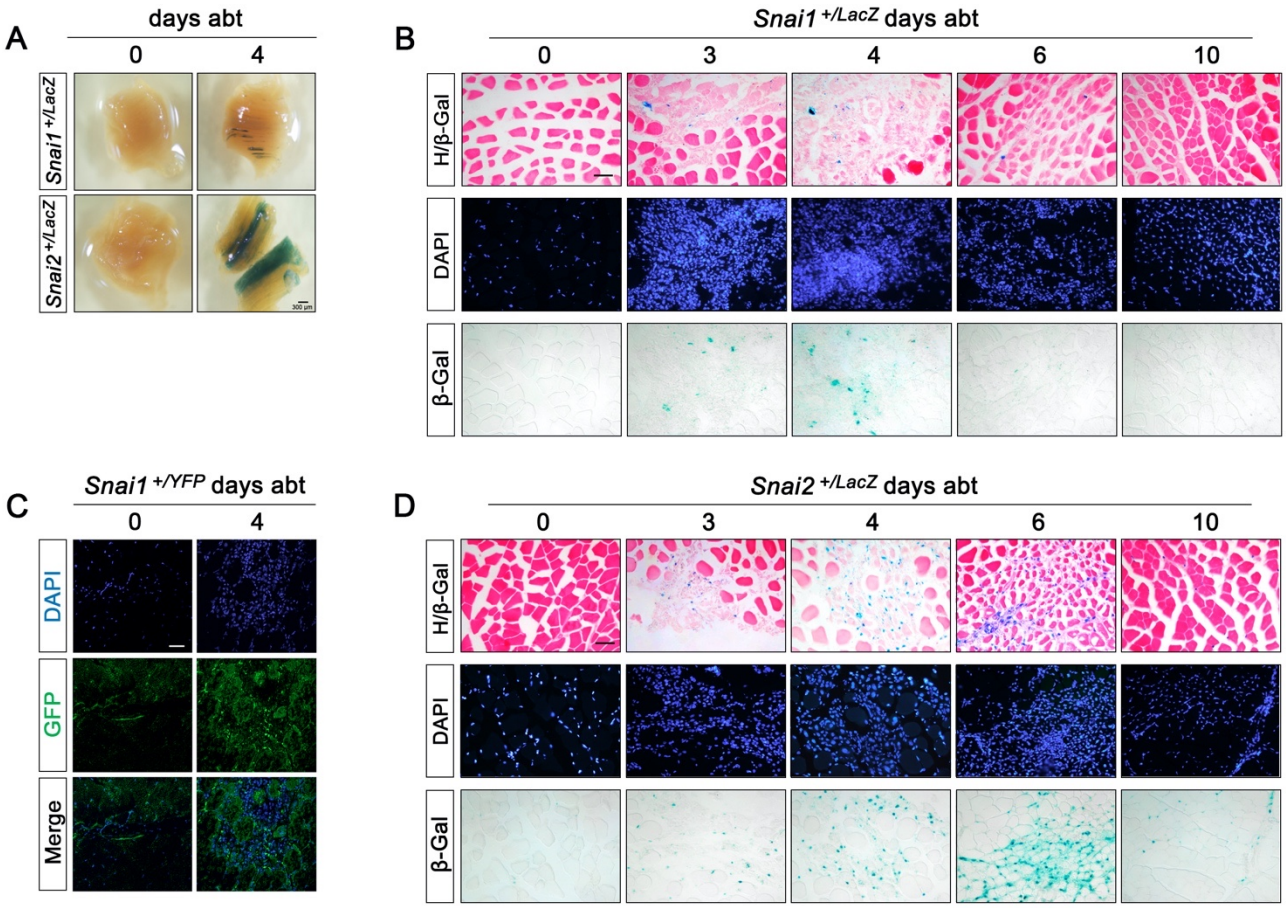

Figure 17. *Snai1* and *Snai2* are upregulated in myoblasts during muscle regeneration.
A) *LacZ* expression in *Snai1*$^{+/LacZ}$ and *Snai2*$^{+/LacZ}$ tibialis anterior muscles at day 0 (untreated) and day 4 after Bupivacaine treatment (abt). Bar, 300 µm. B-D) β-Gal/Hematoxylin, DAPI and β-Gal staining of cross-sections from tibialis anterior muscles in *Snai1*$^{+/LacZ}$ and *Snai2*$^{+/LacZ}$ mice at day 0 (untreated) and days 3, 4, 6 and 10 after Bupivacaine treatment (abt). Bar, 50 µm. C) GFP expression in *Snai1*$^{+/YFP}$ tibialis anterior muscles at day 0 and day 4 after Bupivacaine treatment (abt). Bar, 50 µm.

To confirm the expression of SNAI1 and SNAI2 in proliferating myoblasts, we analyzed their expression in cultured primary myoblasts and C2C12 cells. SNAI1 and SNAI2 were expressed in proliferating C2C12 cells maintained in growth medium and were rapidly down-regulated after switching to low-serum differentiation medium (Figure 18A), showing an expression profile that resembles what obtained for primary myoblasts (Figure 18B, Soleimani *et al.,* 2012).

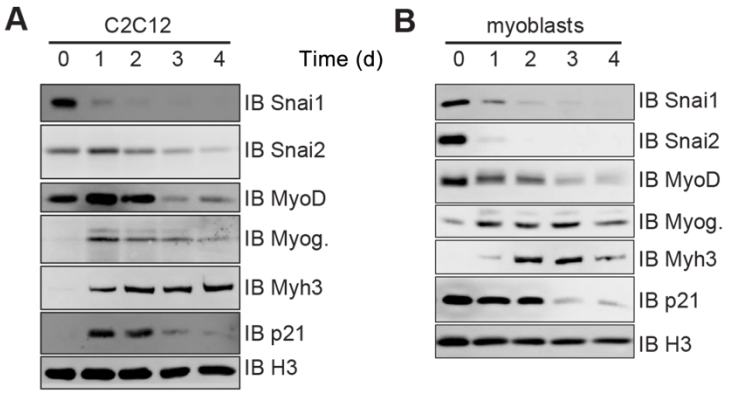

Figure 18. SNAI proteins expression in C2C12 and primary myoblasts. SNAI1 and SNAI2 proteins expression was detected by Western blot analysis of whole cell extracts prepared from proliferating and differentiating C2C12 cells (A) and primary mouse myoblasts (B). Time (d) indicates the days after switching to differentiation medium. Histone H3 expression was used to confirm equal loading. MyoD, Myog and embryonic myosin heavy chain (Myh3) expression were detected as control of myoblasts differentiation.

5.3 Transcriptome analysis of myoblasts silenced for SNAI1

In primary skeletal myoblasts, SNAI1 represses upregulated genes during muscle terminal differentiation and SNAI1 knockdown leads to primary myoblasts precocious cell cycle withdrawal and terminal differentiation (Soleimani *et al.*, 2012). Here, we investigated the role of SNAI1 during the early stage of myogenic differentiation using C2C12 cell line. C2C12 cells represent the most widely used and well-established *in vitro* model for mammalian muscle differentiation. These cells are considerably less prone to spontaneous differentiation than primary myoblasts in the presence of growth factors, making them a good and homogenous model to study transcriptome in proliferating myoblasts. This was confirmed by the lower expression levels of p21 and Myogenin under growth conditions in comparison to primary myoblasts (Figure 18A-B). We transduced C2C12 cells with lentiviral particles for the expression of two different small hairpin RNA (shRNA) targeting SNAI1 and reduced SNAI1 expression by about 80% (Figure 19A) without inducing spontaneous differentiation to myotube in high-serum culture conditions (Figure 19B).

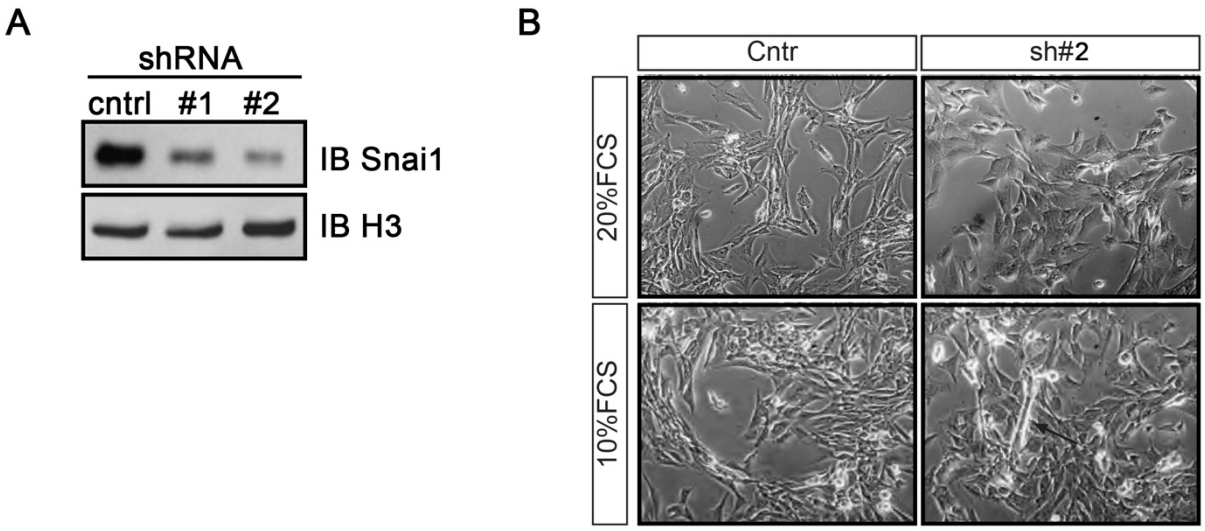

Figure 19. SNAI1 knockdown is not able to induce spontaneous differentiation. A) SNAI1 expression was silenced in C2C12 cells by the administration of lentiviral vector expressing the shRNA#1 and shRNA#2. Control cells were infected with lentiviral vector expressing shRNA for GFP. B) Control cells and SNAI1 knockdown C2C12 myoblasts (sh#2) were seeded in 20% FCS and 10% FCS and morphological analysis was performed. The arrow indicates the presence of a myotube.

Gene expression profiling by microarray analysis revealed that, compared to control transduced cells, about 200 genes had significantly altered expression (fold change ≥3) in SNAI1 knockdown cells (mean expression values obtained with both shRNAs) (Figure 20A). In particular, 64 genes were up-regulated and 139 were down-regulated in silenced cells (p value < 0.05). Among the down-regulated genes, we identified four functional groups of genes involved in angiogenesis, myoblast proliferation and differentiation, extracellular matrix deposition and lipid metabolism. Among the up-regulated genes, we identified a large group of genes involved in Endoplasmic Reticulum stress (ER stress) and a group of genes involved in lipid metabolism. Only a few genes involved in terminal myofiber differentiation were upregulated by SNAI1 silencing, confirming that the ability of C2C12 to maintain an undifferentiated phenotype is not related to SNAI1 expression (Figure 20B). We validated the microarray results by RT-qPCR on selected transcripts for each functional group (Figure 20C).

Keeping in mind that it is a repressor, we looked for new direct target genes of SNAI1. Thus, we studied *Fgf21* and *Atf3,* two of the most regulated genes in the microarray analysis. In muscle differentiation, *Fgf21* is positively regulated by the transcription factor MyoD and it activates expression of the early myogenic genes, promotes cell cycle exit and enhances myogenic differentiation of C2C12 cells (Liu *et al.*, 2017). ATF3 is a transcription factor involved in the ER stress, a complex process involved in myogenesis and other numerous physiological processes (Schmitz *et al.,* 2018). Alter and collaborators showed that ATF3 is transiently expressed during myogenic differentiation, but not during myogenic proliferation (Alter *et al.,* 2011), but nothing else is known about its role in muscle differentiation.

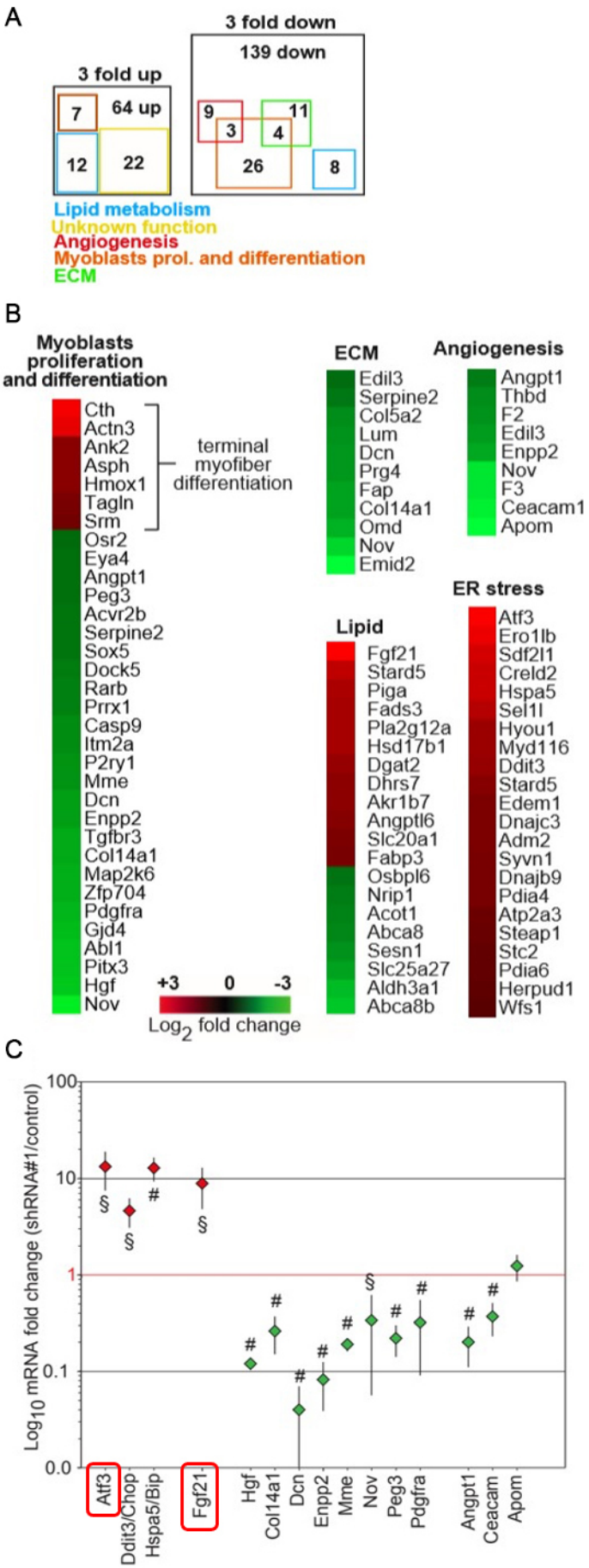

Figure 20. Transcriptome analysis of myoblasts silenced for SNAI1. A) Eulero-Venn diagram of microarray analysis showing functional groups of genes differentially expressed following SNAI1 silencing. Only genes showing more than 3-fold differential expression in both independently silenced cell types vs control cells were counted. (ECM, extra-cellular matrix). B) Heat map of microarray analysis showing genes up- and down-regulated following SNAI1 silencing. C) mRNA expression levels of 10 differentially expressed genes, were analyzed by RT-qPCR. Results were normalized to *Gapdh* mRNA. Mean values from three independent experiments are shown with standard deviations (# $p<0.0$; § $p<0.05$).

5.4 Analysis of FGF21 expression in C2C12 cells and during muscle regeneration

Recent studies have demonstrated that FGF21 has a crucial role during myogenic differentiation (Liu *et al.,* 2017). Taking into account the transcriptome analysis results, the role of the transcription factor SNAI1 on myogenesis and the effect of FGF21 on myogenic differentiation, we hypothesized that SNAI1 could be involved in the repression of *Fgf21* expression. In order to better understand the role of FGF21 in myogenesis and muscle differentiation, we analyzed by RT-qPCR the *Fgf21* expression during muscle regeneration. We observed that *Fgf21* mRNA levels were induced in regenerating muscle 3-4 days after Bupivacaine treatment, with an expression peak at day 4 (Figure 21A). Western blot analysis showed that FGF21 protein expression was induced during muscle regeneration with a maximum at days 4-5 after Bupivacaine treatment and this is the first time that FGF21 has been described to be induced during muscle regeneration *in vivo* (Figure 21A-B). In this experimental model, SNAI1 and *Fgf21* expressions are partially overlapping, but these data are still consistent with the repressive role of SNAI1 on the *Fgf21* expression. In fact, it is important to consider that during muscle regeneration myoblasts are not perfectly synchronized in their differentiation stage and they are not the only cell type present during this process.

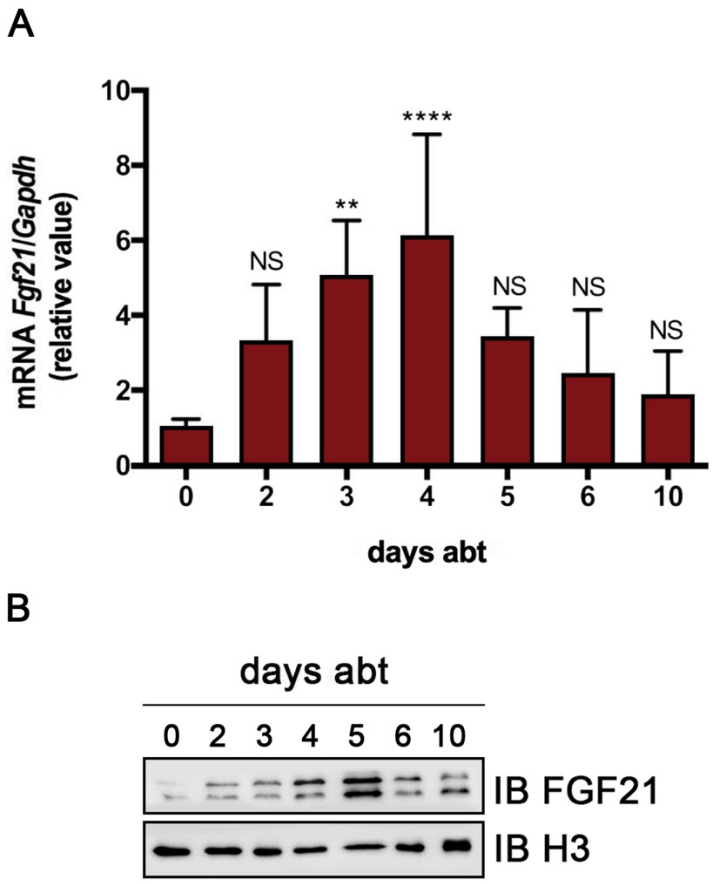

Figure 21. *Fgf21* mRNA and protein expression during muscle regeneration. A) Quantitative evaluation of *Fgf21* mRNA during muscle regeneration by RT-qPCR at different days after Bupivacaine treatment (abt). The values were normalized to *Gapdh* mRNA. Asterisks indicate significant differences (p-values) between expression in untreated muscle (0) and each time point after Bupivacaine treatment (abt). B) FGF21 protein expression was detected by Western blot analysis (B) in whole extracts prepared from regeneration muscle at the indicated days abt. Histone H3 expression was used to confirm equal loading. Data were evaluated from three independent experiments using the one-way analysis of variance ANOVA: **** = P< 0.0001, ** = 0.001<P< 0.01, N.S.= not statistically significance.

To confirm this hypothesis, we analyzed *Fgf21* expression in synchronized differentiating C2C12 cells at different days after switching to differentiation medium (Figure 22A).

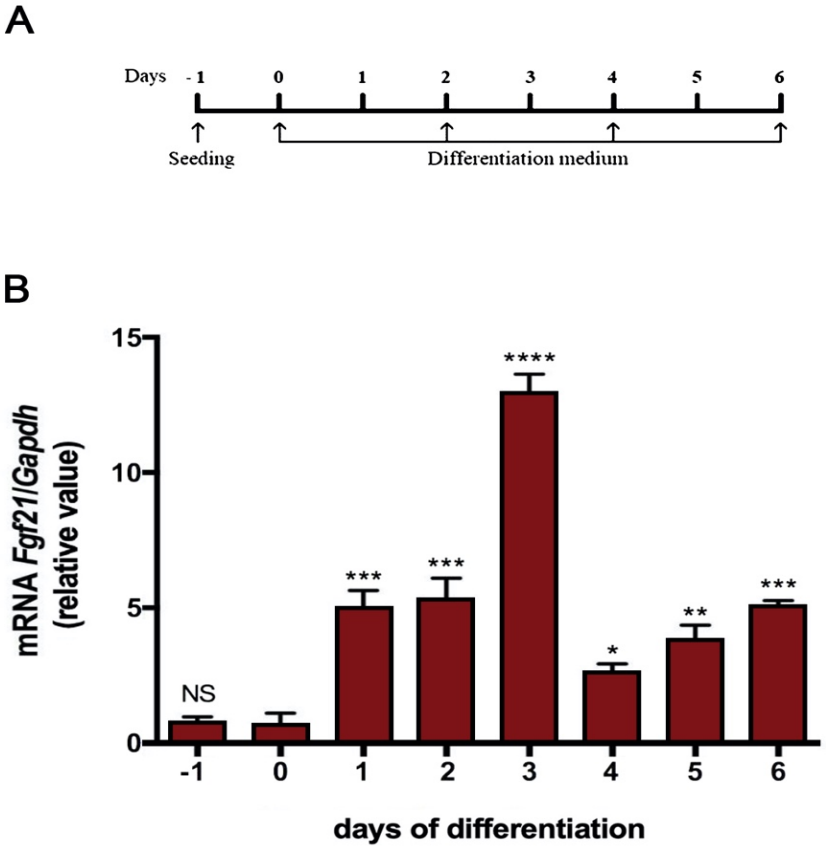

Figure 22. *Fgf21* mRNA and protein expression during C2C12 differentiation. A) The differentiation was induced by culturing C2C12 cells with the differentiation medium from day 0 and changing the medium every two days. B) Quantitative evaluation of *Fgf21* mRNA by RT-qPCR during C2C12 myogenic cell differentiation. Asterisks indicate p-values between expression in proliferating and differentiating C2C12. Data were evaluated from three independent experiments using the one-way analysis of variance ANOVA: **** = P< 0.0001, *** = 0.0001<P< 0.001, ** = 0.001<P< 0.01, * = 0.01<P< 0.05, N.S.= not statistically significance.

Our analysis showed a strong increase of *Fgf21* mRNA expression in differentiating C2C12 cells already on the first day after the switch to differentiation medium with a maximum reached at day 3 (Figure 22B). The *Fgf21* expression pattern perfectly mirrored in reverse the SNAI1 expression, confirming the possible negative regulation of *Fgf21* by SNAI1.

5.5 Analysis of ATF3 expression during muscle regeneration

Similarly, to what performed for *Fgf21*, we investigated ATF3 expression during muscle regeneration both *in vivo* and *in vitro.* ATF3 protein and mRNA were upregulated during muscle regeneration. In particular, Western blot and RT-qPCR analysis revealed that ATF3 expression was induced in regenerating muscle, mainly 2-4 days after Bupivacaine treatment both at the protein and mRNA levels (Figure 23A-B). During synchronized C2C12 differentiation program, as observed for *Fgf21*, also *Atf3* expression was inversely correlated with SNAI1 expression, confirming the possible role of the latter in *Atf3* negative regulation (Figure 23C).

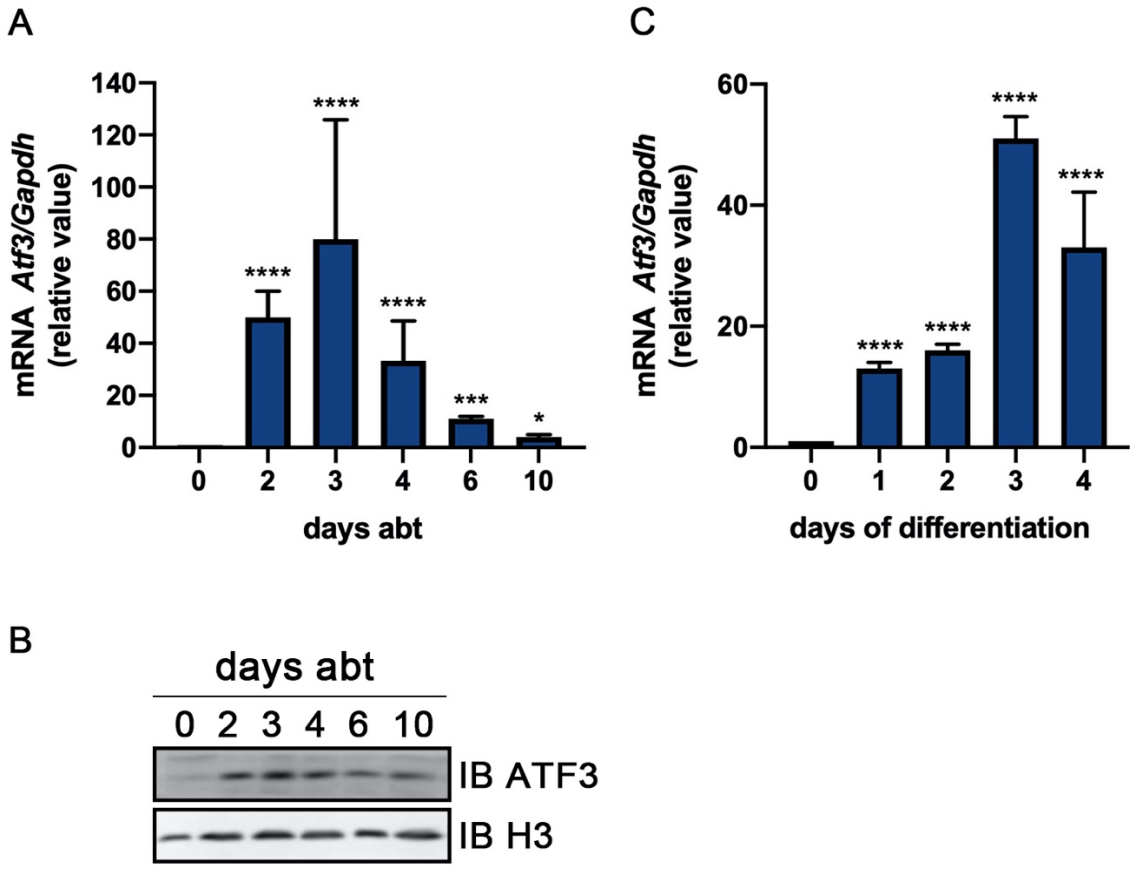

Figure 23. ATF3 protein and mRNA expression during muscle regeneration *in vivo* and *in vitro*. A) Quantitative evaluation of *Atf3* transcript in regenerating muscle by RT-qPCR. The values normalized to *Gapdh* mRNA levels are expressed as the mean ± SD of 3 independent experiments. Asterisks indicate significant differences (p-values) between expression in untreated muscle (0) and each time point after Bupivacaine treatment (abt). B) ATF3 protein expression was detected by Western blot analysis in whole extracts prepared from regeneration muscle at the indicated days after Bupivacaine treatment (abt). Histone H3 expression was used to confirm equal loading. Quantitative evaluation of *Atf3* mRNA by RT-qPCR during C2C12 myogenic cells differentiation. C) Quantitative evaluation of *Fgf21* mRNA by RT-qPCR during C2C12 myogenic cell differentiation. Asterisks indicate p-values between expression in proliferating and differentiating C2C12. Data were evaluated from three independent experiments using the one-way analysis of variance ANOVA: **** = P< 0.0001, *** = 0.0001<P< 0.001, * = 0.01<P< 0.05.

5.6 *Fgf21* and *Atf3* are downregulated in C2C12 cells overexpressing SNAI1

To deeply investigate the repressive role of SNAI1 on *Fgf21* and *Atf3* expression, C2C12 myoblasts were transiently transfected with eighter pCMV6-emty plasmid or pCMV6-SNAI1 plasmid to overexpress the SNAI1 protein (Figure 24A). Myoblasts differentiation was induced 24 hours post-transfection by medium switch. *Fgf21* and *Atf3* expression was analyzed by RT-qPCR at 24, 48, and 72 hours after transfection corresponding to differentiation day -1 (D-1), day 0 (D0) and day 1 (D1), respectively. As expected, *Fgf21* and *Atf3* expressions were increased in C2C12 transfected with the pCMV6-empty vector at D2. At the same time point, *Fgf21* and *Atf3* were downregulated in C2C12 cells overexpressing exogenous SNAI1 compared to the control cells, suggesting that SNAI1 could play a role in the repression of *Fgf21* and *Atf3* expression in proliferating myoblasts (Figure 24B, C).

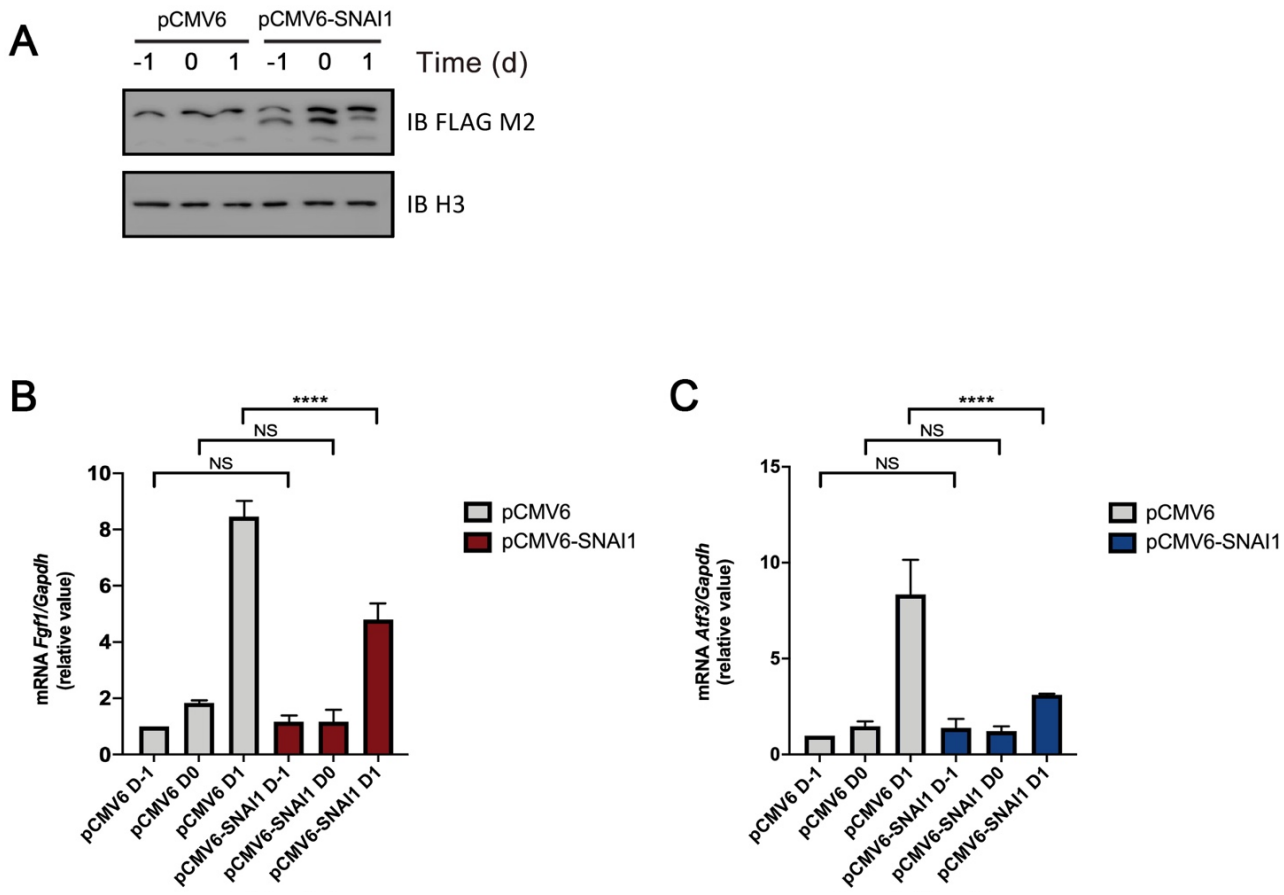

Figure 24. *Fgf21* and *Atf3* are repressed by exogenous SNAI1 overexpression in differentiating myoblasts. A) C2C12 myoblasts were transiently transfected with the pCMV6-emty plasmid or with the pCMV6-SNAI1 plasmid and transfected SNAI1 protein expression was detected by Western blot analysis at 0, 1 and 2 days after the transfection by means of an anti-FLAG antibody. Histone H3 expression was used to confirm equal loading. B-C) Quantitative evaluation of *Fgf21* and *Atf3* transcripts in C2C12 cells overexpressing SNAI1 at 24h (D-1), 48h (D0) and 72h (D1) after transfection. The values were normalized to the *Gapdh* mRNA levels. Histone H3 expression was used to confirm equal loading. Asterisks indicate significant differences (p-values) between expression in control C2C12 cells (pcMV6) and C2C12 cells overexpressing SNAI1 (pcMV6-SNAI1) at the indicated days after the transfection. Data were evaluated from three independent experiments using the one-way analysis of variance ANOVA: **** = P< 0.0001, N.S.= not statistically significance.

5.7 Involvement of SNAI1 transcription factor in the regulation of *Fgf21* expression

To demonstrate the direct action of SNAI1 repressor in the transcriptional regulation of *Fgf21* promoter and to characterize the promoter regions involved in this regulation, we performed a bioinformatic analysis and identified the potential E-box binding sites for SNAI1 (CACCTG, CACGTG and CAGCTG) in the mouse *Fgf21* promoter region sequence. Three clusters of putative SNAI1 binding sites were identified centered around positions -1659 (cluster A), -1000 (cluster B), and +21 (cluster C) respect to the transcriptional start site (TSS; +1). To progressively exclude the

E-boxes, we generated luciferase reporter constructs carrying *Fgf21* promoter regions of different length, spanning from position +166 to -1775, -1681, -1091 and -926 respect to the TSS (Figure 25).

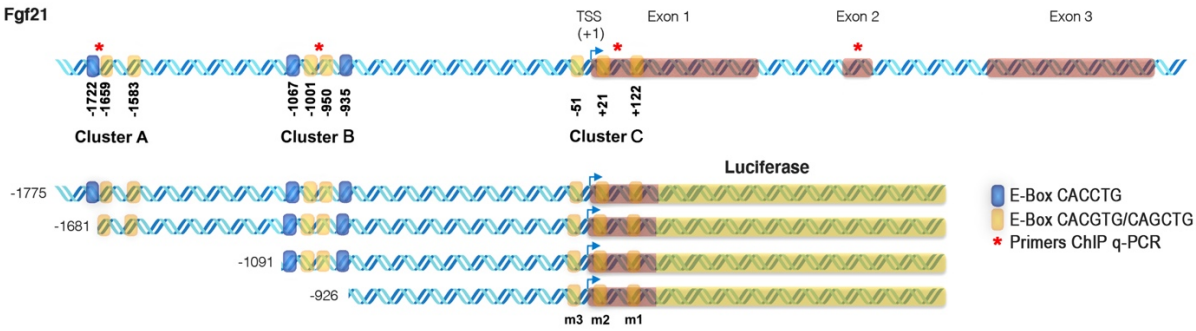

Figure 25. *Fgf21* promoter region and the four promoter fragments cloned into the pGL3-Basic vector. Schematic representation of the *Fgf21* gene and the four promoter fragments, which were cloned into the pGL3-Basic vector, upstream of the luciferase reporter gene. The blue and yellow boxes represent the E-Box CACCTG and CACGTG/CAGCTG, respectively. Positions of the identified E-boxes with respect to the TSS are indicated and referred to the first bp of the CANNTG consensus. The E-boxes are grouped in three clusters. The annealing sites of the primers used for ChIP-qPCR are represented as red asterisk.

pCMV6-SNAI1 expression vector or pCMV6-empty control vector were co-transfected in C2C12 myoblasts together with each of the reporter vectors. The basal activity of the full length *Fgf21* promoter decreased drastically in the -926 deletion mutant. This is in agreement with the observation presented by Liu *et al.* (Liu *et al*., 2017), in which they have described the first E-box of the cluster B in position -1067 as a binding site for the transactivator MYOD and an essential element for the full promoter activity. However, the full length and each of the 3 other promoters with progressive 3' deletions decreased their activity when co-transfected with the SNAI1 expression vector, even though the full length -1775 promoter proved to be the most responsive to SNAI1 repression (Figure 26A-C). This suggests that the E-boxes cluster A and probably C work in concert with each other for full *Fgf21* promoter repression. In the E-box cluster C of the *Fgf21* promoter there are three putative SNAI1 binding site, located at -51 bp, +21 bp and +122 bp respect to the TSS (Figure 25). In order to confirm their involvement in *Fgf21* repression, we introduced single and multiple point-mutations of the three E-boxes in the reporter vector harboring the -926 promoter, to obtain five new promoter mutants named -926m1, -926m2, -926m3, -926m1m3 and -926m1m2m3, respectively. Following the co-transfection of this new set of reporter plasmids with SNAI1 expression plasmid, we observed that only the triple point-mutant -926m1m2m3 was no longer responsive to SNAI1 repressive activity

(Figure 26B-C), suggesting that the three binding sites play a mutual role in SNAI1 recruitment on *Fgf21* promoter.

To further verify and characterize the direct binding of SNAI1 to the *Fgf21* promoter, C2C12 cells were transiently transfected with pCMV6-SNAI1 expression vector or pCMV6 empty control vector and ChIP followed by qPCR was performed. The results confirmed that SNAI1 can effectively bind to the *Fgf21* promoter at the E-box cluster A and C, but not B. No significant signal increase was observed with primers annealing in exon 2 sequence used as negative control (Figure 26D).

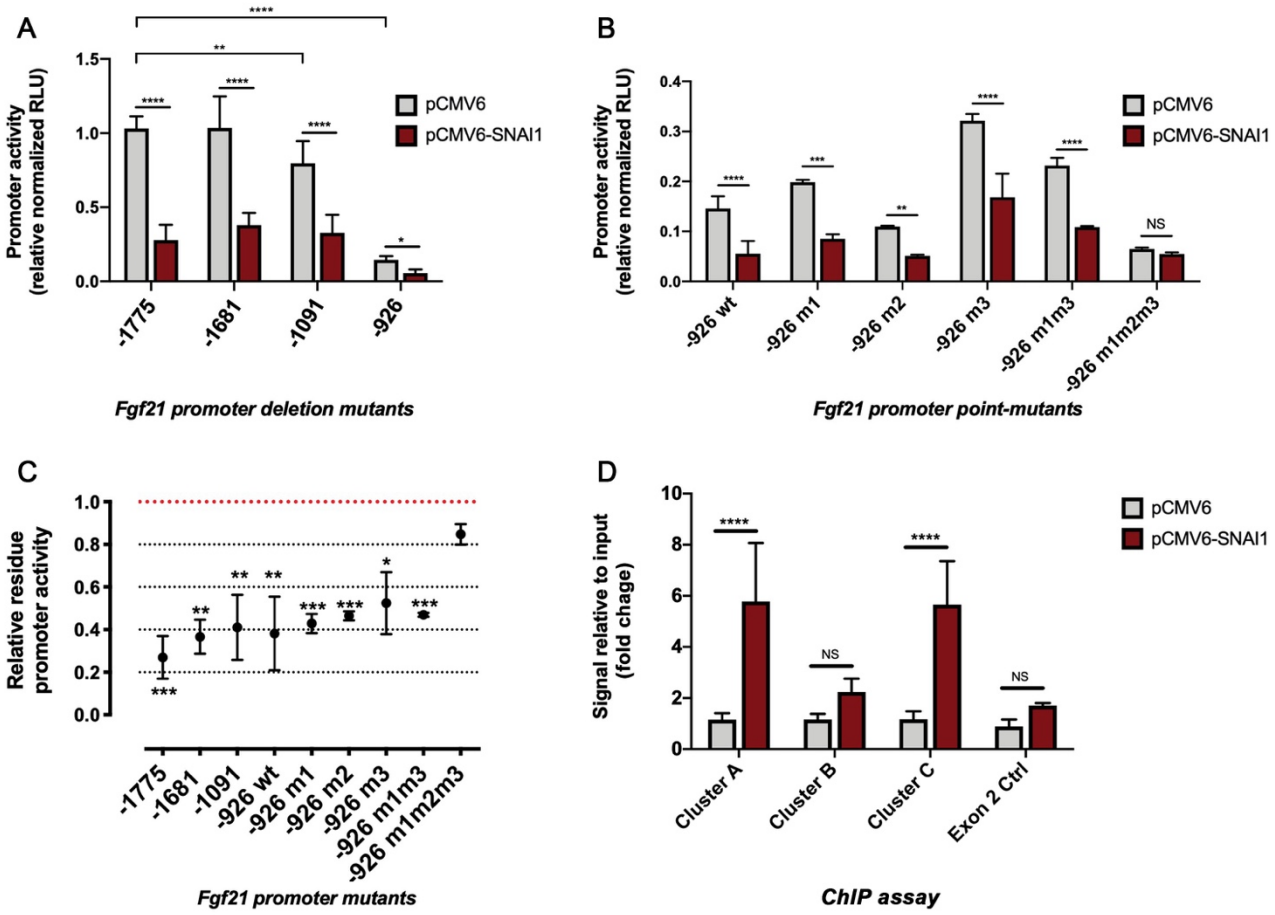

Figure 26. SNAI1 regulates *Fgf21* promoter activity by binding directly to E-box sequences. A) C2C12 myoblasts were transiently co-transfected with the pCMV6-emty plasmid or with the pCMV6-SNAI1 plasmid and each of the reporter plasmids. Luciferase activity measurements in the whole extracts of cells transfected with the reporter vectors carrying the full length (-1775) or deleted fragments *Fgf21* promoter. Asterisks indicate p-values between *Fgf21* promoter deletion mutants luciferase activity in control cells (pcMV6) and cells overexpressing SNAI1 (pcMV6-SNAI1). Asterisks also indicate p-values of the luciferase activity between the -1775 and the -1091 and -926 *Fgf21* promoter deletion mutants in control cells. B) pCMV6-SNAI1 or empty control (pCMV6) vector were transiently co-transfected with the pGL3 luciferase vectors harboring point-mutations in the -926 *Fgf21* promoter sequence and luciferase activity was measured. Asterisks indicate p-values between *Fgf21* promoter point mutants luciferase activity in control cells (pcMV6) and cells overexpressing SNAI1 (pcMV6-SNAI1). C) SNAI1 transcription factor repressive activity is here expressed as relative residue activity of each promoter obtained by normalizing luciferase activity of cells co-transfected with pCMV6-SNAI1 to that of cells co-transfected with empty control vector. P-values represent statistical differences between relative residue activity of each promoter and relative residue activity of promoter -926m1m2m3. D) SNAI1 binds both E-box cluster A and the E-box cluster C in the *Fgf21* promoter region. pCMV6-SNAI1 or empty control (pCMV6) vectors were transiently co-transfected in C2C12 and ChIP assay with anti-FLAG antibody followed by qPCR was performed. Upon normalization to spike-in DNA, results were expressed as signal relative to input. Asterisks indicate p-values between *Fgf21* expression in control cells (pcMV6) and cells overexpressing SNAI1 (pcMV6-SNAI1) at the indicated binding sites. Data were evaluated from three independent experiments using the two-way (A and B) and one way (C and D) analysis of variance (ANOVA): **** = P< 0.0001, *** = 0.0001<P< 0.001, ** = 0.001<P< 0.01, * = 0.01<P< 0.05, N.S.= not statistically significance.

5.8 Cloning of *Atf3* promoter region

To investigate the direct regulatory effect of SNAI1 on the *Atf3* promoter region, we identified the potential binding sites for SNAI1 in the *Atf3* promoter region sequence by bioinformatic analysis and cloned two promoter fragments (from -1943 bp or -1235 bp to +139 bp with respect to the TSS) in front of the firefly luciferase reporter gene. The promoter fragment spanned from -1235 to +139 was designed to exclude the 3 E-boxes CACCTG, putative preferred binding sites for the SNAI factors. Given the difficulty encountered in cloning the *Atf3* promoter sequence directly into the pGL3-Basic vector (probably due to the high GC content of this sequence) (Figure 27), it was necessary to resort to an additional step, using the pCR-Blunt II-TOPO vector. Thus, the two promoter deletions were cloned by the pCR-Blunt II-TOPO system, which is based on topoisomerase reaction instead of ligase. Thus, the two promoter fragments were cloned into the pCR-Blunt II-TOPO vector, within which was successively cloned the fragment Luc+-SV40 late poly(A) signal derived from the pGL3-Basic vector (Figure 28).

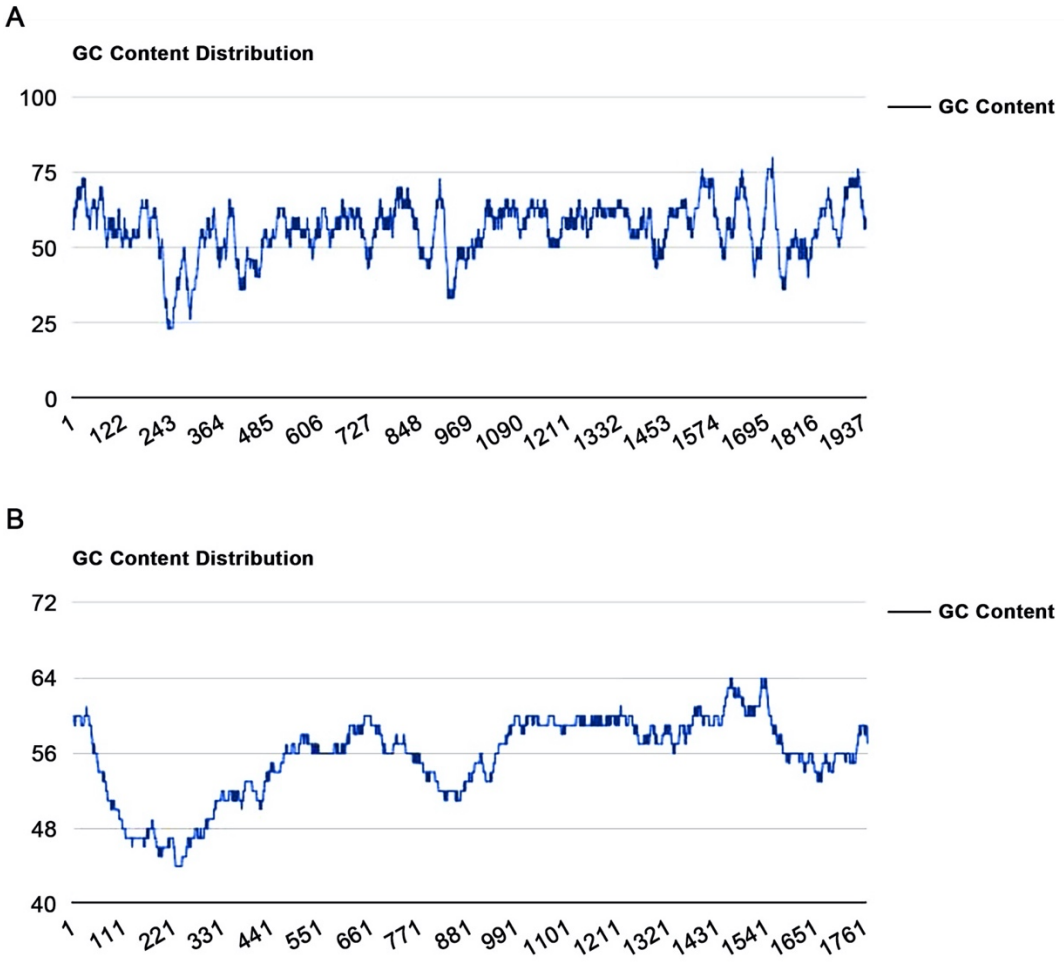

Figure 27. GC content of the *Atf3* promoter. GC content calculated using as parameter the window size of (A) 30 and (B) 200 base pairs.

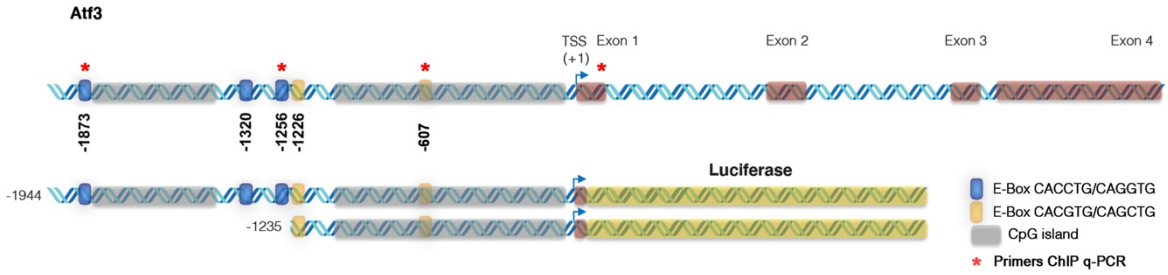

Figure 28. *Atf3* promoter region and its two promoter fragments. Schematic representation of the *Atf3* gene and the two promoter fragments cloned in front of with a luciferase reporter gene. Positions of the identified E-boxes with respect to the TSS are indicated and referred to the first bp of the CANNTG consensus. The cDNA encoding the firefly luciferase is shown in yellow, the CpG island in grey, while the blue and yellow boxes represent the E-Box CACCTG and CACGTG/CAGCTG, respectively. The annealing sites of the primers used for ChIP-qPCR are represented as red asterisk.

5.9 Involvement of SNAI1 in the regulation of *Atf3* expression

pCMV6-SNAI1 expression vector or pCMV6-empty control vector were co-transfected in C2C12 myoblasts together with the *Atf3* promoter constructs and the normalized luciferase activity was measured. The results obtained showed a decrease of *Atf3* levels in presence of SNAI1 in both the promoter constructs tested, indicating that SNAI1 could bind the *Atf3* promoter and that the remaining E-boxes of -1235 promoter deletion mutant were still able to lead SNAI1 repression of the promoter activity (Figure 29A). To verify the direct binding of SNAI1 to *Atf3* promoter, C2C12 cells were transiently transfected with pCMV6-SNAI1 expression vector to overexpress SNAI1 and ChIP followed by q-PCR was performed. The results obtained confirmed that SNAI1 binds the E-Box at -1873bp, as well as the cluster of E-boxes between -1320 bp and -1226 bp but not in the E-box at -607 bp. No significant signal increase was observed with primers annealing in exon 1 sequence that was used as negative control (Figure 29B).

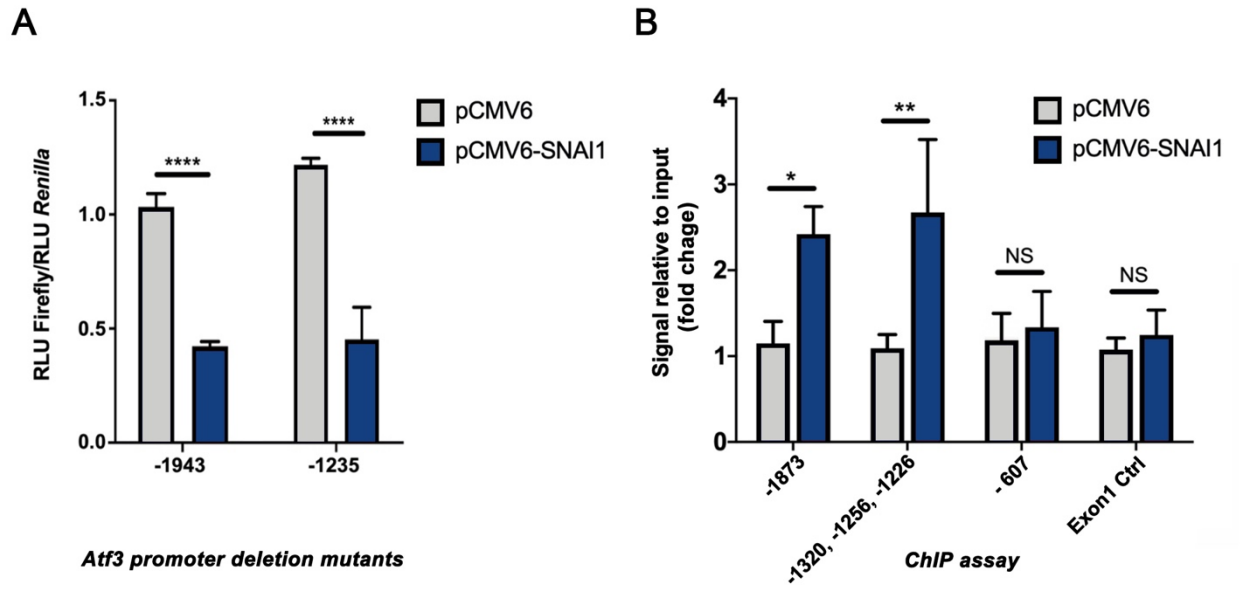

Figure 29. SNAI1 regulates *Atf3* promoter activity by binding directly to E-box sequences. C2C12 myoblasts were transiently co-transfected with the pCMV6-emty plasmid or the pCMV6-SNAI1 plasmid, and the *Atf3* promoter reporter vectors. A) Constructs carrying the full length (-1943) and deletion mutant (-1235) of the *Atf3* promoter region were co-transfected in C2C12 myoblasts together with the pCMV6-SNAI1 or pCMV6-empty vectors, and luciferase activity was measured. Asterisks indicate p-values between *Atf3* promoter deletion mutants luciferase activity in control cells (pcMV6) and cells overexpressing SNAI1 (pcMV6-SNAI1). B) SNAI1 binds both E-box at -1873 bp and the E-box cluster from – 1320 bp to -1226 bp. pCMV6-SNAIl or empty control (pCMV6) vectors were transiently co-transfected in C2C12 and ChIP-qPCR was performed. Upon normalization to spike-in DNA, results were expressed as signal relative to input. Asterisks indicate p-values between *Atf3* expression in control cells (pcMV6) and cells overexpressing SNAI1 (pcMV6-SNAI1) at the indicated binding sites after ChIP analysis. Data were evaluated from three independent experiments using the two-way (A) and one way (B) analysis of variance (ANOVA): **** = P< 0.0001, ** = 0.001<P< 0.01, * = 0.01<P< 0.05, N.S.= not statistically significance.

5.10 Analysis of *Fgf21* expression in C2C12 cells in response to thapsigargin treatment

It has been recently reported that ER stress plays a crucial role in the regulation of the skeletal muscle development (Chen *et al*., 2006; Nakanishi *et al*., 2015; Wei *et al*., 2016). To evaluate *Fgf21* expression during ER stress and the role played by SNAI1 in such regulation, C2C12 cells were treated with thapsigargin, a well characterized ER stress inducing agent, and *Fgf21* mRNA expression was evaluated at different time points. The results showed an induction of the level of *Fgf21* mRNA in cycling C2C12 cells as a consequence of the ER stress induction by thapsigargin (Figure 30A). Afterwards, C2C12 cells were transiently co-transfected with pCMV6-empty vector or pCMV6-SNAI1 to overexpress SNAI1 and the -1775 *Fgf21* promoter reporter plasmid.

After 24 hours from the transfection, cells were treated with thapsigargin, then the luciferase activity of the -1775 *Fgf21* promoter deletion mutant was measured. *Fgf21* expression was upregulated in

response to the thapsigargin treatment and SNAI1 was able to repress thapsigargin induced promoter activity. (Figure 30B).

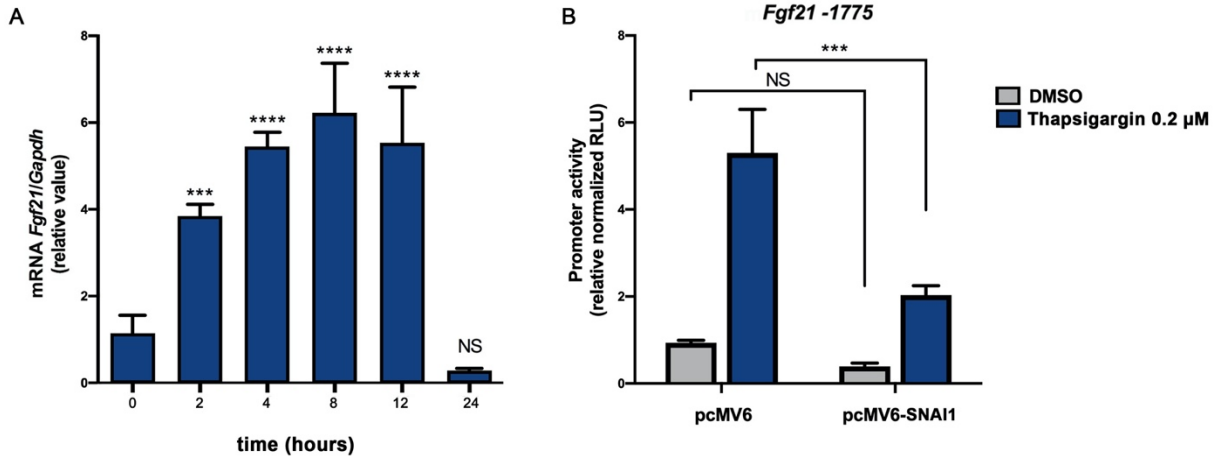

Figure 30. *Fgf21* expression in cycling C2C12 myoblasts after thapsigargin treatment. A) Transcriptional analysis of *Fgf21* levels by RT-qPCR in proliferating C2C12 cells at hour 0, 2, 4, 8, 12 and 24 after thapsigargin treatment. Results were normalized to *Gapdh* mRNA. Asterisks indicate significant differences (p-values) between expression in untreated cells (0) and each time point after thapsigargin treatment. B) C2C12 cells were co-transfected with pCMV6-empty or pCMV6-SNAI1 vectors and with the -1775 *Fgf21* promoter reporter plasmid. After 24 h from the transfection, C2C12 cells were treated with thapsigargin 0.2 µM and after 48 h from the transfection, luciferase activity was measured. Asterisks indicate significant differences (p-values) of the -1775 *Fgf21* promoter deletion mutant luciferase activity between C2C12 control cells (pcMV6) and C2C12 overexpressing SNAI1 (pcMV6-SNAI1) treated with DMSO or thapsigargin. Data were evaluated from three independent experiments using the one-way analysis of variance (ANOVA): **** = P< 0.0001, *** = 0.0001<P< 0.001, N.S.= not statistically significance.

5.11 Involvement of ATF3 in the *Fgf21* expression

ER stress is implicated in *Fgf21* transcriptional induction and ATF3 is a transcription factor induced by ER stress, thus we wondered if *Fgf21* promoter is responsive to ATF3 and if repression of its activity by SNAI1 overexpression could be due to repression of endogenous ATF3 expression by SNAI1 rather than a SNAI1 direct binding of the promoter. C2C12 myoblasts were co-transfected with pCMV6-SNAI1, pCMV6-ATF3 and with the -1755 *Fgf21* promoter reporter plasmid. We observed a significant induction of *Fgf21* promoter activity by overexpression of exogenous ATF3, that, however, was unable counteract the repressive effect of SNAI1 (Figure 31), confirming that SNA1 represses *Fgf21* promoter by direct DNA binding.

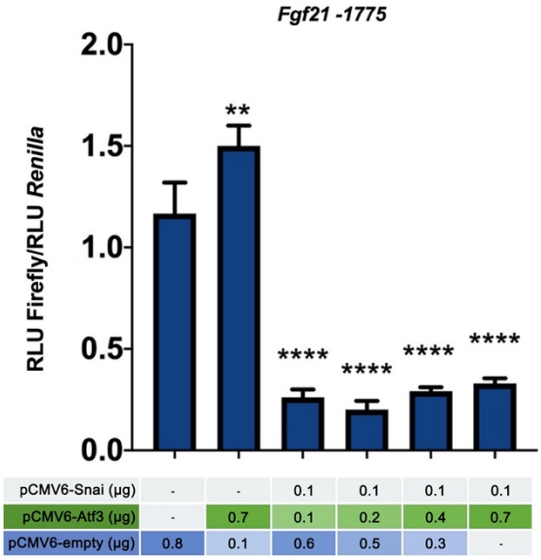

Figure 31. Exogenous ATF3 is unable to rescue repression by SNAI1 of the *Fgf21* promoter. Construct carrying the full length *Fgf21* promoter fragment -1775 was co-transfected in C2C12 myoblasts together with the pCMV6-SNAI1, pCMV6-ATF3 or pCMV6-empty vectors. Asterisks indicate significant differences (p-values) between the -1775 *Fgf21* promoter deletion mutant luciferase activity of the cells transfected with pCMV6- empty vector and cells overexpressing ATF3 or ATF3 and SNAI1. Data were evaluated from three independent experiments using the one-way analysis of variance (ANOVA): **** = P< 0.0001, ** = 0.001<P< 0.01.

5.12 SNAI1 impairs proliferation in C2C12 cells

To confirm the transcriptome analysis obtained by shRNA interference, we generated a C2C12 cell line knockout for SNAI1 by CRISPR-Cas9 genome editing. To obtain that, C2C12 cells were transduced with lentiviral particles for the expression of the endonuclease Cas9 and three different single guide RNA (sgRNA). As negative control, C2C12 cells were transduced with similar particles, but missing the sgRNA sequence in the viral genome. As shown in the Western Blot of the Figure 32A, the cells transduced with the pLCV2-SN3 vector, carrying the single guide RNA #3, were knockout for SNAI1 and were used for the next set of experiments. To investigate SNAI1 knockout effect on C2C12 proliferation and differentiation we analyzed, at the morphological level, the proliferation and differentiation grade by means of bright-field microscopy analysis. No evident differences were observed in myotube number or size comparing the knockout cell line with the control, while C2C12 SNAI1$^{-/-}$ showed a decreased proliferation rate in comparison to parental wild type cells (Figure 32B). To better define this point, we compared the SNAI1 knockout cell line with the control, in high serum culture medium, by immunofluorescence staining of the proliferation

marker Ki67, and we confirmed that C2C12 cells knockout for SNAI1 showed a reduced rate of cell proliferation (Figure 32C-D).

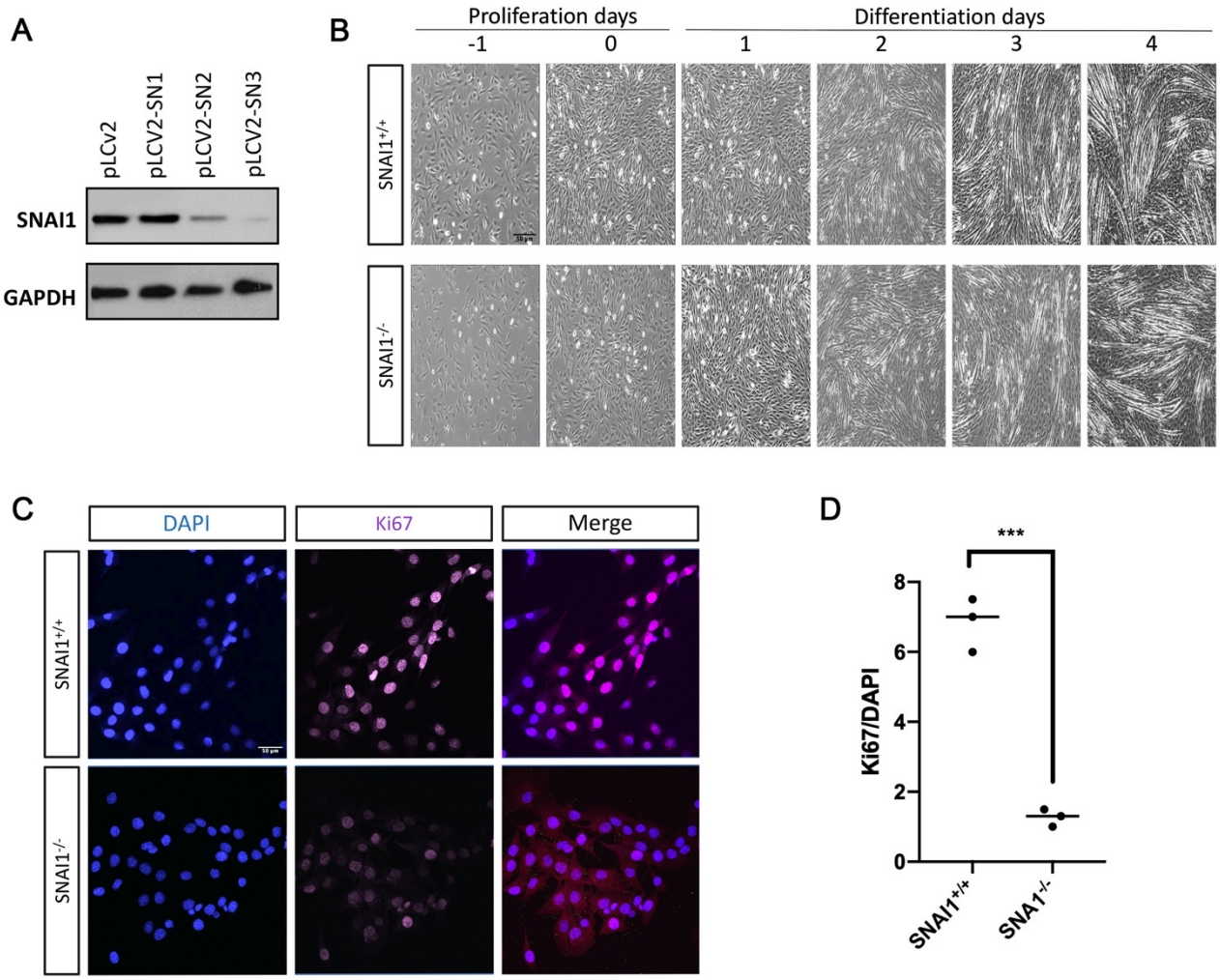

Figure 32. SNAI1 regulates C2C12 cell proliferation. A) CRISPR-Cas9 genome editing technique was used to knockout SNAI1 in C2C12 cell line. The figure represents the expression of SNAI1 in C2C12 cell line infected with Lentivirus expressing pLCV2 (control, empty vector), pLCV2-SN1 (Single Guide RNA #1), pLCV2-SN2 (Single Guide RNA #2) and pLCV2-SN3 (Single Guide RNA #3) respectively. B) Morphological analysis of $SNAI1^{+/+}$ and $SNAI^{-/-}$ C2C12 myoblasts during proliferation and differentiation stages. Cells were seeded at day -1 and the switch to differentiation medium was done at day 0. C) $SNAI1^{+/+}$) and $SNAI^{-/-}$ cell lines were paraformaldehyde fixed and stained with an antibody anti-Ki67 (proliferation marker). D) Ki67/ DAPI positive cells were counted using ImageJ. The graph represents the means ± SD of 4 images per condition from two different experiments. Asterisks indicate significant differences (p-values) between proliferation in $SNAI1^{+/+}$ cells and $SNAI^{-/-}$ cells. Data were evaluated using the t-test analysis, *** = 0.0001<P< 0.001.

5.13 *Fgf21* and *Atf3* are repressed by the transcription factor SNAI1

Silencing of SNAI1 expression by shRNA induced a significant upregulation of several genes, including *Fgf21*and *Atf3*. In order to confirm the SNAI1 involvement in *Fgf21* and *Atf3* regulation in myoblasts, we performed RT-qPCR analysis, comparing the *Fgf21* and *Atf3* expression in C2C12 SNAI1$^{-/-}$ and control cell line. A significant increased level of *Fgf21* and *Atf3* expression was observed in proliferating SNAI1 knockout myoblasts (D-1) compared with the control cells. As expected, in differentiated cells (D4) not expressing anymore SNAI1, *Fgf21* and *Atf3* were strongly upregulated, but no variation was detected between control cells and SNAI1 knockout cell line (Figure 33).

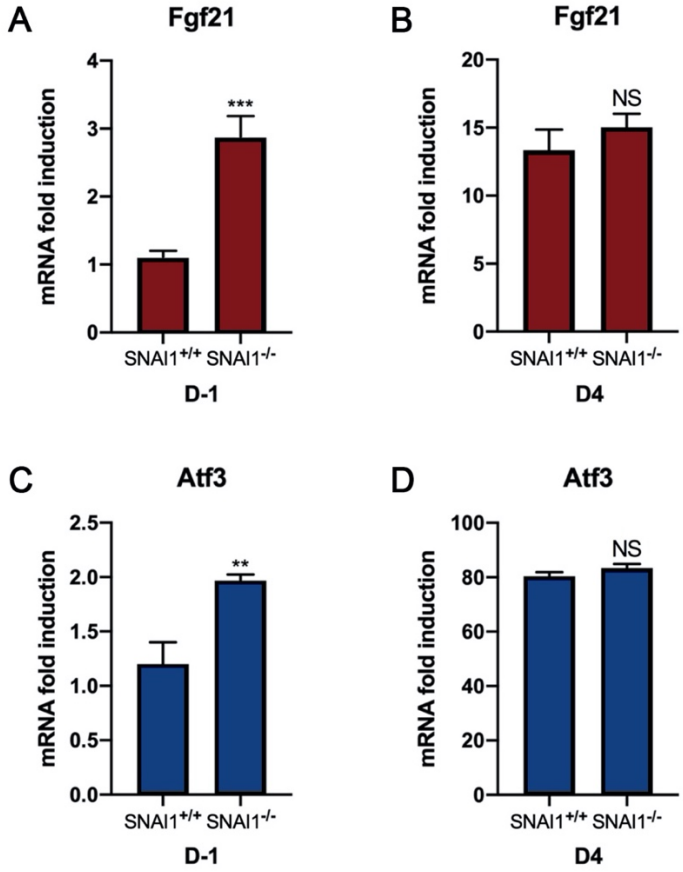

Figure 33. SNAI1 knockout by CRIPR-Cas9 genome editing confirms the repressive role of SNAI1 of the *Fgf21* and *Atf3* expression. Quantitative evaluation of *Fgf21* and *Atf3* transcripts in C2C12 SNAI1$^{+/+}$ e C2C12 SNAI1$^{-/-}$ by RT-qPCR. Asterisks indicate significant differences (p-values) between expression in SNAI1$^{+/+}$ cells and SNAI$^{-/-}$ cell. The values normalized to the *Gapdh* mRNA levels are expressed as the mean ± SD of 3 independent experiments using the t-test analysis. *** = 0.0001<P< 0.001, ** = 0.001<P< 0.01, NS= not statistically significance.

6. DISCUSSION

Skeletal muscles have the peculiar ability to regenerate following damage. After an acute injury or trauma, degeneration is induced, followed by regeneration processes that involve different cell populations, including a resident population of muscle cells, the satellite cells. Indeed, in the absence of any environmental stimuli, the satellite cells are in a quiescent state and are located in a specialized niche between the sarcolemma and the basal lamina. Following an injury or disease, satellite cells become activated, proliferate, migrate to the damaged areas, and eventually differentiate, giving rise to newly forming myofiber (Rappolee *et al.*, 1992; Guardiola *et al*., 2017). In this process, the MRFs such as MyoD, Myog, Myf5 and MRF4 play a crucial role to direct satellite cells to terminal differentiation (Seale *et al.,* 2014). MRFs recognize and bind the same E-box (5'-CANNTG-3') recognized by SNAI proteins, this indicates that SNAI proteins might compete with MRFs for the same binding sequences and could have a role in myogenesis (Kataoka *et al.*, 2000; Braun *et al.*, 1991; Mauhin *et al.*, 1993).

SNAI1 and SNAI2 are DNA-binding transcription factors widely expressed in mesodermal cells, including myoblasts and have been shown to act as transcriptional repressors by recruiting HDAC1/2 (Bolos *et. al.,* 2012; Hajra *et al*., 2002; Peinado *et al.,* 2007).

Our data showed that *in vitro*, during myogenesis, SNAI transcription factors are expressed during satellite cells proliferation and are rapidly downregulated when satellite cells start to differentiate. Moreover, using wild type mice and *Snai* knock-in transgenic mice, we demonstrated that *Snai1* and *Snai2* are overexpressed during muscle regeneration at 3-4 days after the injury, when quiescent satellite cells are activated and in a proliferative state. In the *in vivo* experiments, *Snai1* and *Snai2* show a different temporal expression: *Snai1* decreases at the beginning of the differentiation program, while *Snai2* is detected also later, suggesting that it could also be expressed in other cell types during muscle regeneration, such as macrophages and Fibro/Adipogenic progenitors (FAPs).

Even though targeted experiments of double staining for SNAI proteins and cell-specific markers are needed to better clarify this point, these data indicate that SNAI1 may function in early myogenic program during muscle regeneration. Accordingly, the absence of SNAI1 in C2C12 Crispr-Cas9 gene edited cells leads to a decreased proliferation. The transition from proliferation to differentiation is a critical step in muscle development. SNAI1 is important in myogenic cells proliferation and it could regulate the entry of myogenic cells in the differentiation program because there is a rapid decrease of SNAI1 at the onset of the differentiation. In this context, among the genes downregulated by the silencing of SNAI1, we found the hepatocyte growth factor (HGF), suggesting that SNAI1 is necessary for the HGF expression in myoblasts. HGF is known to activate satellite cells, through its

receptor c-Met (expressed also in quiescent satellite cells), to promote myoblasts proliferation and to inhibit their terminal differentiation (Leshem *et al.*, 2000). Thus, SNAI1-dependent HGF expression could be one way for SNAI1 to promote myoblasts proliferation and their undifferentiated state.
The analysis of the transcriptome in C2C12 myoblasts silenced for SNAI1 has identified several target genes, but only few genes involved in terminal myofiber differentiation. This is in contrast with the data obtained by Soleimani and colleagues, which describe SNAI1 as an inhibitor of terminal differentiation of primary myoblasts (Soleimani *et al.,* 2012). However, in the presence of growth factors, C2C12 cells are considerably less prone to spontaneous differentiation than primary myoblasts, and this was confirmed by their resistance to differentiation even in absence of SNAI1 expression. This makes them a good model to study SNAI1 effect on transcriptome in proliferating myoblasts without the influence of an ongoing differentiation process. In this cell system, among the genes most repressed by SNAI1, we selected *Fgf21* and *Atf3*, which have been never described as SNAI1 targets and have, however, shown to play a role regulating muscle differentiation. Previous studies have reported that FGF21 is upregulated during myogenic differentiation of myoblasts and is positively regulated by the transcription factor MyoD. FGF21 promotes the myogenic differentiation and the switch of muscle fiber from anaerobic myofiber to aerobic myofiber via FGF21-SIRT1-AMPK- PGC1a axis (Liu *et al.*, 2017). Less is known about the direct involvement of ATF3 in terminal differentiation of myoblasts. ATF3 is a transcription factor involved in the induction of ER stress that has a crucial role in myogenesis (Schmitz *et al.,* 2018). Recent studies showed that ATF3 is transiently expressed during myogenic differentiation, but not during myogenic proliferation and it is a negative regulator of some inflammatory genes in skeletal muscle damage (Fernández-Verdejo *et al.,* 2017; Alter *et al*., 2011).

We showed, both *in vitro* and *in vivo,* that *Fgf21* and *Atf3* are expressed during myogenesis at the beginning of the differentiation program, when SNAI1 expression decreases, confirming the SNAI1 repressive role on *Fgf21* and *Atf3* expression. Moreover, we found that SNAI1 overexpression downregulates *Fgf21* and *Atf3* transcripts and negatively regulates *Fgf21* and *Atf3* by direct binding to their promoter regions. By ChIP assay, we described that SNAI1 binds the E-boxes of the *Fgf21* promoter located in the regions between -1722 and -1583 bp (Cluster A) and between -51 and +122 bp (Cluster C), but it doesn't bind the putative binding sites between -1067 and -935 bp (Cluster B). However, due to methodology limitation, we are not able to discriminate among the E-boxes within the same cluster recognized by SNAI1.

This because the E-boxes within the same cluster are confined in a DNA region smaller than 200 bp in size, but the chromatin complexes cleaved by the pAG-Mnase are about 200 bp.

Interestingly, it has been suggested that MyoD binds the E-box at -1067 bp of the *Fgf21* promoter enhancing myogenic differentiation (Liu *et al.,* 2017). With our study, we show that SNAI1 binding sites do not overlap with MyoD-targeted E-box in the *Fgf21* promoter, suggesting that their opposite effect on the *Fgf21* transcription is not a simple competition for the binding sites. Since SNAI1 is expressed during satellite cells proliferation and it decreases concurrently with the increasing of MyoD expression when satellite cells start to differentiate, we suppose that *Fgf21* could be repressed by SNAI1 during the early stage of myogenesis and subsequently activated by MyoD by binding different E-boxes and engaging chromatin modifiers with opposing activities.

We also found that SNAI1 directly binds the *Atf3* promoter in the E-box positioned at -1873 bp and in the E-box cluster between -1320 and -1220 bp with respect to the TSS. Again, we are not able to discriminate among the E-boxes present within the cluster between -1320 and -1220 bp bound by SNAI1 for the technical reasons mentioned above. There is no evidence about the possible involvement of MyoD in the regulation of *Atf3.* Further studies are necessary to indagate if the mechanism indicate for *Fgf21* could be also postulated for *Atf3,* since our studies demonstrated that SNAI1 represses *Atf3* expression during satellite cells proliferation, and which is the precise role of ATF3 in muscle differentiation. Recent studies have demonstrated that ER stress plays a crucial role in the regulation of the skeletal muscle development (Chen *et al.*, 2006; Nakanishi *et al.*, 2015; Wei *et al*., 2016). Through the analysis of the transcriptome in myoblasts silenced for the expression of SNAI1, we identified several regulated genes related to ER stress. Since ER stress is implicated in *Fgf21* induction, we evaluated *Fgf21* expression during ER stress, treating proliferating C2C12 cells with thapsigargin as ER stress inducing agent, and we found that *Fgf21* expression increases in response to ER stress. Moreover, thapsigargin-induced *Fgf21* expression is strongly downmodulated by overexpression of SNAI1, demonstrating that SNAI1 and ER stress act with opposite effect on *Fgf21* transcriptional regulation. Hernadez *et al.* showed that ATF3 is able to bind *Fgf21* promoter and upregulate its expression. However, we demonstrate that, during proliferation stage of myoblasts, ATF3 alone is not able to counteract *Fgf21* repression mediated by SNAI1. Targeted silencing of ATF3 is necessary to validate its involvement in *Fgf21* induction triggered by myoblasts differentiation.

In summary, we described that the transcription factor SNAI1 plays a role in early myogenic program both *in vitro* and *in vivo* in part by directly repressing *Fgf21* and *Atf3* through binding their promoters during myoblast proliferation. The downregulation of SNAI1 at the beginning of differentiation program is *per sè* sufficient to unlock the expression of *Fgf21* and *Atf3,* that consequently participate in the myogenic differentiation. SNAI1 downregulation, mediated by the withdrawal of growth

factor, determines the entry of myogenic cells in the differentiation program and leads to the activation of ER stress and ATF3. Since SNAI1 is absent and is not able to repress *Fgf21* at the beginning of the differentiation, we suppose that ER stress and ATF3 positively regulate *Fgf21* expression leading to myogenic differentiation (Figure 34). Further targeted experiments are needed to confirm this latter hypothesis.

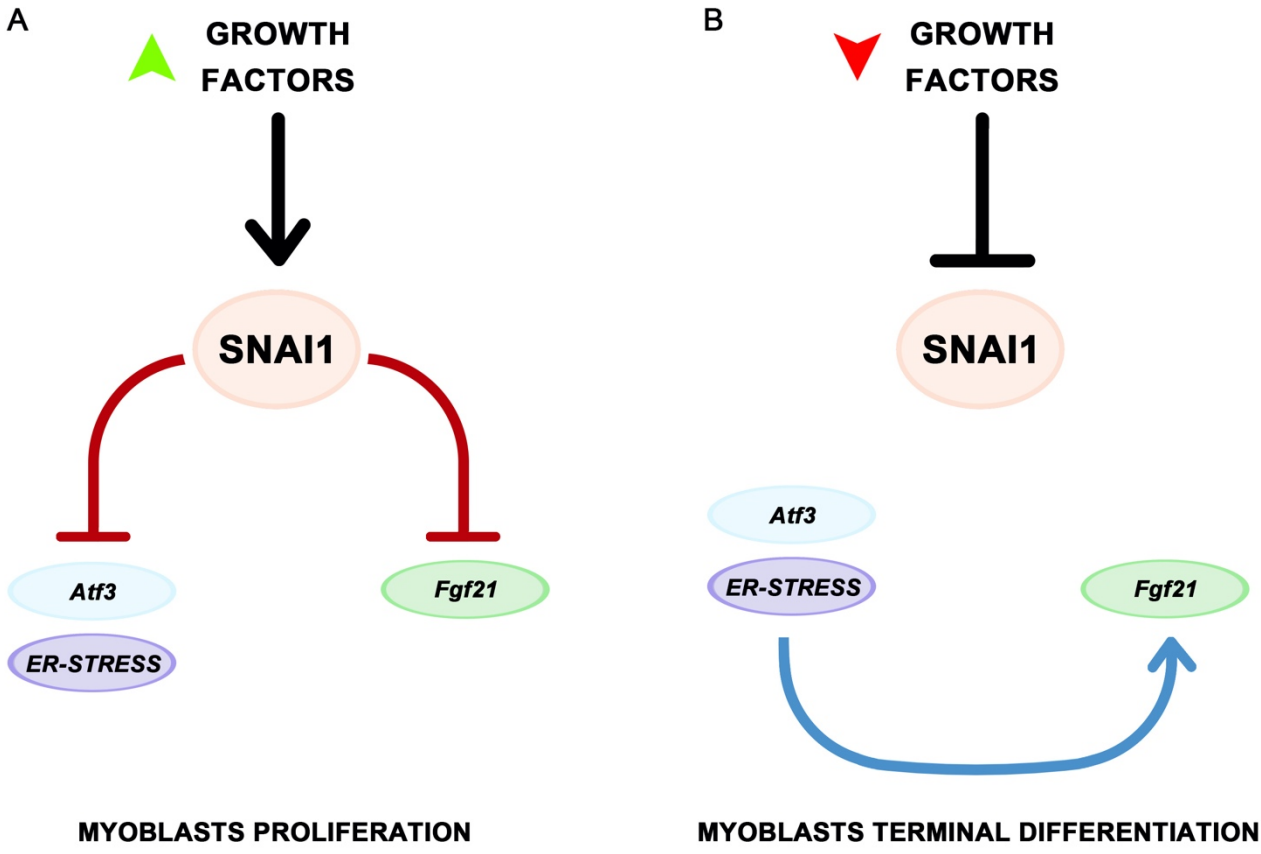

Figure 34. Suggested mechanism by which SNAI1 regulates myogenesis. A) During myoblasts proliferation, growth factors activate SNAI1. The transcription factor SNAI1 binds directly *Atf3* and *Fgf21* promoters and negatively regulates their expression. B) During myoblasts terminal differentiation, the loss of SNAI1, due to the growth factors reduction, activates ER stress and *Atf3* that positively regulate *Fgf21*.

7. REFERENCES

- Acosta-Alvear D, Zhou Y, Blais A, Tsikitis M, Lents N H, Arias C, Lennon C J, Kluger Y, Dynlacht B D. (2007). XBP1 controls diverse cell type- and condition- specific transcriptional regulatory networks. Mol Cell., 27:53–66.
- Afroze D, Kumar A. (2019). ER stress in skeletal muscle remodeling and myopathies. *FEBS J*., 286(2):379-398.
- Alter J, Bengal E. (2011). Stress-induced C/EBP homology protein (CHOP) represses MyoD transcription to delay myoblast differentiation. PLoS One., 6(12):e29498.
- Anna Meiliana, Nurrani Mustika Dewi, Andi Wijaya. (2015). Molecular Regulation and Rejuvenation of Muscle Stem (Satellite) Cell Aging. The Indonesian Biomedical Journal, 7(2):73.
- Barrallo-Gimeno A, Nieto M A. (2005). The Snail genes as inducers of cell movement and survival: implications in development and cancer. Development, 132, 315-61.
- Batlle E M, Sancho E, Franci C, Dominguez D, Monfar M, Baulida J, Garcia de Herreros A. (2000). The transcription factor Snail is a repressor of E-cadherin gene expression in epithelial tumour cells. Nat. Cell. Biol., 2(2), 84-9.
- Blais A, Tsikitis M, Acosta-Alvear D, Sharan R, Kluger Y, Dynlacht B D. (2005). An initial blueprint for myogenic differentiation. Genes Dev., 19:553–69. 45.
- Bolos V, Peinado H, Perez-Moreno M A, Fraga M F, Esteller M, Cano A. (2003). The transcription factor Slug represses E-cadherin expression and induces epithelial to mesenchymal transitions: a comparison with Snail and E47 repressors. J. Cell Sci., 116, 499-511.
- Bourlay J L, Dennefeld C, Alberga A. (1987). The *Drosophila* development gene snail encodes a protein with nucleic acid binding fingers. Nature, 330, 395-8.
- Bradley C K, Norton C R, Chen Y, Han X, Booth C J, Yoon J K, Krebs L T, Gridley T. (2013). The Snail family gene Snai3 Is not essential for embryogenesis in mice. PLoS, 8(6), e65344.
- Braun T, Arnold H H. (1991). The four human muscle regulatory helix-loop-helix proteins Myf3-Myf6 exhibit similar hetero-dimerization and DNA binding properties. Nucleic Acids Res., 19(20), 5645-51.
- Buorlay J L, Dennefeld C, Alberga A. (1987). The *Drosophila* development gene snail encodes a protein with nucleic acid binding fingers. Nature, 330, 395-8.
- Campion D R. (1984) The muscle satellite cell: a review. Int. Rev. Cytol., 87, 225-51.

- Camporez J P, Asrih M, Zhang D, Kahn M, Samuel V T, Jurczak M J, Jornayvaz F R. (2015). Hepatic insulin resistance and increased hepatic glucose production in mice lacking Fgf21. J. Endocrinol., 226, 207-17.
- Cano A, Perez-Moreno M A, Rodrigo I, Locascio A, Blanco M J, Del Barrio M G, Portillo F, Nieto M A. (2000). The transcription factor Snail controls epithelial-mesenchymal transitions by repressing E-cadherin expression. Nat. Cell Biol., 2, 76-83.
- Cao S S, Kaufman R J. (2013). Targeting endoplasmic reticulum stress in metabolic disease. Expert Opin. Ther. Tar., 17(4), 437-48.
- Chang N C, Rudnicki M A. (2014). Satellite cells: the architects of skeletal muscle. Curr Top Dev Biol, 107:161-81.
- Chargé S B, Rudnicki M A. (2004). Cellular and molecular regulation of muscle regeneration. Physiol Rev, 84(1):209-38.
- Chen B P, Liang G, Whelan J, Hai T. (1994). ATF3 and ATF3 delta Zip. Transcriptional repression versus activation by alternatively spliced isoforms. J Biol Chem, 3;269(22):15819-26.
- Chen J F, Mandel E M, Thomson J M, Wu Q, Callis T E, Hammond S M, Conlon F L, Wang D. (2006). The role of microRNA-1 and microRNA-133 in skeletal muscle proliferation and differentiation. Nat. Genet., 38(2), 228-33.
- De Craene B, Van Roy F, Berx G. (2005). Unraveling signalling cascades for the Snail family of transcription factors. Cell Signal., 17(5), 535-47.
- Decary S, Mouly V, Hamida C B, Sautet A, Barbet J P, Butler-Browne G S. (1997). Replicative potential and telomere length in human skeletal muscle: implications for satellite cell-mediated gene therapy. Hum Gene Ther, 8(12):1429-38.
- Decary S, Mouly V, Hamida C B, Sautet A, Barbet J P, Butler-Browne G S. (1997) Replicative potential and telomere length in human skeletal muscle: implications for satellite cell-mediated gene therapy. Hum. Gene. Ther., 8(12), 1429-38.
- Dominguez D, Montserrat-Sentis B, Virgos-Soler A, Guaita S, Grueso J, Porta M, Puig I, Baulida J, Franci C, Garcia de Herreros A. (2003). Phosphorylation regulates the subcellular location and activity of the Snail transcriptional repressor. Mol. Cell. Biol., 23(14), 5078-89.
- Edagawa M, Kawauchi J, Hirata M, Goshima H, Inoue M, Okamoto T, Murakami A, Maehara Y, Kitajima S. (2014). Role of Activating Transcription Factor 3 (ATF3) in Endoplasmic Reticulum (ER) Stress-induced Sensitization of p53-deficient Human Colon Cancer Cells to Tumor Necrosis Factor (TNF)-related Apoptosis-inducing Ligand (TRAIL)-

mediated Apoptosis through Up-regulation of Death Receptor 5 (DR5) by Zerumbone and Celecoxib. J. Biol. Chem., 289(31), 21544-61.

- Espineda C E, Chang J H, Twiss J, Rajasekran S A, Rajasekran A K. (2004). Repression of Na/K-ATPase beta1-subunit by the transcription factor snail in carcinoma. Mol. Biol. Cell., 15, 1364-73.
- Fernández-Verdejo R, Vanwynsberghe A M, Hai T, Deldicque L, Francaux M. (2017). Activating transcription factor 3 regulates chemokine expression in contracting C_2C_{12} myotubes and in mouse skeletal muscle after eccentric exercise. Biochem Biophys Res Commun., 14;492(2):249-254.
- Galvagni F, Cantini M, Oliviero S. (2002) The utrophin gene is transcriptionally up-regulated in regenerating muscle. J Biol Chem, 277(21):19106-13.
- Gjymishka A, Su N, Kilberg M S. (2009). Transcriptional induction of the human asparagine synthetase gene during the unfolded protein response does not require the ATF6 and IRE1/XBP1 arms of the pathway. Biochem. J., 417, 695–703.
- Grande M T, Sánchez-Laorden B, López-Blau C, De Frutos C A, Boutet A, Arévalo M, Rowe R G, Weiss S J, López-Novoa J M, Nieto M A. (2015). Snail1-induced partial epithelial-to-mesenchymal transition drives renal fibrosis in mice and can be targeted to reverse established disease. Nat Med, 21(9):989-97.
- Grau Y, Carteret C, Simpson P. (1984). Mutations and chromosomal rearrangements affecting the expression of snail, a gene involved in embryonic patterning in *Drosophila melanogaster*. Genetics, 108(2), 347-60.
- Guaita S, Puig I, Franci C, Garrido M, Dominguez D, Batlle E, Sancho E, Dedhar S, Garcia de Herreros A, Baulida J. (2002). Snail induction of epithelial to mesenchymal transition in tumor cells is accompanied by MUC1 repression and ZEB1 expression. J. Biol. Chem. 277(42), 39209-16.
- Guridi M, Tintignac L A, Lin S, Kupr B, Castets P, Ruegg M A. (2015). Activation of mTORC1 in skeletal muscle regulates whole-body metabolism through FGF21. Sci. Signal., 8(402), ra113.
- Hai T, Curran T. (1991) Cross-family dimerization of transcription factors Fos/Jun and ATF/CREB alters DNA binding specificity. Proc Natl Acad Sci U S A, 1;88(9):3720-4.
- Hai T, Wolfgang C D, Marsee D K, Allen A E, Sivaprasad U. (1999) ATF3 and stress responses. Gene Expr, 7(4-6):321-35.

- Hai T W, Liu F, Coukos W J, Green M R. (1989). Transcription factor ATF cDNA clones: An extensive family of leucine zipper proteins able to selectively form DNA-binding heterodimers. Genes Dev., 3, 2083–90.
- Haring M, Offermann S, Danker T, Horst I, Peterhansel C, Stam M. (2007). Chromatin immunoprecipitation: optimization, quantitative analysis and data normalization. *Plant Methods*, 3:11.
- Alberts B, Johnson A, Lewis J, Morgan D, Raff M, Roberts K, Walter P. (2015) Biologia molecolare della cellula. 6th edizione, Trad. a cura di Pagano A, Bologna, Zanichelli (tit. orig. Molecular biology of the cell), 734.
- Hashimoto Y, Zhang C, Kawauchi J, Imoto I, Adachi M T, Inazawa J, Amagasa T, Hai T, Kitajima S. (2002). An alternatively spliced isoform of transcriptional repressor ATF3 and its induction by stress stimuli. Nucleic Acids Res., 30(11):2398-406.
- Hemavathy K, Ashraf S I, Ip Y T. (2000). Snail/slug family of repressors: slowly going into the fast lane of development and cancer. Gene, 257(1),1-12.
- Herranz N, Pasini D, Diaz V M, Franci C, Gutierrez A, Dave N, Escriva M, Hernandez Muñoz I, Di Croce L, Helin K, Garcia de Herreros A, Peiro S. (2008). Polycomb complex 2 is required for E-cadherin repression by the Snail1 trascription factor. Mol. Cell. Biol., 28(15), 4772.
- Ikenouchi J, Matsuda M, Furuse M, Tsukita S. (2003). Regulation of tight junctions during the epithelium-mesenchyme transition: direct repression of the gene expression of claudins/occluding by Snail. J. Cell Sci., 116, 1959-67.
- Itoh N. (2014). FGF21 as a hepatokine, adipokine, and myokine in metabolism and disease. Front Endocrinol (Lausanne), 7;5:107.
- Izumiya Y, Bina H A, Ouchi N, Akasaki Y, Kharitonenkov A, Walsh K. (2008). FGF21 is an Akt-regulated myokine. FEBS Lett., 582(27), 3805-10.
- Jägle S, Busch H, Freihen V, Beyes S, Schrempp M, Boerries M, Hecht A. (2017). SNAIL1-mediated downregulation of FOXA proteins facilitates the inactivation of transcriptional enhancer elements at key epithelial genes in colorectal cancer cells. PLoS Genet., 13(11):e1007109.
- Jiang H, Wek S A, McGrath B C, Lu D, Hai T, Harding H P, Wang X, Ron D, Cavener D R, Wek R C. (2004). Activating transcription factor 3 is integral to the Eukaryotic initiation factor 2 kinase stress response. Mol. Cell. Biol., 24(3), 1365-77.
- Jiang R, Lan Y, Norton C R, Sundberg J P, Gridley T. (1998). The Slug gene is not essential for mesoderm or neural crest development in mice. Dev Biol., 198(2):277-85.

- Jiménez-Amilburu V, Salmeron C, Codina M, Navarro I, Capilla E, Gutierrez J. (2013). Insuline-like growth factors effects on the expression of myogenic regulatory factors in gilthead sea bream muscle cells. Gen. Comp. Endocrinol., 188(1), 151-8.
- Kajita M, McClinc K N, Wade P A. (2004). Aberrant expression of the transcription factors snail and slug alters the response to genotoxic stress. Mol. Cell. Biol., 24(17), 310-9.
- Kataoka H, Murayama T, Yokode M, Mori S, Sano H, Ozaki H, Yokota Y, Nishikawa S, Kita T. (2000). A novel snail-related transcription factor Smuc regulates basic helix-loop-helix transcription factor activities via specific E-box motifs. Nucleic Acids Res., 28(2): 626-633.
- Kaufman R J. (1999). Stress signaling from the lumen of the endoplasmic reticulum: coordination of gene transcriptional and translational controls. Genes Dev., 13(10), 1211-33.
- Kim J Y, Kim Y M, Yang C H, Cho S K, Lee J W, Cho M. (2012). Functional regulation of Slug/Snail2 activity is dependent on GSK-3β mediated phosphorylation. FEBS J., 279(16), 2929-39.
- Ku H C, Cheng C F. (2020). Master Regulator Activating Transcription Factor 3 (ATF3) in Metabolic Homeostasis and Cancer. Front Endocrinol (Lausanne), 14;11:556.
- Chen J F, Mandel E M, Thomson J M, Wu Q, Callis T E, Hammond S M, Conlon F L, Wang D Z. (2006). The role of microRNA-1 and microRNA-133 in skeletal muscle proliferation and differentiation. Nat. Genet., 38(2), 228-33.
- Lau M, Leung P C K. (2012). The PI3K/Akt/mTOR signaling pathway mediates insulin-like growth factor 1-induced E-cadherin down-regulation and cell proliferation in ovarian cancer cells. Cancer Lett., 326(2), 191-8.
- Leptin M. (1991). Twist and Snail as positive and negative regulators during Drosophila development. Genes Dev., 5, 1568-76.
- Lin Y, Li X Y, Willis A L, Liu C, Chen G, Weiss S J. (2014). Snail1-dependent control of embryonic stem cell pluripotency and lineage commitment. Nat Commun., 5:3070.
- Lin Y, Dong C, Zhou B P. (2014). Epigenetic regulation of EMT: The Snail story. Curr. Pharm Des., 20(11):1698-705.
- Litwiniuk A, Pijet B, Pijet-Kucicka M, Gajewska M, Pajak B, Orzechowski A. (2016). FOXO1 and GSK-3β are main target of inculin-mediated myogenesis in C2C12 muscle cells. PLoS One, 11(1), e0146726.
- Liu X, Wang Y, Zhao S, Li X. (2017). Fibroblast Growth Factor 21 Promotes C2C12 Cells Myogenic Differentiation by Enhancing Cell Cycle Exit. Biomed Res Int., 2017:1648715.
- Lu D, Wolfgang C D, Hai T. (2006). Activating transcription factor 3, a stress-inducible gene, suppresses Ras-stimulated tumorigenesis. J Biol Chem., 14;281(15):10473-81.

- Malhotra J D, Kaufman R J. (2007). The endoplasmic reticulum and the unfolded protein response. Semin. Cell. Dev. Biol., 18(6), 716-31.
- Manzanares M, Locascio A, Nieto M A. (2001). The increasing complexity of the Snail gene superfamily in metazoan evolution. Trends in genetics, 17(4), 178-81.
- Markan K R, Naber M C, Ameka M K, Anderegg M D, Mangelsdorf D J, Kliewew S A, Mohammadi M, Potthoff M J. (2014). Circulating FGF21 is liver derived and enhances glucose uptake during refeeding and overfeeding. Diabetes, 63(12), 4057-63.
- Martinez-Alvarez C, Blanco M J, Perez R, Rabadan M A, Aparicio M, Resel E, Martinez T, Nieto M A. (2004). Snail family members and cell survival in physiological and pathological cleft palates. Dev. Biol., 265(1), 207-18.
- Mauhin V, Lutz Y, Dennefeld C, Alberga A. (1993). Definition of the DNA-binding site repertoire for the Drosophila transcription factor SNAIL. Nucleic Acids Res., 21(17): 3951-3957.
- Nakanishi K, Dohmae N, Morishima N. (2007). Endoplasmic reticulum stress increases myofiber formation in vitro. FASEB J., 21:2994–3003.
- Nakanishi K, Sudo T, Morishima N. (2005). Endoplasmic reticulum stress signaling transmitted by ATF6 mediates apoptosis during muscle development. J Cell Biol., 169:555–60.
- Nakanishi K, Kikiguchi K, Yonemura S, Nakano A, Morishima N. (2015). Transient Ca2+ depletion from the endoplasmic reticulum is critical for skeletal myoblast differentiation. FASEB J., 29(5), 2137-49.
- Nakayama H, Scott I.C, Cross J.C. (1998). The transition to endoreduplication in trophoblast giant cells is regulated by the mSNA zinc finger transcription factor. Dev. Biol., 199, 150-63.
- Nieto M.A. The snail superfamily of zinc-finger transcription factors. (2002). Nat Rev Mol Cell Biol., 3(3):155-66.
- Nüsslein-Volhard C, Wieschaus E, Kluding H. (1984). Mutations affecting the pattern of the larval cuticle in Drosophila melanogaster. Wilhelm Roux's Arch. Dev. Biol., 193(5), 267-82.
- Osorio L A, Farfan N M, Castellon E A, Contreras H R. (2016). Snail transcription factor increases the motility and invasive capacity of prostate cancer cells. Mol. Med. Rep., 13(1), 778-786.
- Otto A, Schmidt C, Luke G, Allen S, Valasek P, Muntoni F, Lawrence-Watt D, Patel K. (2008). Canonical Wnt signalling induces satellite-cell proliferation during adult skeletal muscle regeneration. J. Cell. Sci., 121, 2939-50.

- Pálmer H G, Larriba M J, García J M, Ordóñez-Morán P, Peña C, Peiró S, Puig I, Rodríguez R, De la Fuente R, Bernad A, Pollán M, Bonilla F, Gamallo C, De Herreros A G, Muñoz A. (2004). The transcription factor SNAIL represses vitamin D receptor expression and responsiveness in human colon cancer. Nat Med., 10(9), 917-9.
- Peinado H, Ballerstar E, Esteller M, Cano A. (2004). Snail mediates E-Cadherin repression by the recruitment of the Sin3A/histone deacetylase 1 (HDAC1)/HDAC2 complex. Mol. Cell. Biol., 24, 306-319.
- Peinado H, Olmeda D, Cano A. (2007). Snail, ZEB and bHLH factors in tumor progression: an alliance against the epithelial phenotype? Nat. Rev. Cancer, 7, 415-28.
- Peirò S, Escriva M, Puig I, Barbera M J, Dave N, Herranz N, Larriba M J, Takkunen M, Franci C, Muño A, Virtanen I, Baulida J, Garcia de Herreros A. (2006). Snail1 transcriptional repressor binds to its own promotes and controls its expression. Nuc. Acids Res., 34(7), 2077-84.
- Phillips S, Kuperwasser C. (2014). SLUG: critical regulator of epithelial cell identity in breast development and cancer. Cell Adhes. Migrat., 8(6), 578-87.
- Planavila A, Redondo I, Hondares E, Vinciguerra M, Munts C, Iglesias R, Gabrielli L A, Sitges M, Giralt M, Van Bilsen M, Villarroya F. (2013). Fibroblast growth factor 21 protects against cardiac hypertrophy in mice. Nat. Commun., 4, 2019.
- Planavila A, Redondo-Angulo I, Ribas F, Garrabou G, Casademont J, Giralt M, Villarroya F. (2015). Fibroblast growth factor 21 protects the heart from oxidative stress. Cardiovasc. Res., 106, 19-31.
- Rappolee D A, Werb Z. (1992). Macrophage-Derived Growth Factors. Curr. Top. Microbiol. Immunol., 181, 87-140.
- Ribas F, Villarroya J, Hondares E, Giralt M, Villarroya F. (2014). FGF21 expression and release in muscle cells: involvement of MyoD and regulation by mitochondria-driven signaling. Biochem. J., 463, 191-9.
- Rowe R G, Li X Y, Hu Y, Saunders T L, Virtanen I, Garcia de Herreros A, Becker K F, Ingvarsen S, Engelholm L H, Bommer G T, Fearon E R, Weiss S J. (2009) Mesenchymal cells reactivate Snail1 expression to drive three-dimensional invasion programs. J Cell Biol., 184(3):399-408.
- Sabourin L A, Rudnicki M A. (2000). The molecular regulation of myogenesis. Clin. Genet., 57(1), 16-25.
- Schaap F G, Kremer A E, Lamers W H, Jansen P L M, Gaemers I C. (2013). Fibroblast growth factor 21 is induced by endoplasmic reticulum stress. Biochimie, 95(4), 692-9.

- Schmalbruch H, Al-Amood W S, Lewis D M. (1991) Morphology of long-term denervated rat soleus muscle and the effect of chronic electrical stimulation. J Physiol., 441:233-41.
- Schmalbruch H, Jensen H J, Bjaerg M, Kamieniecka Z, Kurland L. (1991) A new mouse mutant with progressive motor neuronopathy. J Neuropathol Exp Neurol., 50(3):192-204.
- Schmitz M L, Shaban M S, Albert B V, Gökçen A, Kracht M. (2018). The Crosstalk of Endoplasmic Reticulum (ER) Stress Pathways with NF-κB: Complex Mechanisms Relevant for Cancer, Inflammation and Infection. Biomedicines., 6(2), 58.
- Seale P, Ishibashi J, Holterman C, Rudnicki M A. (2004). Muscle satellite cell-specific genes identified by genetic profiling of MyoD-deficient myogenic cell. Dev. Biol., 275(2), 287-300.
- Seale P, Rudnicki M A. (2000). A New Look at the Origin, Function, and "Stem-Cell" Status of Muscle Satellite Cells. Developmental Biology, 218, 115–124
- Singh K, Dilworth F J. (2013). Differential modulation of cell cycle progression distinguishes members of the myogenic regulatory factor family of transcription factors. FEBS J., 280(17):3991-4003.
- Soleimani V D, Yin H, Jahani-Asl A, Ming H, Kockx C E, Van Ijcken W F, Grosveld F, Rudnicki M A. (2012). Snail regulates MyoD binding-site occupancy to direct enhancer switching and differentiation-specific transcription in myogenesis. Mol. Cell., 47(3), 457-68.
- Stewart C E H, Rotwein P. (1996). Growth, differentiation, and survival: multiple physiological functions for insulin-like growth factors. Physiol. Rev., 76, 1005-26.
- Sweetman D, Goljanek K, Rathjen T, Oustanina S, Braun T, Dalmay T, Munsterberg A. (2008). Specific requirements of MRFs for the expression of muscle specific microRNAs, miR1, miR-206 and miR-133. Dev. Biol., 321, 491–9.
- Tanaka S, Terada K, Nohno T. (2011). Canonical Wnt signaling is involved in switching from cell proliferation to myogenic differentiation of mouse myoblast cells. J. Mol. Signal., 6, 12.
- Thiery J P. (2002). Epithelial-mesenchymal transitions in tumour progression. Nat Rev Cancer, 2(6):442-54.

- Thiery J P, Sleeman J P. (2006) Complex networks epithelial-mesenchymal transitions. Nat. Rev. Mol. Cell. Biol., 7(2), 131-42.
- Tidball J G, Daniel T L. (1986) Myotendinous junctions of tonic muscle cells: structure and loading. Cell Tissue Res., 245(2):315-22.
- Tidball J G, Dorshkind K, Wehling-Henricks M. (2014). Shared signaling systems in myeloid cell-mediated muscle regeneration. Development, 141(6):1184-96.
- Tidball J G, O'Halloran T, Burridge K. (1986) Talin at myotendinous junctions. J Cell Biol., 103(4):1465-72.

- Tidball J G. (2017) Regulation of muscle growth and regeneration by the immune system. Nat Rev Immunol., 17(3):165-178.
- Ustanina S, Carvajal J, Rigby P, Braun T. (2007). The myogenic factor Myf5 supports efficient skeletal muscle regeneration by enabling transient myoblast amplification. Stem Cells., 25(8):2006-16.
- Van der Velden J L, Langen R C, Kelders M C, Wouters E F, Janssen-Heininger Y M, Schols A M. (2006). Inhibition of glycogen synthase kinase-3beta activity is sufficient to stimulate myogenic differentiation. Am. J. Physiol. Cell. Physiol., 290(2), 453-62.
- Vega S, Morales A V, Ocaña O H, Valdés F, Fabregat I, Nieto M A. (2004). Snail blocks the cell cycle and confers resistance to cell death. Genes Dev., 18(10):1131-43.
- Wan X, Lu X, Xiao Y, Lin Y, Zhu H, Ding T, Yang Y, Huang Y, Zhang Y, Liu Y, Xu Z, Xia J, Li X. (2014). ATF4- and CHOP-dependent induction of FGF21 through endoplasmic reticulum stress. Biomed. Res. Int., 2014(18), 807874.
- Wang M, Kaufman R J. (2016). Protein misfolding in the endoplasmic reticulum as a conduit to human disease. Nature, 529, 326-35.
- Wang Y, Liu X, Hou L, Wu W, Zhao S, Xiong Y. (2016). Fibroblast growth factor 21 suppresses adipogenesis in pig intramuscular fat cells. Int. J. Mol. Sci., 17, 11.
- Wei Y, Tao X, Xu H, Chen Y, Zhu L, Tang G, Li M, Jiang A, Shuai S, Ma J, Jin L, Wen A, Wang Q, Zhu G, Xie M, Wu J, He T, Jiang Y, Li X. (2016). Role of miR-181a-5p and endoplasmic reticulum stress in the regulation of myogenic differentiation. Gene, 592(1), 60-70.
- Wu Y, Evers B M, Zhou B P. (2009). Small C-terminal domain phosphate enhances Snail activity through dephosphorylation. J. Biol. Chem., 284(1), 640-8.
- Wu Z Q, Li X Y, Hu C Y, Ford M, Kleer C G, Weiss S J. (2012). Canonical Wnt signaling regulates Slug activity and links epithelial-mesenchymal transition with epigenetic breast cancer 1, early onset (BRCA1) repression. Proc. Natl. Acad. Sci., 109(41), 16654-9.
- Xu L, Su L, Liu X. (2012). PKCδ regulates death receptor 5 expression induced by PS-341 through ATF4-ATF3/CHOP axis in human lung cancer cells. Mol. Cancer Ther., 11, 2174–82.
- Y Leshem, D B Spicer, R Gal-Levi, O Halevy. (2000). Hepatocyte growth factor (HGF) inhibits skeletal muscle cell differentiation: a role for the bHLH protein twist and the cdk inhibitor p27. J Cell Physiol., 184(1):101-9.
- Yablonka-Reuveni Z. (2011) The skeletal muscle satellite cell: still young and fascinating at 50. J Histochem Cytochem., 59(12):1041-59.

- Yaffe D, Saxel O. (1977). Serial passaging and differentiation of myogenic cells isolated from dystrophic mouse muscle. *Nature*, 270, 725–727.
- Yang C, Yang J, Fan Z, Yang J. (2016). Activating transcription factor 3 – an endogenous inhibitor of myocardial ischemia-reperfusion injury. Mol. Med. Rep., 13(1), 9-12.
- Yang Y J, Li Z B, Zhang G R, Wu L J, Yu J Y, Hu L J, Zhou Y L, Wang H D, Liang D. (2016). Snail-induced epithelial-mesenchymal transition in gastric carcinoma cells and generation of cancer stem cell characteristics. Genet. Mol. Res., 15(3).
- Yang Z, Rayala S, Nguyen D, Vadlamudi R K, Chen S, Kumar R. (2005). Pak1 phosphorylation of Snail, a master regulator of epithelial-to-mesenchyme transition, modulates Snail's subcellular localization and functions. Cancer Res., 65, 3179-3184.
- Ye X, Weinberg R A. (2015). Epithelial-Mesenchymal Plasticity: A Central Regulator of Cancer Progression. Trends Cell Biol., 25(11):675-686.
- Yin H, Price F, Rudnicki M A. (2013). Satellite cells and the muscle stem cell niche. Physiol Rev., 93(1):23-67.
- Yook J I, Li X, Ota I, Fearon E R, Weiss S J, (2005). Wnt-dependent regulation of the Ecadherin repressor Snail. J. Biol. Chem., 280, 11740-8.
- Yu Y, He J, Li S, Song L, Guo X, Yao W, Zou D, Gao X, Liu Y, Bai F, Ren G, Li D. (2016). Fibroblast growth factor 21 (FGF21) inhibits macrophage-mediated inflammation by activating Nrf2 and suppressing the NF-κB signaling pathway. Int. Immunopharmacol., 38, 144-52.
- Zammit P S. (2017). Function of the myogenic regulatory factors Myf5, MyoD, Myogenin and MRF4 in skeletal muscle, satellite cells and regenerative myogenesis. Semin Cell Dev Biol., 72:19-32.
- Zhang C, Huang Z, Gu J, Yan X, Lu X, Zhou S, Wang S, Shao M, Zhang F, Cheng P, Feng W, Tan Y, Li X. (2015). Fibroblast growth factor 21 protects the heart from apoptosis in a diabetic mouse model via extracellular signal-regulated kinase 1/2-dependent signaling pathway. Diabetologia, 58, 1937-48.
- Zhou B P, Deng J, Xia W, Xu J, Li Y M, Gunduz M, Hung M. (2004). Dual regulation of Snail by GSK-3β-mediated phosphorylation in control of epithelial-mesenchymal transition. Nat Cell Biol, 6(10):931-40.
- Zink W, Graf B M, Sinner B, Martin E, Fink R H, Kunst G. (2002). Differential effects of Bupivacaine on intracellular Ca2+ regulation: potential mechanisms of its myotoxicity. Anesthesiology, 97(3), 710-6.

8. ACKNOWLEDGEMENT

First and foremost, I am extremely grateful to my tutors, Prof. Federico Galvagni and Prof. Maurizio Orlandini for their invaluable advice, continuous support, and patience during my PhD study. Their immense knowledge and plentiful experience have encouraged me in all the time of my academic research and daily life. I would also like to offer my special thanks to Prof. Libero Vitiello for his help and suggestions about the muscle regeneration experiments on wild type mice. I would also like to show my gratitude to Dr. Stephen J. Weiss for welcoming me in his lab at University of Michigan, allowing me to grow both as researcher and person. Finally, I would like to express my gratitude to my parents Agostino and Vittoria, my sister Alessandra and my partner Vincenzo. Without their tremendous understanding and encouragement in the past few years, it would be impossible for me to complete my study.